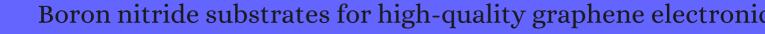
CITATION REPORT List of articles citing



DOI: 10.1038/nnano.2010.172 Nature Nanotechnology, 2010, 5, 722-6.

Source: https://exaly.com/paper-pdf/48516246/citation-report.pdf

Version: 2024-04-23

This report has been generated based on the citations recorded by exaly.com for the above article. For the latest version of this publication list, visit the link given above.

The third column is the impact factor (IF) of the journal, and the fourth column is the number of citations of the article.

#	Paper	IF	Citations
2300	Ballistic Transport in Graphene Antidot Lattices.		
2299	Ultraconfined Plasmonic Hotspots Inside Graphene Nanobubbles.		
2298	Photocharge Trapping in Two-Sheet Reduced Graphene OxideTi0.87O2 Heterostructures and Their Photoreduction and Photomemory Applications.		
2297	Chemical Interaction-Guided, Metal-Free Growth of Large-Area Hexagonal Boron Nitride on Silicon-Based Substrates.		
2296	Large-Velocity Saturation in Thin-Film Black Phosphorus Transistors.		
2295	Inducing Strong Superconductivity in WTe2 by a Proximity Effect.		
2294			
2293	Black Phosphorus High-Frequency Transistors with Local Contact Bias.		
2292	Room Temperature Graphene Mid-Infrared Bolometer with a Broad Operational Wavelength Range.		
2291	Large scale growth and characterization of atomic hexagonal boron nitride layers. 2010 , 10, 3209-15		1961
2290	Nanomaterials: Graphene rests easy. <i>Nature Nanotechnology</i> , 2010 , 5, 699-700	28.7	40
2289	Local compressibility measurements of correlated states in suspended bilayer graphene. 2010 , 105, 250	5806	129
2288	Graphene/Substrate Charge Transfer Characterized by Inverse Photoelectron Spectroscopy. 2010 , 114, 21618-21624		58
2287	Imaging ellipsometry of graphene. 2010 , 97, 231901		85
2286	Broken-symmetry states in doubly gated suspended bilayer graphene. 2010 , 330, 812-6		316
2285	Graphene field-effect transistors based on boron nitride gate dielectrics. 2010,		60
2284	Transport in kinked bi-layer graphene interconnects. 2011 ,		

(2011-2011)

2283	Unique photoemission from single-layer graphene on a SiO2 layer by a substrate charging effect. 2011 , 47, 8608-10	6
2282	Global and Local Oxidation Behavior of Reduced Graphene Oxide. 2011 , 115, 7956-7966	34
2281	Boron nitride substrates for high mobility chemical vapor deposited graphene. 2011 , 98, 242105	305
2280	Controlled modulation of electronic properties of graphene by self-assembled monolayers on SiO2 substrates. 2011 , 5, 1535-40	92
2279	Imaging universal conductance fluctuations in graphene. 2011 , 5, 3622-7	16
2278	Mechanism for puddle formation in graphene. 2011 , 84,	43
2277	Graphene magnetoresistance device in van der Pauw geometry. 2011 , 11, 2973-7	37
2276	Graphene pn Junction: Electronic Transport and Devices. 2011 , 467-508	1
2275	Direct growth of graphene/hexagonal boron nitride stacked layers. 2011 , 11, 2032-7	413
2274	Adhesion and electronic structure of graphene on hexagonal boron nitride substrates. 2011, 84,	230
2273	. 2011 , 32, 1349-1351	22
2272	Charge storage in mesoscopic graphitic islands fabricated using AFM bias lithography. 2011 , 22, 245302	24
2271	RANDOM WALK TO GRAPHENE. 2011 , 25, 4055-4080	10
2270	Graphene microwave transistors on sapphire substrates. 2011 , 99, 113502	40
2269	Local electronic properties of graphene on a BN substrate via scanning tunneling microscopy. 2011 , 11, 2291-5	475
2268	Capacitance of graphene bilayer as a probe of layer-specific properties. 2011 , 84,	24
2267	Graphene veils and sandwiches. 2011 , 11, 3290-4	49
2266	Anomalous paramagnetism in graphene on hexagonal boron nitride substrates. 2011 , 84,	16

2265	ddn in suspended bilayer graphene: The interplay of disorder and band gap. 2011, 84,	8
2264	Quasiparticle band gap engineering of graphene and graphone on hexagonal boron nitride substrate. 2011 , 11, 5274-8	186
2263	Electrical transport properties of graphene on SiO2 with specific surface structures. 2011 , 110, 024513	142
2262	BN/Graphene/BN Transistors for RF Applications. 2011 , 32, 1209-1211	157
2261	Landau level spectra and the quantum Hall effect of multilayer graphene. 2011, 83,	66
2260	Graphene: materials in the Flatland. 2011 , 181, 1299	32
2259	Ballistic transport of graphene pnp junctions with embedded local gates. 2011 , 22, 415203	25
2258	Wafer-scale graphene/ferroelectric hybrid devices for low-voltage electronics. 2011 , 93, 17002	67
2257	Shot noise and conductivity at high bias in bilayer graphene: Signatures of electron-optical phonon coupling. 2011 , 84,	15
2256	Electrostatic doping of graphene through ultrathin hexagonal boron nitride films. 2011 , 11, 4631-5	107
2255	Mapping the density of scattering centers limiting the electron mean free path in graphene. 2011 , 11, 4612-8	84
2254	Electronic properties of edge-functionalized zigzag graphene nanoribbons on SiO2 substrate. 2011 , 22, 265702	6
2253	Chirality-assisted electronic cloaking of confined States in bilayer graphene. 2011 , 107, 156603	47
2252	Ultimate RF Performance Potential of Carbon Electronics. 2011 , 59, 2739-2750	88
2251	Toward tunable band gap and tunable dirac point in bilayer graphene with molecular doping. 2011 , 11, 4759-63	127
2250	Correlated charged impurity scattering in graphene. 2011 , 107, 206601	110
2249	Magneto-transport properties of exfoliated graphene on GaAs. 2011 , 110, 043712	16
2248	In-plane and tunneling pressure sensors based on graphene/hexagonal boron nitride heterostructures. 2011 , 99, 133109	65

2247	Quantum Hall effect and Landau-level crossing of Dirac fermions in trilayer graphene. 2011 , 7, 621-625	182
2246	Direct growth of graphene pad on exfoliated hexagonal boron nitride surface. 2011 , 3, 3089-93	80
2245	Enhanced thermoelectric power in dual-gated bilayer graphene. 2011 , 107, 186602	60
2244	Measurement of the 월1/3 fractional quantum hall energy gap in suspended graphene. 2011 , 106, 046801	66
2243	Interfacial interactions between local defects in amorphous SiO2 and supported graphene. 2011 , 84,	34
2242	Stability of boron nitride bilayers: Ground-state energies, interlayer distances, and tight-binding description. 2011 , 83,	122
2241	Quantized conductance of a suspended graphene nanoconstriction. 2011 , 7, 697-700	128
2240	A role for graphene in silicon-based semiconductor devices. 2011 , 479, 338-44	556
2239	Nobel Lecture: Graphene: Materials in the Flatland*. 2011 , 83, 837-849	584
2238	Nobel Lecture: Random walk to graphene*. 2011 , 83, 851-862	286
2237	Wafer-scale graphene integrated circuit. 2011 , 332, 1294-7	730
2236	Dirac cones reshaped by interaction effects in suspended graphene. 2011 , 7, 701-704	577
2235	Transfer of CVD-grown monolayer graphene onto arbitrary substrates. 2011 , 5, 6916-24	1059
2234	Micrometer-scale ballistic transport in encapsulated graphene at room temperature. 2011 , 11, 2396-9	1203
2233	Engineering a Robust Quantum Spin Hall State in Graphene via Adatom Deposition. 2011, 1,	244
2232	High-frequency performance of graphene field effect transistors with saturating IV-characteristics. 2011 ,	27
2231	Signatures of disorder in the minimum conductivity of graphene. 2011 , 11, 1319-22	24
2230	Chemical vapor deposition and etching of high-quality monolayer hexagonal boron nitride films. 2011 , 5, 7303-9	162

2229	Formation of monolayer and few-layer hexagonal boron nitride nanosheets via surface segregation. 2011 , 3, 2854-8		55
2228	Fluorinating Hexagonal Boron Nitride/Graphene Multilayers into Hybrid Diamondlike Nanofilms with Tunable Energy Gap. 2011 , 115, 21678-21684		21
2227	Semiclassical magnetotransport in graphene n-p junctions. 2011 , 84,		35
2226	Electronic and optical properties of a circular graphene quantum dot in a magnetic field: Influence of the boundary conditions. 2011 , 84,		75
2225	Tunable metallhsulator transition in double-layer graphene heterostructures. 2011 , 7, 958-961		417
2224	Non-thermal ablation of graphite by ultrashort pulsed fs-laser radiation. 2011,		
2223	Coulomb drag and high-resistivity behavior in double-layer graphene. 2011 , 95, 18001		43
2222	Magnetic Skyrmions Could Act as Qubits. 2011 , 4,		1
2221	Hexagonal Boron Nitride as a New Ultraviolet Luminescent Material and Its Application. 2011 , 8, 977-98	39	55
2220	Scanning tunnelling microscopy and spectroscopy of ultra-flat graphene on hexagonal boron nitride. 2011 , 10, 282-5		985
2219	Single-layer MoS2 transistors. <i>Nature Nanotechnology</i> , 2011 , 6, 147-50	28.7	10521
2218			/
	Nanoelectronics: Making light of electrons. <i>Nature Nanotechnology</i> , 2011 , 6, 196-7	28.7	
2217	Nanoelectronics: Making light of electrons. <i>Nature Nanotechnology</i> , 2011 , 6, 196-7 Nanomaterials: Exfoliating the inorganics. <i>Nature Nanotechnology</i> , 2011 , 6, 200-1	28.7	21
2217	Nanomaterials: Exfoliating the inorganics. <i>Nature Nanotechnology</i> , 2011 , 6, 200-1	ĺ	107
,	Nanomaterials: Exfoliating the inorganics. <i>Nature Nanotechnology</i> , 2011 , 6, 200-1	ĺ	
2216	Nanomaterials: Exfoliating the inorganics. <i>Nature Nanotechnology</i> , 2011 , 6, 200-1 Microscopic polarization in bilayer graphene. 2011 , 7, 649-655	ĺ	107
2216	Nanomaterials: Exfoliating the inorganics. <i>Nature Nanotechnology</i> , 2011 , 6, 200-1 Microscopic polarization in bilayer graphene. 2011 , 7, 649-655 Multicomponent fractional quantum Hall effect in graphene. 2011 , 7, 693-696	ĺ	107 347

2211	Giant nonlocality near the Dirac point in graphene. 2011 , 332, 328-30	217
2210	Graphene Sensors. 2011 , 11, 3161-3170	290
2209	Toward intrinsic graphene surfaces: a systematic study on thermal annealing and wet-chemical treatment of SiO2-supported graphene devices. 2011 , 11, 767-71	412
2208	Conductivity of graphene on boron nitride substrates. 2011 , 83,	33
2207	Ripples and layers in ultrathin MoS2 membranes. 2011 , 11, 5148-53	286
2206	Graphene plasmonics: a platform for strong light-matter interactions. 2011 , 11, 3370-7	2008
2205	Giant spin-Hall effect induced by the Zeeman interaction in graphene. 2011 , 107, 096601	47
2204	Quantifying defects in graphene via Raman spectroscopy at different excitation energies. 2011 , 11, 3190-6	2228
2203	New directions in science and technology: two-dimensional crystals. 2011 , 74, 082501	185
2202	Electronic Transport in Graphene Heterostructures. 2011 , 2, 101-120	65
2201	Transport in graphene nanostructures. 2011 , 6, 271-293	55
2200	Hunting for monolayer boron nitride: optical and Raman signatures. 2011 , 7, 465-8	791
2199	Atomically thin mica flakes and their application as ultrathin insulating substrates for graphene. 2011 , 7, 2491-7	62
2198	High-performance graphene devices on SiO / Si substrate modified by highly ordered self-assembled monolayers. 2011 , 23, 2464-8	93
2197	"Chemical blowing" of thin-walled bubbles: high-throughput fabrication of large-area, few-layered BN and C(x) -BN nanosheets. 2011 , 23, 4072-6	184
2196	Site-specific transfer-printing of individual graphene microscale patterns to arbitrary surfaces. 2011 , 23, 3938-43	50
	, 25, 5956-45	
2195	Zufallswege zum Graphen (Nobel-Aufsatz). 2011 , 123, 7100-7122	21

2193	Fortschritte bei Ammoniak-Boran: verbessertes Recycling und Einsatz als Vorstufe fil BN-Einzelschichten. 2011 , 123, 10470-10472	12
2192	Random walk to graphene (Nobel lecture). 2011 , 50, 6966-85	118
2191	Graphene: materials in the Flatland (Nobel lecture). 2011 , 50, 6986-7002	133
2190	Advances with ammonia-borane: improved recycling and use as a precursor to atomically thin BN films. 2011 , 50, 10288-9	48
2189	Direct growth of few layer graphene on hexagonal boron nitride by chemical vapor deposition. 2011 , 49, 2522-2525	125
2188	Quantum inductance and high frequency oscillators in graphene nanoribbons. 2011 , 22, 165203	12
2187	Raman spectra of graphene exfoliated on insulating crystalline substrates. 2011 , 13, 063018	19
2186	Characteristics of CVD graphene nanoribbon formed by a ZnO nanowire hardmask. 2011 , 22, 295201	26
2185	Optical and transport gaps in gated bilayer graphene. 2011 , 84,	15
2184	Dielectric capping effects on binary and ternary topological insulator surface states. 2011 , 84,	5
2184	Dielectric capping effects on binary and ternary topological insulator surface states. 2011 , 84, A transfer technique for high mobility graphene devices on commercially available hexagonal boron nitride. 2011 , 99, 232104	271
	A transfer technique for high mobility graphene devices on commercially available hexagonal	
2183	A transfer technique for high mobility graphene devices on commercially available hexagonal boron nitride. 2011 , 99, 232104 Magneto-optical Faraday and Kerr effects in topological insulator films and in other layered	271
2183 2182 2181	A transfer technique for high mobility graphene devices on commercially available hexagonal boron nitride. 2011, 99, 232104 Magneto-optical Faraday and Kerr effects in topological insulator films and in other layered quantized Hall systems. 2011, 84,	271 125
2183 2182 2181	A transfer technique for high mobility graphene devices on commercially available hexagonal boron nitride. 2011, 99, 232104 Magneto-optical Faraday and Kerr effects in topological insulator films and in other layered quantized Hall systems. 2011, 84, Transport scattering time probed through rf admittance of a graphene capacitor. 2011, 83,	271 125 27
2183 2182 2181 2180	A transfer technique for high mobility graphene devices on commercially available hexagonal boron nitride. 2011, 99, 232104 Magneto-optical Faraday and Kerr effects in topological insulator films and in other layered quantized Hall systems. 2011, 84, Transport scattering time probed through rf admittance of a graphene capacitor. 2011, 83, Vertical field-effect transistor based on wave-function extension. 2011, 84,	2711252722
2183 2182 2181 2180	A transfer technique for high mobility graphene devices on commercially available hexagonal boron nitride. 2011, 99, 232104 Magneto-optical Faraday and Kerr effects in topological insulator films and in other layered quantized Hall systems. 2011, 84, Transport scattering time probed through rf admittance of a graphene capacitor. 2011, 83, Vertical field-effect transistor based on wave-function extension. 2011, 84, Enhanced thermal conductivity and isotope effect in single-layer hexagonal boron nitride. 2011, 84,	271 125 27 22 290

(2012-2011)

2175	graphene. 2011 , 107, 155502	41
2174	Effect of interlayer bare tunneling on electron-hole coherence in graphene bilayers. 2011 , 84,	15
2173	Carrier-induced antiferromagnet of graphene islands embedded in hexagonal boron nitride. 2011 , 84,	69
2172	Fabrication and performance of graphene nanoelectromechanical systems. 2011 , 29, 050801	44
2171	Magnetic moments and Kondo effect near vacancies and resonant scatterers in graphene. 2011, 83,	33
2170	Carrier transport mechanism in graphene on SiC(0001). 2011 , 84,	77
2169	Transport through graphene on SrTiO3. 2011 , 107, 225501	73
2168	Ni(111) graphene h-BN junctions as ideal spin injectors. 2011 , 84,	63
2167	Robust one-dimensional wires in lattice mismatched bilayer graphene. 2011 , 98, 251902	13
2166	Electron tunneling through atomically flat and ultrathin hexagonal boron nitride. 2011, 99, 243114	348
2166 2165	Electron tunneling through atomically flat and ultrathin hexagonal boron nitride. 2011 , 99, 243114 Hexagonal Boron Nitride Nanowalls Synthesized by Unbalanced RF Magnetron Sputtering. 2011 , 1307, 1	348
2165	Hexagonal Boron Nitride Nanowalls Synthesized by Unbalanced RF Magnetron Sputtering. 2011 ,	348
2165	Hexagonal Boron Nitride Nanowalls Synthesized by Unbalanced RF Magnetron Sputtering. 2011 , 1307, 1 UV-LIGHT-ASSISTED OXIDATIVE sp3 HYBRIDIZATION OF GRAPHENE. 2011 , 06, 409-418	
2165 2164	Hexagonal Boron Nitride Nanowalls Synthesized by Unbalanced RF Magnetron Sputtering. 2011 , 1307, 1 UV-LIGHT-ASSISTED OXIDATIVE sp3 HYBRIDIZATION OF GRAPHENE. 2011 , 06, 409-418	36
2165 2164 2163 2162	Hexagonal Boron Nitride Nanowalls Synthesized by Unbalanced RF Magnetron Sputtering. 2011, 1307, 1 UV-LIGHT-ASSISTED OXIDATIVE sp3 HYBRIDIZATION OF GRAPHENE. 2011, 06, 409-418 GRAPHENE: MATERIALS IN THE FLATLAND. 2011, 25, 4081-4106 Chemical vapor deposition-assembled graphene field-effect transistor on hexagonal boron nitride.	36 19
2165 2164 2163 2162 2161	Hexagonal Boron Nitride Nanowalls Synthesized by Unbalanced RF Magnetron Sputtering. 2011, 1307, 1 UV-LIGHT-ASSISTED OXIDATIVE sp3 HYBRIDIZATION OF GRAPHENE. 2011, 06, 409-418 GRAPHENE: MATERIALS IN THE FLATLAND. 2011, 25, 4081-4106 Chemical vapor deposition-assembled graphene field-effect transistor on hexagonal boron nitride. 2011, 98, 262103	36 19 48
2165 2164 2163 2162 2161	Hexagonal Boron Nitride Nanowalls Synthesized by Unbalanced RF Magnetron Sputtering. 2011, 1307, 1 UV-LIGHT-ASSISTED OXIDATIVE sp3 HYBRIDIZATION OF GRAPHENE. 2011, 06, 409-418 GRAPHENE: MATERIALS IN THE FLATLAND. 2011, 25, 4081-4106 Chemical vapor deposition-assembled graphene field-effect transistor on hexagonal boron nitride. 2011, 98, 262103 Theory of Coulomb drag for massless Dirac fermions. 2012, 14, 063033	36 19 48 40

2157 SEMICONDUCTING GRAPHENE. 2012 , 02, 1230009	5
Tunable Magnetic Properties of Rhombohedral Graphite Thin Films: Effects of Insulating Substrate on Magnetic Properties. 2012 , 51, 02BN04	
2155 Electronic Structure Modulation of Graphene by Metal Electrodes. 2012 , 51, 085102	2
Advancing quasi-freestanding epitaxial graphene electronics through integration of wafer scale hexagonal boron nitride dielectrics. 2012 ,	
Density functional studies of the defect-induced electronic structure modifications in bilayer boronitrene. 2012 , 367, 012004	0
2152 Magnetoresistance of Bilayer Graphene in Parallel Magnetic Fields. 2012 , 81, 013702	4
2151 Scanning tunneling microscopy with InAs nanowire tips. 2012 , 101, 243101	4
2150 Reactive-ion-etched graphene nanoribbons on a hexagonal boron nitride substrate. 2012 , 101, 203103	40
2149 Multiple Dirac fermions from a topological insulator and graphene superlattice. 2012 , 85,	10
2148 Effect of carrier mobility on magnetothermoelectric transport properties of graphene. 2012 , 86,	19
2147 Mechanism of near-field Raman enhancement in two-dimensional systems. 2012 , 85,	46
2146 Renormalization-group potential for quantum Hall effects. 2012 , 85,	3
2145 Band-edge transitions in hexagonal boron nitride epilayers. 2012 , 101, 051110	42
Kinetic theory of Coulomb drag in two monolayers of graphene: From the Dirac point to the Fermi liquid regime. 2012 , 86,	13
Nonlinear resistivity and heat dissipation in monolayer graphene. 2012 , 85,	34
2142 Unraveling the acoustic electron-phonon interaction in graphene. 2012 , 85,	91
2141 Screening and collective modes in gapped bilayer graphene. 2012 , 86,	20
Hexagonal boron nitride intercalated multi-layer graphene: a possible ultimate solution to ultra-scaled interconnect technology. 2012 , 2, 012191	12

(2012-2012)

2139	The integration of high-k dielectric on two-dimensional crystals by atomic layer deposition. 2012 , 100, 152115	111
2138	The role of substrate for transport in graphene. 2012 ,	3
2137	Density fluctuation effects on the exciton condensate in double-layer graphene. 2012, 86,	15
2136	Phonon engineering in nanostructures: Controlling interfacial thermal resistance in multilayer-graphene/dielectric heterojunctions. 2012 , 101, 113111	45
2135	Ultrasensitive and Wide-Bandwidth Thermal Measurements of Graphene at Low Temperatures. 2012 , 2,	48
2134	Atomic-scale transport in epitaxial graphene. 2011 , 11, 114-9	149
2133	Transconductance fluctuations as a probe for interaction-induced quantum Hall states in graphene. 2012 , 109, 056602	29
2132	Epitaxial growth and demonstration of hexagonal BN/AlGaN p-n junctions for deep ultraviolet photonics. 2012 , 100, 061121	76
2131	High-temperature behavior of supported graphene: Electron-phonon coupling and substrate-induced doping. 2012 , 86,	28
2130	Field-induced quantum Hall ferromagnetism in suspended bilayer graphene. 2012 , 85,	24
2129	Tunneling spectroscopy of graphene-boron-nitride heterostructures. 2012, 85,	64
2128	Substrate-induced chiral states in graphene. 2012 , 86,	35
2127	Single-particle tunneling in doped graphene-insulator-graphene junctions. 2012, 111, 043711	126
2126	Exploring carrier transport phenomena in a CVD-assembled graphene FET on hexagonal boron nitride. 2012 , 23, 125706	24
2125	Graphene for future electronics. 2012 , T146, 014025	28
2124	Graphene quilts for thermal management of high-power GaN transistors. 2012 , 3, 827	369
2123	Annealing Temperature and Substrate Effects on the Raman Spectra of Transferred CVD Graphene. 2012 , 1407, 93	
2122	CVD-Graphene Complementary Logic on Ultra-thin Multilayer Hexagonal Boron Nitride. 2012 , 1407, 151	

2121 Low-voltage graphene transistors based on self-assembled monolayer nanodielectrics. **2012**, 1451, 179-184

2120 E	Experimental Review of Graphene. 2012 , 2012, 1-56	303
2119 E	Electronic Properties of Graphene/h-BN Bilayer Superlattices. 2012 , 81, 103701	13
2118	Semiconducting hexagonal boron nitride for deep ultraviolet photonics. 2012,	9
2117	Development of superconducting interference device based on graphene. 2012 , 400, 042064	2
	Fabrication of graphene/polypyrrole nanotube/MnO2nanotube composite and its supercapacitor application. 2012 , 58, 30403	14
2115	Theoretical aspects of the fractional quantum Hall effect in graphene. 2012 , T146, 014017	6
2771	Surface Potential Variations in Graphene Induced by Nanostructured Crystalline Ionic Substrates. 2012 , 5, 045103	1
2113	Diamagnetism of Graphene with Gap in Nonuniform Magnetic Field. 2012 , 81, 024702	12
2112 [Defects and doping and their role in functionalizing graphene. 2012 , 37, 1187-1194	56
2111	Science and Engineering Beyond Moore's Law. 2012 , 100, 1720-1749	160
	Suppression of short-range scattering via hydrophobic substrates and the fractional quantum Hall effect in graphene. 2012 , 6, 376-378	2
2109 (Graphene plasmonics. 2012 , 6, 749-758	2152
	Electronics and optoelectronics of two-dimensional transition metal dichalcogenides. <i>Nature</i> Nanotechnology, 2012 , 7, 699-712	10871
2107 (Graphene-GaAs/AlxGa1⊠As heterostructure dual-function field-effect transistor. 2012 , 101, 202104	16
	A stable "flat" form of two-dimensional crystals: could graphene, silicene, germanene be minigap semiconductors?. 2012 , 12, 1045-52	160
2105	Thermal and Thermoelectric Transport in Nanostructures and Low-Dimensional Systems. 2012 , 16, 79-116	108
2104 E	Electronic Transport in Graphene. 2012 , 17-49	

2103 Ultrathin oxide films by atomic layer deposition on graphene. 2012 , 12, 3706-10	66
2102 Encyclopedia of Nanotechnology. 2012 , 968-978	
Quasi-periodic nanoripples in graphene grown by chemical vapor deposition and its impact on charge transport. 2012 , 6, 1158-64	111
Optical properties of bulk semiconductors and graphene/boron nitride: The Bethe-Salpeter equation with derivative discontinuity-corrected density functional energies. 2012 , 86,	40
2099 Quantum dots at room temperature carved out from few-layer graphene. 2012 , 12, 6096-100	67
2098 Transport in Graphene: Studying Layers of BN, SiC, and SiO2. 2012 , 6, 18-25	2
2097 Graphene applications in electronics and photonics. 2012 , 37, 1225-1234	144
2096 Thickness identification of two-dimensional materials by optical imaging. 2012 , 23, 495713	77
2095 Contact-induced spin polarization in graphene/h-BN/Ni nanocomposites. 2012 , 112, 114303	17
2094 Modeling of a vertical tunneling graphene heterojunction field-effect transistor. 2012 , 101, 033503	38
2093 Charges driving under the influence. 2012 , 8, 862-863	2
2092 Graphene field-effect transistors as room-temperature terahertz detectors. 2012 , 11, 865-71	725
2091 Toward the synthesis of wafer-scale single-crystal graphene on copper foils. 2012 , 6, 9110-7	488
High quality 2D crystals made by anodic bonding: a general technique for layered materials. 2012 , 23, 505709	36
Hexagonal boron nitride nanowalls: physical vapour deposition, 2D/3D morphology and spectroscopic analysis. 2012 , 45, 135302	19
$_{20}88$ Morphology dependence of radial elasticity in multiwalled boron nitride nanotubes. 2012 , 101, 10310)9 10
Electronic structure and quantum transport properties of trilayers formed from graphene and boron nitride. 2012 , 4, 5490-8	52
Electronic and Quantum Transport Properties of Heterobilayers of Graphene Nanoribbons and Zinc-Porphyrin Tapes. 2012 , 116, 8167-8173	4

2085	Encapsulating graphene by ultra-thin alumina for reducing process contaminations. 2012 , 249, 2526-2529	2
2084	Transport behaviors of graphene 2D field-effect transistors on boron nitride substrate. 2012 ,	1
2083	Anomalous insulator-metal transition in boron nitride-graphene hybrid atomic layers. 2012, 86,	41
2082	Nonlinear Dinear Transition of Magnetoelectric Effect in Magnetic Graphene Nanoflakes on Substrates. 2012 , 116, 626-631	12
2081	Transport in graphene on BN and SiC. 2012 ,	6
2080	Transport in graphene on boron nitride. 2012,	1
2079	System-level performance optimization and benchmarking for on-chip graphene interconnects. 2012 ,	3
2078	Growth selectivity of hexagonal-boron nitride layers on Ni with various crystal orientations. 2012 , 2, 111-115	66
2077	Anomalous energy-gap behaviour of armchair BC3 ribbons due to enhanced Econjugation. 2012 , 22, 20881	10
2076	Self-Assembly of Cobalt-Phthalocyanine Molecules on Epitaxial Graphene on Ir(111). 2012 , 116, 20433-20437	67
2075	Performance and Energy-per-Bit Modeling of Multilayer Graphene Nanoribbon Conductors. 2012 , 59, 2753-2761	64
2074	Cross-sectional imaging of individual layers and buried interfaces of graphene-based heterostructures and superlattices. 2012 , 11, 764-7	664
2073	Magnetic behavior and clustering effects in Mn-doped boron nitride sheets. 2012 , 24, 326003, 1-7	4
2072	Strained silicon nanowire array MOSFETs with high-k/metal gate stack. 2012 ,	1
2071	Electronic transport at monolayer-bilayer junctions in epitaxial graphene on SiC. 2012, 86,	79
2070	Origin of the relatively low transport mobility of graphene grown through chemical vapor deposition. 2012 , 2, 337	148
2069	Synthesis and characterization of hexagonal boron nitride film as a dielectric layer for graphene devices. 2012 , 6, 8583-90	388
2068	Effective cleaning of hexagonal boron nitride for graphene devices. 2012 , 12, 4449-54	92

2067 Photon-Assisted CVD Growth of Graphene Using Metal Adatoms As Catalysts. 2012 , 116, 18263-18269	3
2066 Biaxial compressive strain engineering in graphene/boron nitride heterostructures. 2012 , 2, 893	101
2065 Tunable magnetic states in hexagonal boron nitride sheets. 2012 , 101, 132405	25
2064 Graphite and Hexagonal Boron-Nitride have the Same Interlayer Distance. Why?. 2012 , 8, 1360-9	208
Establishing the Role of Graphite as a Shaping Agent of Vanadium Aluminum Mixed (Hydr)oxides and Their Physicochemical Properties and Catalytic Functionalities. 2012 , 2, 322-336	15
2062 The influence of substrate in determining the band gap of metallic carbon nanotubes. 2012 , 12, 4843-7	24
High-resolution x-ray absorption studies of core excitons in hexagonal boron nitride. 2012 , 101, 191604	13
2060 Long-wavelength local density of states oscillations near graphene step edges. 2012 , 108, 016801	32
Stamp transferred suspended graphene mechanical resonators for radio frequency electrical readout. 2012 , 12, 198-202	99
2058 Graphene based heterostructures. 2012 , 152, 1275-1282	158
2058 Graphene based heterostructures. 2012, 152, 1275-1282 2057 Quantum transport in double-gated graphene devices. 2012, 152, 1301-1305	158 16
2057 Quantum transport in double-gated graphene devices. 2012 , 152, 1301-1305	16
Quantum transport in double-gated graphene devices. 2012 , 152, 1301-1305 2056 Issues with characterizing transport properties of graphene field effect transistors. 2012 , 152, 1311-1316	16 16
Quantum transport in double-gated graphene devices. 2012 , 152, 1301-1305 2056 Issues with characterizing transport properties of graphene field effect transistors. 2012 , 152, 1311-1316 2055 Integrating functional oxides with graphene. 2012 , 152, 1365-1374 Large-area graphene synthesis and its application to interface-engineered field effect transistors.	16 16 37
Quantum transport in double-gated graphene devices. 2012, 152, 1301-1305 2056 Issues with characterizing transport properties of graphene field effect transistors. 2012, 152, 1311-1316 2055 Integrating functional oxides with graphene. 2012, 152, 1365-1374 Large-area graphene synthesis and its application to interface-engineered field effect transistors. 2012, 152, 1350-1358	16 16 37 26
2057 Quantum transport in double-gated graphene devices. 2012, 152, 1301-1305 2056 Issues with characterizing transport properties of graphene field effect transistors. 2012, 152, 1311-1316 2055 Integrating functional oxides with graphene. 2012, 152, 1365-1374 2054 Large-area graphene synthesis and its application to interface-engineered field effect transistors. 2012, 152, 1350-1358 2053 Graphene on SrTiO3. 2012, 152, 1795-1799	16 16 37 26

2049	Understanding and controlling the substrate effect on graphene electron-transfer chemistry via reactivity imprint lithography. 2012 , 4, 724-32	407
2048	Probing charge scattering mechanisms in suspended graphene by varying its dielectric environment. 2012 , 3, 734	103
2047	Chemical vapor deposition-derived graphene with electrical performance of exfoliated graphene. 2012 , 12, 2751-6	321
2046	Advances in 2D boron nitride nanostructures: nanosheets, nanoribbons, nanomeshes, and hybrids with graphene. 2012 , 4, 6908-39	611
2045	How close can one approach the Dirac point in graphene experimentally?. 2012, 12, 4629-34	136
2044	Transfer-free electrical insulation of epitaxial graphene from its metal substrate. 2012 , 12, 4503-7	105
2043	Dual-gated bilayer graphene hot-electron bolometer. <i>Nature Nanotechnology</i> , 2012 , 7, 472-8 28.7	335
2042	Interaction-enhanced coherence between two-dimensional Dirac layers. 2012 , 85,	58
2041	Condensation of electron-hole pairs in a two-layer graphene system: Correlation effects. 2012, 86,	66
2040	All graphene-based thin film transistors on flexible plastic substrates. 2012 , 12, 3472-6	198
2039	A facile route to recover intrinsic graphene over large scale. 2012 , 6, 7781-8	68
2038	A roadmap for graphene. 2012 , 490, 192-200	6640
2037	Ab initio studies of electronic and optical properties of graphene and grapheneBN interface. 2012 , 258, 8338-8342	26
2036	Strong enhancement of light-matter interaction in graphene coupled to a photonic crystal nanocavity. 2012 , 12, 5626-31	204
2035	Renormalization of the graphene dispersion velocity determined from scanning tunneling spectroscopy. 2012 , 109, 116802	73
2034	Graphene: an emerging electronic material. 2012 , 24, 5782-825	603
2033	Electronic and transport properties of a biased multilayer hexagonal boron nitride. 2012 , 85, 1	10
2032	Graphene bilayer structures with superfluid magnetoexcitons. 2012 , 7, 145	15

2031 Laser induced non-thermal deposition of ultrathin graphite. 2012 , 100, 151606	14
2030 Mapping Dirac quasiparticles near a single Coulomb impurity on graphene. 2012 , 8, 653-657	99
2029 Planar tunneling measurements of the energy gap in biased bilayer graphene. 2012 , 112, 094510	
2028 Integer quantum Hall effect in gapped single-layer graphene. 2012 , 86,	25
2027 Graphene plasmon waveguiding and hybridization in individual and paired nanoribbons. 2012 , 6, 431	1-40 564
2026 Step like surface potential on few layered graphene oxide. 2012 , 101, 263109	17
Anomalous response of supported few-layer hexagonal boron nitride to DC electric fields: a confined water effect?. 2012 , 23, 175703	15
Quantum Hall effect, screening, and layer-polarized insulating states in twisted bilayer graphene. 2012 , 108, 076601	107
2023 Understanding Graphene via Raman Scattering. 2012 , 49-90	3
2022 Transport through graphene quantum dots. 2012 , 75, 126502	114
Transport through graphene quantum dots. 2012 , 75, 126502 2021 Gate-controllable negative differential conductance in graphene tunneling transistors. 2012 , 27, 105	<u> </u>
2021 Gate-controllable negative differential conductance in graphene tunneling transistors. 2012 , 27, 105	5018 13
Gate-controllable negative differential conductance in graphene tunneling transistors. 2012 , 27, 105 2020 Field-effect tunneling transistor based on vertical graphene heterostructures. 2012 , 335, 947-50	5018 13 1991
Gate-controllable negative differential conductance in graphene tunneling transistors. 2012, 27, 105 2020 Field-effect tunneling transistor based on vertical graphene heterostructures. 2012, 335, 947-50 Theory of interfacial plasmon-phonon scattering in supported graphene. 2012, 86, Mobility enhancement and highly efficient gating of monolayer MoS2transistors with polymer	5018 13 1991 56
Gate-controllable negative differential conductance in graphene tunneling transistors. 2012, 27, 105 2020 Field-effect tunneling transistor based on vertical graphene heterostructures. 2012, 335, 947-50 2019 Theory of interfacial plasmon-phonon scattering in supported graphene. 2012, 86, 2018 Mobility enhancement and highly efficient gating of monolayer MoS2transistors with polymer electrolyte. 2012, 45, 345102 Nanoscale electron diffraction and plasmon spectroscopy of single- and few-layer boron nitride.	5018 13 1991 56 118
Gate-controllable negative differential conductance in graphene tunneling transistors. 2012, 27, 105 2020 Field-effect tunneling transistor based on vertical graphene heterostructures. 2012, 335, 947-50 2019 Theory of interfacial plasmon-phonon scattering in supported graphene. 2012, 86, 2018 Mobility enhancement and highly efficient gating of monolayer MoS2transistors with polymer electrolyte. 2012, 45, 345102 Nanoscale electron diffraction and plasmon spectroscopy of single- and few-layer boron nitride. 2012, 85, Ab initio and semi-empirical van der Waals study of graphene-boron nitride interaction from a	5018 13 1991 56 118 41

2013 Graphene and Carbon Nanotube Applications in Mobile Devices. 2012 , 59, 2876-2887	12
Graphene on incommensurate substrates: Trigonal warping and emerging Dirac cone replicas with halved group velocity. 2012 , 86,	70
2011 Charge inhomogeneity determines oxidative reactivity of graphene on substrates. 2012 , 6, 8335-41	55
2010 Diamondization of chemically functionalized graphene and graphene-BN bilayers. 2012 , 14, 8179-84	48
2009 Production and processing of graphene and 2d crystals. 2012 , 15, 564-589	745
Self-assembly mechanisms of short atomic chains on single-layer graphene and boron nitride. 2012 , 86,	23
Solvent exfoliation of transition metal dichalcogenides: dispersibility of exfoliated nanosheets varies only weakly between compounds. 2012 , 6, 3468-80	535
2006 Graphene-based flexible and stretchable thin film transistors. 2012 , 4, 4870-82	125
2005 Graphene nanoelectronics: Overview from post-silicon perspective. 2012 ,	О
Strength, plasticity, interlayer interactions and phase transition of low-dimensional nanomaterials under multiple fields. 2012 , 25, 221-243	6
2003 Low-dimensional boron nitride nanomaterials. 2012 , 15, 256-265	297
2002 Graphene Electronics for RF Applications. 2012 , 13, 114-125	27
2001 A Newtonian approach to extraordinarily strong negative refraction. 2012 , 488, 65-9	30
Single-step exfoliation and chemical functionalisation of graphene and hBN nanosheets with nickel phthalocyanine. 2012 , 22, 23246	14
1999 Oxygen radical functionalization of boron nitride nanosheets. 2012 , 134, 18758-71	362
1998 Resonant tunnelling diodes based on graphene/h-BN heterostructure. 2012 , 45, 325104	51
1997 Phase coexistence of clusters and islands: europium on graphene. 2012 , 14, 023022	34
Dielectric strength, optical absorption, and deep ultraviolet detectors of hexagonal boron nitride epilayers. 2012 , 101, 171112	95

(2012-2012)

1995	Long-range atomic ordering and variable interlayer interactions in two overlapping graphene lattices with stacking misorientations. 2012 , 85,	26
1994	Identifying hexagonal boron nitride monolayers by transmission electron microscopy. 2012 , 18, 558-67	7
1993	Electrochemical properties comparison of the polypyrrole nanotube and polyaniline nanofiber applied in supercapacitor. 2012 , 57, 30702	16
1992	Ab initio study of energy-band modulation in graphene-based two-dimensional layered superlattices. 2012 , 22, 23821	17
1991	Long-distance spin transport in high-mobility graphene on hexagonal boron nitride. 2012 , 86,	164
1990	Cascading wafer-scale integrated graphene complementary inverters under ambient conditions. 2012 , 12, 3948-53	51
1989	Angle-dependent carrier transmission in graphene p-n junctions. 2012 , 12, 4460-4	57
1988	Two distinct phases of bilayer graphene films on Ru(0001). 2012 , 6, 9299-304	18
1987	Graphene and boron nitride lateral heterostructures for atomically thin circuitry. 2012, 488, 627-32	650
1986	Logic Inverter Implemented with CVD-Assembled Graphene FET on Hexagonal Boron Nitride. 2012 , 11, 619-623	9
1985	Effect of Dimensionality on the Photocatalytic Behavior of Carbon-Titania Nanosheet Composites: Charge Transfer at Nanomaterial Interfaces. 2012 , 3, 1760-5	163
1984	Les promesses du graphfie. 2012 , 100, 101-107	
1983	Implanted bottom gate for epitaxial graphene on silicon carbide. 2012 , 45, 154006	5
1982	Mechanical properties of freely suspended atomically thin dielectric layers of mica. 2012 , 5, 550-557	70
1981	Fermi velocity engineering in graphene by substrate modification. 2012 , 2,	269
1980	Electronic compressibility of layer-polarized bilayer graphene. 2012 , 85,	112
1979	Transport/magnetotransport of high-performance graphene transistors on organic molecule-functionalized substrates. 2012 , 12, 964-9	54
1978	Tunable and sizable band gap of single-layer graphene sandwiched between hexagonal boron nitride. 2012 , 4, e6-e6	140

1977	The electronic property of graphene adsorbed on the siloxane and silanol surface structures of SiO2: A theoretical prediction. 2012 , 101, 253107	6
1976	Why the Band Gap of Graphene Is Tunable on Hexagonal Boron Nitride. 2012 , 116, 3142-3146	88
1975	Large scale metal-free synthesis of graphene on sapphire and transfer-free device fabrication. 2012 , 4, 3050-4	103
1974	Liquid phase growth of graphene on silicon carbide. 2012 , 50, 5076-5084	14
1973	Magnetic states and optical properties of single-layer carbon-doped hexagonal boron nitride. 2012 , 100, 253115	58
1972	Precision quantization of Hall resistance in transferred graphene. 2012 , 100, 164106	25
1971	Mechanical cleaning of graphene. 2012 , 100, 073110	119
1970	Enhanced current-rectification in bilayer graphene with an electrically tuned sloped bandgap. 2012 , 4, 7842-6	12
1969	Unipolar transport in bilayer graphene controlled by multiple p-n interfaces. 2012 , 100, 163115	12
1968	Boron nitride on Cu(111): an electronically corrugated monolayer. 2012 , 12, 5821-8	168
1967	Spatially Resolved Compositional Analysis of a BCN Thin Film Grown on a Ni Substrate by Chemical Vapor Deposition. 2012 , 1451, 151-156	
1966	Negligible environmental sensitivity of graphene in a hexagonal boron nitride/graphene/h-BN sandwich structure. 2012 , 6, 9314-9	85
1965	Temperature dependence of the conductivity of graphene on boron nitride. 2012, 85,	31
1964	Coulomb drag in grapheneBoron nitride heterostructures: Effect of virtual phonon exchange. 2012 , 86,	17
1963	Growth of atomically thin hexagonal boron nitride films by diffusion through a metal film and precipitation. 2012 , 45, 385304	37
1962	Water-gated charge doping of graphene induced by mica substrates. 2012 , 12, 648-54	146
1961	Transport behaviors in graphene field effect transistors on boron nitride substrate. 2012,	1
1960	Toward the controlled synthesis of hexagonal boron nitride films. 2012 , 6, 6378-85	242

1959	Epitaxial Growth of Hexagonal Boron Nitride on Ir(111). 2012 , 116, 157-164	57
1958	Hybrid graphene/organic semiconductor field-effect transistors. 2012 , 101, 033309	28
1957	Cleaning graphene using atomic force microscope. 2012 , 111, 064904	51
1956	Graphene-based quantum Hall effect metrology. 2012 , 37, 1255-1264	10
1955	Impurity and edge roughness scattering in graphene nanoribbons: the Boltzmann approach. 2012 , 24, 455303	8
1954	Gate-defined confinement in bilayer graphene-hexagonal boron nitride hybrid devices. 2012 , 12, 4656-60	88
1953	Controlling the electrical behavior of semiconducting carbon nanotubes via tube contact. 2012 , 8, 220-4	7
1952	Investigating the mechanism of hysteresis effect in graphene electrical field device fabricated on SiOIsubstrates using Raman spectroscopy. 2012 , 8, 2833-40	101
1951	Ultra-thin and flat mica as gate dielectric layers. 2012 , 8, 2178-83	25
1950	Hybrid graphene-quantum dot phototransistors with ultrahigh gain. <i>Nature Nanotechnology</i> , 2012 , 7, 363-8	1588
1950 1949		1588 17
1949	7, 363-8 Tunable spin-orbit interaction in trilayer graphene exemplified in electric-double-layer transistors.	, in the second
1949	7, 363-8 Tunable spin-orbit interaction in trilayer graphene exemplified in electric-double-layer transistors. 2012, 12, 2212-6	17
1949	Tunable spin-orbit interaction in trilayer graphene exemplified in electric-double-layer transistors. 2012, 12, 2212-6 Deformation and scattering in graphene over substrate steps. 2012, 108, 096601 Spin and valley quantum Hall ferromagnetism in graphene. 2012, 8, 550-556	17 77
1949 1948 1947	Tunable spin-orbit interaction in trilayer graphene exemplified in electric-double-layer transistors. 2012, 12, 2212-6 Deformation and scattering in graphene over substrate steps. 2012, 108, 096601 Spin and valley quantum Hall ferromagnetism in graphene. 2012, 8, 550-556	17 77 255
1949 1948 1947 1946	Tunable spin-orbit interaction in trilayer graphene exemplified in electric-double-layer transistors. 2012, 12, 2212-6 Deformation and scattering in graphene over substrate steps. 2012, 108, 096601 Spin and valley quantum Hall ferromagnetism in graphene. 2012, 8, 550-556 Interplay between sublattice and spin symmetry breaking in graphene. 2012, 85, Integration of hexagonal boron nitride with quasi-freestanding epitaxial graphene: toward	17 77 255 25
1949 1948 1947 1946	Tunable spin-orbit interaction in trilayer graphene exemplified in electric-double-layer transistors. 2012, 12, 2212-6 Deformation and scattering in graphene over substrate steps. 2012, 108, 096601 Spin and valley quantum Hall ferromagnetism in graphene. 2012, 8, 550-556 Interplay between sublattice and spin symmetry breaking in graphene. 2012, 85, Integration of hexagonal boron nitride with quasi-freestanding epitaxial graphene: toward wafer-scale, high-performance devices. 2012, 6, 5234-41	17 77 255 25 104

1941	Optical coupling of surface plasmons between graphene sheets. 2012 , 100, 131111	260
1940	Double-layer graphene and topological insulator thin-film plasmons. 2012 , 85,	84
1939	Electron-Electron Interactions in Graphene: Current Status and Perspectives. 2012 , 84, 1067-1125	833
1938	Plasmons and near-field amplification in double-layer graphene. 2012 , 85,	89
1937	Structure and electronic transport in graphene wrinkles. 2012 , 12, 3431-6	463
1936	Towards Rationally Designed Graphene-Based Materials and Devices. 2012 , 213, 1091-1100	19
1935	van der Waals epitaxy of MoSilayers using graphene as growth templates. 2012 , 12, 2784-91	788
1934	Emergence of superlattice Dirac points in graphene on hexagonal boron nitride. 2012 , 8, 382-386	793
1933	Understanding surfactant/graphene interactions using a graphene field effect transistor: relating molecular structure to hysteresis and carrier mobility. 2012 , 28, 8579-86	46
1932	Laser-thinning of MoS⊡on demand generation of a single-layer semiconductor. 2012 , 12, 3187-92	471
1931	Hot electron cooling by acoustic phonons in graphene. 2012 , 109, 056805	108
1930	Large Variations of the Raman Signal in the Spectra of Twisted Bilayer Graphene on a BN Substrate. 2012 , 3, 796-9	30
1929	Comparison of microscopic models for disorder in bilayer graphene: Implications for density of states and optical conductivity. 2012 , 85,	7
1928	Engineering the electronic structure of graphene. 2012 , 24, 4055-69	99
1927	Binary and ternary atomic layers built from carbon, boron, and nitrogen. 2012 , 24, 4878-95	197
1926	Anisotropic photoresponse properties of single micrometer-sized GeSe nanosheet. 2012 , 24, 4528-33	196
1925	Synthesis of monolithic graphene-graphite integrated electronics. 2011 , 11, 120-5	192
1924	Large-scale synthesis of high-quality hexagonal boron nitride nanosheets for large-area graphene electronics. 2012 , 12, 714-8	444

1923	Preparation of High Concentration Dispersions of Exfoliated MoS2 with Increased Flake Size. 2012 , 24, 2414-2421	437
1922	Control of valley polarization in monolayer MoS2 by optical helicity. <i>Nature Nanotechnology</i> , 2012 , 7, 494-8	2670
1921	Tailoring electrical transport across grain boundaries in polycrystalline graphene. 2012 , 336, 1143-6	469
1920	Artificially stacked atomic layers: toward new van der Waals solids. 2012 , 12, 3518-25	187
1919	Graphene/metal contacts: bistable states and novel memory devices. 2012 , 24, 2614-9	30
1918	Quantum capacitance and density of states of graphene. 2012 , T146, 014009	23
1917	Nucleation and growth of single crystal graphene on hexagonal boron nitride. 2012, 50, 329-331	83
1916	Boron nitride substrate-induced reversible hydrogen storage in bilayer solid matrix via interlayer spacing. 2012 , 37, 9677-9687	11
1915	Graphene: synthesis and applications. 2012 , 15, 86-97	663
1914	Strain-tunable band gap in graphene/h-BN hetero-bilayer. 2012 , 73, 818-821	38
1913	Impact of calcium on transport property of graphene. 2012 , 152, 60-63	8
1912	Graphene growth on h-BN by molecular beam epitaxy. 2012 , 152, 975-978	86
1911	Stable forms of two-dimensional crystals and graphene. 2012 , 407, 1964-1968	4
1910	Scanning probe microscopy of graphene. 2012 , 44, 743-759	27
1909	Graphite flake self-retraction response based on potential seeking. 2012 , 7, 185	8
1908	Single-gate bandgap opening of bilayer graphene by dual molecular doping. 2012 , 24, 407-11	212
1907	Boron nitride growth on metal foil using solid sources. 2013 , 31, 041804	15
1906	Extremely confined terahertz surface plasmon-polaritons in graphene-metal structures. 2013 , 103, 071103	66

1905	Aharonov-Bohm effect and giant magnetoresistance in graphene nanoribbon rings. 2013, 88,	13
	Copper-vapor-assisted chemical vapor deposition for high-quality and metal-free single-layer graphene on amorphous SiO2 substrate. 2013 , 7, 6575-82	133
1903	Van der Waals heterostructures. 2013 , 499, 419-25	6627
1902	Magnetic-like field inducing negative Dirac mass in graphene on hexagonal boron nitride. 2013, 52, 70-76	3
1901	Direct imaging of charged impurity density in common graphene substrates. 2013 , 13, 3576-80	60
1900	3D graphene-Fe3O4 nanocomposites with high-performance microwave absorption. 2013 , 15, 13038-43	281
1899	Optical Third-Harmonic Generation in Graphene. 2013 , 3,	133
1898	Epitaxial growth of single-domain graphene on hexagonal boron nitride. 2013, 12, 792-7	745
1897	Spin filtering in graphene nanoribbons with Mn-doped boron nitride inclusions. 2013 , 178, 1347-1351	19
1896	Examining graphene field effect sensors for ferroelectric thin film studies. 2013 , 13, 4374-9	55
1895	Topological phase transition in a graphene system with a coexistence of Coulomb interaction, staggered potential, and intrinsic spin-orbit coupling. 2013 , 88,	9
1894	Short-range potential scattering and its effect on graphene mobility. 2013 , 12, 76-84	17
1893	Large current modulation and spin-dependent tunneling of vertical graphene/MoS2 heterostructures. 2013 , 7, 7021-7	80
1892	Excitation processes modeling in two-layer graphene. 2013,	1
	First-Principles Investigations of Metal (Cu, Ag, Au, Pt, Rh, Pd, Fe, Co, and Ir) Doped Hexagonal Boron Nitride Nanosheets: Stability and Catalysis of CO Oxidation. 2013 , 117, 17319-17326	246
1890	. 2013 , 101, 1766-1779	88
	Nonequilibrium dynamics of photoexcited electrons in graphene: Collinear scattering, Auger processes, and the impact of screening. 2013 , 88,	128
1888	Graphene interconnects fully encapsulated in layered insulator hexagonal boron nitride. 2013, 24, 355202	28

(2013-2013)

1887	Surface polar optical phonon scattering of carriers in graphene on various substrates. 2013 , 103, 081606	33
1886	Fabrication of large area hexagonal boron nitride thin films for bendable capacitors. 2013 , 6, 602-610	42
1885	Thickness dependent band gap and effective mass of BN/graphene/BN and graphene/BN/graphene heterostructures. 2013 , 610, 27-32	26
1884	. 2013 , 101, 1670-1688	25
1883	Fabrication and transfer of flexible few-layers MoS2 thin film transistors to any arbitrary substrate. 2013 , 7, 8809-15	158
1882	Topological classification of crystalline insulators with space group symmetry. 2013 , 88,	111
1881	Estimation of residual carrier density near the Dirac point in graphene through quantum capacitance measurement. 2013 , 102, 173507	33
1880	Graphene electronics for terahertz electron-beam radiation. 2013 , 24, 375205	15
1879	Ballistic interferences in suspended graphene. 2013 , 4, 2342	141
1878	Raman Spectroscopy. 2013 , 753-802	3
1878	Raman Spectroscopy. 2013 , 753-802 Tunable superlattice in graphene to control the number of Dirac points. 2013 , 13, 3990-5	3 57
1877		
1877	Tunable superlattice in graphene to control the number of Dirac points. 2013 , 13, 3990-5 Tuning the bandgap of exfoliated InSe nanosheets by quantum confinement. 2013 , 25, 5714-8	57
1877 1876	Tunable superlattice in graphene to control the number of Dirac points. 2013 , 13, 3990-5 Tuning the bandgap of exfoliated InSe nanosheets by quantum confinement. 2013 , 25, 5714-8	57 419
1877 1876 1875	Tunable superlattice in graphene to control the number of Dirac points. 2013, 13, 3990-5 Tuning the bandgap of exfoliated InSe nanosheets by quantum confinement. 2013, 25, 5714-8 Quantum Hall effect in gapped graphene heterojunctions. 2013, 88, Flexible and transparent MoS2 field-effect transistors on hexagonal boron nitride-graphene	57 419 13
1877 1876 1875 1874	Tuning the bandgap of exfoliated InSe nanosheets by quantum confinement. 2013, 25, 5714-8 Quantum Hall effect in gapped graphene heterojunctions. 2013, 88, Flexible and transparent MoS2 field-effect transistors on hexagonal boron nitride-graphene heterostructures. 2013, 7, 7931-6 Tunable doping and band gap of graphene on functionalized hexagonal boron nitride with	57 419 13 800
1877 1876 1875 1874	Tuning the bandgap of exfoliated InSe nanosheets by quantum confinement. 2013, 25, 5714-8 Quantum Hall effect in gapped graphene heterojunctions. 2013, 88, Flexible and transparent MoS2 field-effect transistors on hexagonal boron nitride-graphene heterostructures. 2013, 7, 7931-6 Tunable doping and band gap of graphene on functionalized hexagonal boron nitride with hydrogen and fluorine. 2013, 15, 5067-77	57 419 13 800 65

1869	Ballistic versus diffusive transport in graphene. 2013 , 88,		14
1868	Slow gold adatom diffusion on graphene: effect of silicon dioxide and hexagonal boron nitride substrates. 2013 , 117, 4305-12		28
1867	Step flow versus mosaic film growth in hexagonal boron nitride. 2013 , 135, 2368-73		72
1866	Vibration responses of h-BN sheet to charge doping and external strain. 2013 , 139, 214708		5
1865	Substrate engineering by hexagonal boron nitride/SiO2 for hysteresis-free graphene FETs and large-scale graphene p-n junctions. 2013 , 8, 2446-52		21
1864	Graphene nanoribbon based negative resistance device for ultra-low voltage digital logic applications. 2013 , 102, 043114		24
1863	High-quality multiterminal suspended graphene devices. 2013 , 13, 5165-70		23
1862	The effects of the crystalline orientation of Cu domains on the formation of nanoripple arrays in CVD-grown graphene on Cu. 2013 , 1, 7819		27
1861	Ultrathin high-temperature oxidation-resistant coatings of hexagonal boron nitride. 2013 , 4, 2541		418
1860	Giant quasiparticle bandgap modulation in graphene nanoribbons supported on weakly interacting surfaces. 2013 , 103, 133107		28
1859	High-surface area ceramic-derived boron-nitride and its hydrogen uptake properties. 2013 , 1, 1014-1017		23
1858	Deep Sub-Wavelength Multimode Tunable In-Plane Plasmonic Lenses Operating at Terahertz Frequencies. 2013 , 3, 550-557		9
1857	Suppression of thermally activated carrier transport in atomically thin MoS2 on crystalline hexagonal boron nitride substrates. 2013 , 5, 9572-6		60
1856	The thermal stability of graphene in air investigated by Raman spectroscopy. 2013 , 44, 1018-1021		155
1855	Mechanism of the effects of low temperature Al2O3 passivation on graphene field effect transistors. 2013 , 53, 182-187		41
1854	Bonding, stability, and electronic properties of the BC3 honeycomb monolayer structure on NbB2(0001). 2013 , 88,		12
1853	Graphene-MoS2 hybrid structures for multifunctional photoresponsive memory devices. <i>Nature Nanotechnology</i> , 2013 , 8, 826-30	8.7	1065
1852	Solvothermal-induced conversion of one-dimensional multilayer nanotubes to two-dimensional hydrophilic VOx nanosheets: synthesis and water treatment application. 2013 , 5, 10389-94		14

(2013-2013)

1851	Photovoltaic infrared photoresponse of the high-mobility graphene quantum Hall system due to cyclotron resonance. 2013 , 88,	13
1850	One-dimensional electrical contact to a two-dimensional material. 2013 , 342, 614-7	1676
1849	Pacific Ocean heat content during the past 10,000 years. 2013 , 342, 617-21	50
1848	h-BN monolayer on the Ni(111) surface: a potential catalyst for oxidation. 2013 , 5, 10404-8	37
1847	Electrical properties of scandium nitride epitaxial films grown on (100) magnesium oxide substrates by molecular beam epitaxy. 2013 , 114, 093704	25
1846	Ballistic-like supercurrent in suspended graphene Josephson weak links. 2013 , 4, 2716	68
1845	The role of surface oxygen in the growth of large single-crystal graphene on copper. 2013 , 342, 720-3	868
1844	Solid-source growth and atomic-scale characterization of graphene on Ag(111). 2013 , 4,	95
1843	Structure and electronic properties of Au intercalated hexagonal-boron-nitride/graphene bilayer. 2013 , 49, 111-116	8
1842	Dielectric screening of the Kohn anomaly of graphene on hexagonal boron nitride. 2013 , 88,	50
1841	Stability of graphitic-like zinc oxide layers under carriers doping: a first-principles study. 2013 , 5, 12111-4	9
1840	Controlled growth of atomically thin In2Se3 flakes by van der Waals epitaxy. 2013 , 135, 13274-7	156
1839	Intrinsic lifetime of Dirac plasmons in graphene. 2013 , 88,	57
1838	Epitaxial Growth and Electronic Properties of Large Hexagonal Graphene Domains on Cu(111) Thin Film. 2013 , 6, 075101	65
1837	A computational investigation of CO oxidation on ruthenium-embedded hexagonal boron nitride nanosheet. 2013 , 1011, 5-10	98
1836	Substrate-enhanced superconductivity in Li-decorated graphene. 2013 , 104, 47013	33
1835	Chiral superfluid States in hybrid graphene heterostructures. 2013 , 111, 086804	18
1834	Laminar MoS2 membranes for molecule separation. 2013 , 49, 10718-20	212

1833	Electron-electron interactions in bilayer graphene quantum dots. 2013, 88,	26
1832	First-principles identifications of superstructures of germanene on Ag(111) surface and h-BN substrate. 2013 , 15, 16853-63	49
1831	Continuous growth of hexagonal graphene and boron nitride in-plane heterostructures by atmospheric pressure chemical vapor deposition. 2013 , 7, 10129-38	156
1830	Electron-beam assisted growth of hexagonal boron-nitride layer. 2013 , 13, 1365-1369	7
1829	Helium ion microscopy of graphene: beam damage, image quality and edge contrast. 2013 , 24, 335702	65
1828	Mn atomic layers under inert covers of graphene and hexagonal boron nitride prepared on Rh(111). 2013 , 6, 887-896	21
1827	Field-effect transistors based on two-dimensional materials for logic applications. 2013 , 22, 098505	20
1826	Liquid Exfoliation of Layered Materials. 2013 , 340, 1226419-1226419	2604
1825	Structural, electronic, and optical properties of hybrid silicene and graphene nanocomposite. 2013 , 139, 154704	79
1824	Evolution of physical and electronic structures of bilayer graphene upon chemical functionalization. 2013 , 135, 18866-75	39
1823	Electron interactions and gap opening in graphene superlattices. 2013 , 111, 266801	116
1822	Generic miniband structure of graphene on a hexagonal substrate. 2013 , 87,	198
1821	Enhanced photodetection in graphene-integrated photonic crystal cavity. 2013 , 103, 241109	61
1820	Band-like transport in high mobility unencapsulated single-layer MoS2 transistors. 2013 , 102, 173107	316
1819	Stepwise Reduction of Immobilized Monolayer Graphene Oxides. 2013 , 25, 4839-4848	12
1818	Synthesis of few-to-monolayer graphene on rutile titanium dioxide. 2013 , 55, 168-175	17
1817	Doping mechanisms in graphene-MoS2 hybrids. 2013 , 103, 251607	95
1816	Multiscale modeling of screening effects on conductivity of graphene in weakly bonded graphene-dielectric heterostructures. 2013 , 12, 722-729	1

1815	Synthesis of highly crystalline sp2-bonded boron nitride aerogels. 2013 , 7, 8540-6	79
1814	Chip-integrated ultrafast graphene photodetector with high responsivity. 2013 , 7, 883-887	768
1813	Isolation of high quality graphene from Ru by solution phase intercalation. 2013 , 103, 121602	19
1812	2D layered insulator hexagonal boron nitride enabled surface passivation in dye sensitized solar cells. 2013 , 5, 11275-82	40
1811	Two-dimensional transition metal honeycomb realized: Hf on Ir(111). 2013, 13, 4671-4	89
1810	A first-principles study on the effect of biaxial strain on the ultimate performance of monolayer MoS2-based double gate field effect transistor. 2013 , 113, 163708	47
1809	Eigenfrequencies of the randomly pinned drum and conductivity of graphene. 2013, 88,	3
1808	Realization of graphene field-effect transistor with high-IHCa2Nb3O10 nanoflake as top-gate dielectric. 2013 , 103, 023113	10
1807	Etched graphene quantum dots on hexagonal boron nitride. 2013 , 103, 073113	37
1806	Energy levels of exciton in a gapped graphene sheet. 2013 , 114, 073702	5
1805	Graphene based field effect transistors: Efforts made towards flexible electronics. 2013 , 89, 177-188	68
1804	Batch-fabricated high-performance graphene Hall elements. 2013 , 3, 1207	61
1803	Interface between Graphene and SrTiO3(001) Investigated by Scanning Tunneling Microscopy and Photoemission. 2013 , 117, 21006-21013	13
1802	Optically active heterostructures of graphene and ultrathin MoS2. 2013 , 175-176, 35-42	35
1801	Electronic structural Moir[pattern effects on MoS2/MoSe2 2D heterostructures. 2013 , 13, 5485-90	255
1800	Three-Dimensional Graphene Nano-Networks with High Quality and Mass Production Capability via Precursor-Assisted Chemical Vapor Deposition. 2013 , 3,	115
1799	Low Temperature Graphene Synthesis from Poly(methyl methacrylate) Using Microwave Plasma Treatment. 2013 , 6, 115102	11
1798	Rapid-thermal-annealing surface treatment for restoring the intrinsic properties of graphene field-effect transistors. 2013 , 24, 405301	49

1797	Improving chemical vapor deposition graphene conductivity using molybdenum trioxide: An in-situ field effect transistor study. 2013 , 103, 263117	25
1796	Substrate surface corrugation effects on the electronic transport in graphene nanoribbons. 2013 , 103, 143506	15
1795	Suspended single-layer MoS2 devices. 2013 , 114, 164509	51
1794	Gate dependent Raman spectroscopy of graphene on hexagonal boron nitride. 2013 , 25, 505304	8
1793	The distorted K1 soft mode of hexagonal-BN sheet and effects of charge doping. 2013 , 103, 183106	8
1792	Infrared absorption by graphenelBN heterostructures. 2013 , 15, 123009	26
1791	Dielectric environment effect on carrier mobility of graphene double-layer structure. 2013 , 103, 033102	14
1790	Quantitative determination of scattering mechanism in large-area graphene on conventional and SAM-functionalized substrates at room temperature. 2013 , 5, 5784-93	24
1789	Inductively heated synthesized graphene with record transistor mobility on oxidized silicon substrates at room temperature. 2013 , 103, 183115	19
1788	Indirect exchange interaction between magnetic adatoms in monolayer MoS2. 2013, 87,	38
1787	Optical properties of boron nitride single crystals. 2013,	
1786	2D electronics: Graphene and beyond. 2013 ,	15
1785	High-contrast electrooptic modulation of a photonic crystal nanocavity by electrical gating of graphene. 2013 , 13, 691-6	151
1784	Growth of a two-dimensional dielectric monolayer on quasi-freestanding graphene. <i>Nature</i> Nanotechnology, 2013 , 8, 41-5	78
1783	Applications of Graphene. 2013 , 333-437	6
1782	Properties of Graphene. 2013 , 61-127	5
1781	Characterisation Techniques. 2013 , 229-332	5
1780	Supercollision cooling in undoped graphene. 2013 , 9, 109-112	149

(2013-2013)

1779	Graphene-like two-dimensional materials. 2013 , 113, 3766-98		3191
1778	Disordered graphene and boron nitride in a microwave tight-binding analog. 2013 , 87,		25
1777	Ab initio optical study of graphene on hexagonal boron nitride and fluorographene substrates. 2013 , 1, 1618		35
1776	Scalable synthesis of uniform few-layer hexagonal boron nitride dielectric films. 2013 , 13, 276-81		149
1775	Fabrication, optimization, and use of graphene field effect sensors. 2013 , 85, 509-21		84
1774	Vertical field-effect transistor based on graphene-WS2 heterostructures for flexible and transparent electronics. <i>Nature Nanotechnology</i> , 2013 , 8, 100-3	3.7	1342
1773	Carbon nanomaterials for electronics, optoelectronics, photovoltaics, and sensing. 2013 , 42, 2824-60		941
1772	Electrically tunable transverse magnetic focusing in graphene. 2013, 9, 225-229		123
1771	Vertically stacked multi-heterostructures of layered materials for logic transistors and complementary inverters. 2013 , 12, 246-52		705
1770	Tunable transport gap in narrow bilayer graphene nanoribbons. 2013 , 3, 1248		41
1769	Monolayer graphene/hexagonal boron nitride heterostructure. 2013 , 54, 396-402		49
1768	Preparation of a boron nitride single layer on a polycrystalline Rh surface. 2013 , 264, 838-844		6
1767	Plasmons and their interaction with electrons in trilayer graphene. 2013 , 88,		4
1766	Measurement of the Electronic Thermal Conductance Channels and Heat Capacity of Graphene at Low Temperature. 2013 , 3,		40
1765	Resonant and nondissipative tunneling in independently contacted graphene structures. 2013, 87,		31
1764	Molecular beam epitaxial growth of graphene using cracked ethylene. 2013 , 378, 404-409		2
1763	Hydrazine-based n-type doping process to modulate Dirac point of graphene and its application to complementary inverter. 2013 , 14, 1586-1590		23
1762	. 2013 , 117, 4800-4807		22

1761	Pseudosaturation and Negative Differential Conductance in Graphene Field-Effect Transistors. 2013 , 60, 985-991	20	
1760	Exfoliation of hexagonal boron nitride by molten hydroxides. 2013 , 25, 2200-4	218	
1759	Two-stage metal-catalyst-free growth of high-quality polycrystalline graphene films on silicon nitride substrates. 2013 , 25, 992-7	99	
1758	Increased mobility for layer-by-layer transferred chemical vapor deposited graphene/boron-nitride thin films. 2013 , 102, 103115	19	
1757	Spatially resolved photocurrents in graphene nanoribbon devices. 2013 , 102, 043106	14	
1756	Understanding the catalyst-free transformation of amorphous carbon into graphene by current-induced annealing. 2013 , 3,	72	
1755	Nonvolatile memory cells based on MoS2/graphene heterostructures. 2013 , 7, 3246-52	762	
1754	A review of carbon nanotube- and graphene-based flexible thin-film transistors. 2013 , 9, 1188-205	237	
1753	Graphene: promises, facts, opportunities, and challenges in nanomedicine. 2013 , 113, 3407-24	563	
1752	Influence of extrinsic factors on accuracy of mobility extraction in graphene metal-oxide-semiconductor field effect transistors. 2013 , 102, 093121	15	
1751	In-plane heterostructures of graphene and hexagonal boron nitride with controlled domain sizes. Nature Nanotechnology, 2013 , 8, 119-24	7 687	
1750	Hyperbolic metamaterials based on multilayer graphene structures. 2013 , 87,	224	
1749	Synthesis of patched or stacked graphene and hBN flakes: a route to hybrid structure discovery. 2013 , 13, 933-41	162	
1748	Fast and reliable identification of atomically thin layers of TaSe2 crystals. 2013 , 6, 191-199	53	
1747	Review of chemical vapor deposition of graphene and related applications. 2013, 46, 2329-39	100	7
1746	Observing atomic collapse resonances in artificial nuclei on graphene. 2013 , 340, 734-7	175	
1745	SymFET: A Proposed Symmetric Graphene Tunneling Field-Effect Transistor. 2013 , 60, 951-957	82	
1744	Enhanced optical response of hybridized VO//graphene films. 2013 , 5, 2632-6	29	

1743	Evidence for a spin phase transition at charge neutrality in bilayer graphene. 2013 , 9, 154-158	115
1742	Interaction phenomena in graphene seen through quantum capacitance. 2013 , 110, 3282-6	197
1741	Photoemission spectra of massless Dirac fermions on the verge of exciton condensation. 2013 , 87,	9
1740	Field effect doping of graphene in metal dielectric graphene heterostructures: A model based upon first-principles calculations. 2013 , 87,	30
1739	A hydrothermal anvil made of graphene nanobubbles on diamond. 2013 , 4, 1556	58
1738	Electron-hole pairing in topological insulator heterostructures in the quantum Hall state. 2013, 87,	1
1737	Impurity induced non-bulk stacking in chemically exfoliated h-BN nanosheets. 2013 , 5, 2290-4	18
1736	Progress, challenges, and opportunities in two-dimensional materials beyond graphene. 2013 , 7, 2898-926	3414
1735	Structure, stability and defects of single layer hexagonal BN in comparison to graphene. 2013 , 25, 045009	38
1734	Raman spectroscopy as a versatile tool for studying the properties of graphene. <i>Nature</i> Nanotechnology, 2013 , 8, 235-46	4466
1734 1733		4466 287
1733	Nanotechnology, 2013 , 8, 235-46	
1733	Nanotechnology, 2013, 8, 235-46 Two-dimensional semiconductors: recent progress and future perspectives. 2013, 1, 2952	287
1733 1732	Nanotechnology, 2013, 8, 235-46 Two-dimensional semiconductors: recent progress and future perspectives. 2013, 1, 2952 Spontaneous symmetry breaking and dynamic phase transition in monolayer silicene. 2013, 110, 085504	287
1733 1732 1731	Nanotechnology, 2013, 8, 235-46 Two-dimensional semiconductors: recent progress and future perspectives. 2013, 1, 2952 Spontaneous symmetry breaking and dynamic phase transition in monolayer silicene. 2013, 110, 085504 Temperature-Dependent Raman Studies and Thermal Conductivity of Few-Layer MoS2. 2013, 117, 9042-9047	287 193 487
1733 1732 1731 1730	Nanotechnology, 2013, 8, 235-46 Two-dimensional semiconductors: recent progress and future perspectives. 2013, 1, 2952 Spontaneous symmetry breaking and dynamic phase transition in monolayer silicene. 2013, 110, 085504 Temperature-Dependent Raman Studies and Thermal Conductivity of Few-Layer MoS2. 2013, 117, 9042-9047 All-graphene photodetectors. 2013, 7, 5052-7 Crystallographic orientation of early domains in CVD graphene studied by Raman spectroscopy.	287 193 487 86
1733 1732 1731 1730 1729	Two-dimensional semiconductors: recent progress and future perspectives. 2013, 1, 2952 Spontaneous symmetry breaking and dynamic phase transition in monolayer silicene. 2013, 110, 085504 Temperature-Dependent Raman Studies and Thermal Conductivity of Few-Layer MoS2. 2013, 117, 9042-9047 All-graphene photodetectors. 2013, 7, 5052-7 Crystallographic orientation of early domains in CVD graphene studied by Raman spectroscopy. 2013, 568-569, 146-150 Flexural electromechanical coupling: a nanoscale emergent property of boron nitride bilayers. 2013	287 193 487 86

1725	The role of external defects in chemical sensing of graphene field-effect transistors. 2013 , 13, 1962-8	107
1724	Charge-carrier screening in single-layer graphene. 2013 , 110, 146802	47
1723	Graphene-based electrodes for electrochemical energy storage. 2013 , 6, 1388	631
1722	Superior thermal conductivity of polymer nanocomposites by using graphene and boron nitride as fillers. 2013 , 163, 41-45	55
1721	Electronic properties of the MoS2-WS2 heterojunction. 2013 , 87,	378
1720	Thermal conductivity and phonon transport in suspended few-layer hexagonal boron nitride. 2013 , 13, 550-4	454
1719	Borocarbonitrides, BxCyNz. 2013 , 1, 5806	121
1718	Unique role of self-assembled monolayers in carbon nanomaterial-based field-effect transistors. 2013 , 9, 1144-59	33
1717	Photo-oxidation of Graphene in the Presence of Water. 2013 , 117, 1453-1456	37
1716	Resonant tunnelling and negative differential conductance in graphene transistors. 2013 , 4, 1794	451
1715	Silicene on Substrates: A Way To Preserve or Tune Its Electronic Properties. 2013, 117, 10353-10359	215
1714	The Restorative Effect of Fluoropolymer Coating on Electrical Characteristics of Graphene Field-Effect Transistors. 2013 , 34, 559-561	13
1713	Adsorption of nucleobase pairs on hexagonal boron nitride sheet: hydrogen bonding versus stacking. 2013 , 15, 10767-76	48
1712	Optical field enhancement by strong plasmon interaction in graphene nanostructures. 2013 , 110, 187401	75
1711	Graphene-analogous low-dimensional materials. 2013 , 58, 1244-1315	600
1710	Effect of surface morphology on friction of graphene on various substrates. 2013 , 5, 3063-9	124
1709	Grains and grain boundaries in highly crystalline monolayer molybdenum disulphide. 2013, 12, 554-61	1590
1708	Controlled charge trapping by molybdenum disulphide and graphene in ultrathin heterostructured memory devices. 2013 , 4, 1624	504

1707 Strong light-matter interactions in heterostructures of atomically thin films. 2013 , 340, 1311-4	1850
First-principles analysis of MoS2/Ti2C and MoS2/Ti2CY2 (Y=F and OH) all-2D semiconductor/me contacts. 2013 , 87,	tal 133
1705 . 2013 , 101, 1740-1765	72
1704 Graphene Field-Effect Transistors Based on BoronNitride Dielectrics. 2013, 101, 1609-1619	114
1703 Boron nitride nanopores: highly sensitive DNA single-molecule detectors. 2013 , 25, 4549-54	182
1702 Large-Area 2-D Electronics: Materials, Technology, and Devices. 2013 , 101, 1638-1652	39
Facile synthesis of large-area ultrathin hexagonal BN films via self-limiting growth at the molter BDBurface. 2013 , 9, 1353-8	n 23
1700 Massive Dirac fermions and Hofstadter butterfly in a van der Waals heterostructure. 2013 , 340,	1427-30 1092
Reversible intercalation of hexagonal boron nitride with Brfisted acids. 2013 , 135, 8372-81	69
1698 Carbon Doping of Hexagonal Boron Nitride by Using CO Molecules. 2013 , 117, 9332-9339	35
1697 Highly defective graphene: A key prototype of two-dimensional Anderson insulators. 2013 , 6, 32	26-334 43
Quantitatively enhanced reliability and uniformity of high-ldielectrics on graphene enabled by self-assembled seeding layers. 2013 , 13, 1162-7	57
Growth and low-energy electron microscopy characterization of monolayer hexagonal boron nitride on epitaxial cobalt. 2013 , 6, 335-347	93
1694 Selective decoration of Au nanoparticles on monolayer MoS2 single crystals. 2013 , 3, 1839	342
Electronic and optical properties of graphene and graphitic ZnO nanocomposite structures. 201 138, 124706	82
1692 Extreme monolayer-selectivity of hydrogen-plasma reactions with graphene. 2013 , 7, 1324-32	86
Optical probing of the electronic interaction between graphene and hexagonal boron nitride. 2 0 7, 1533-41	013 , 48
Synthesis of monolayer graphene having a negligible amount of wrinkles by stress relaxation. 2 0 13, 2496-9	013 , 30

1689	Gigahertz integrated graphene ring oscillators. 2013 , 7, 5588-94	58
1688	Sensing behavior of atomically thin-layered MoS2 transistors. 2013 , 7, 4879-91	987
1687	. 2013 , 101, 1536-1556	38
1686	Tight-binding model for graphene Ebands from maximally localized Wannier functions. 2013, 87,	36
1685	Disorder imposed limits of mono- and bilayer graphene electronic modification using covalent chemistry. 2013 , 13, 809-17	55
1684	Self-modulated band gap in boron nitride nanoribbons and hydrogenated sheets. 2013 , 5, 6381-7	52
1683	Near-ideal electrical properties of InAs/WSe2 van der Waals heterojunction diodes. 2013 , 102, 242101	64
1682	Intrinsic plasmons in two-dimensional Dirac materials. 2013 , 87,	57
1681	Electric-field screening in atomically thin layers of MoSIIthe role of interlayer coupling. 2013, 25, 899-903	122
1680	Where does the current flow in two-dimensional layered systems?. 2013 , 13, 3396-402	193
1679	Chemical vapour deposition growth of large single crystals of monolayer and bilayer graphene. 2013 , 4, 2096	422
1678	Ultralight three-dimensional boron nitride foam with ultralow permittivity and superelasticity. 2013 , 13, 3232-6	152
1677	Molecular self-assembly on graphene on SiO2 and h-BN substrates. 2013 , 13, 3199-204	106
1676	Influence of Interface Structure on the Properties of ZnO/Graphene Composites: A Theoretical Study by Density Functional Theory Calculations. 2013 , 117, 10536-10544	66
1675	Gigahertz quantized charge pumping in graphene quantum dots. <i>Nature Nanotechnology</i> , 2013 , 8, 417-2 0 8.7	99
1674	Sub-10 nm gate length graphene transistors: operating at terahertz frequencies with current saturation. 2013 , 3, 1314	83
1673	Repeated and controlled growth of monolayer, bilayer and few-layer hexagonal boron nitride on Pt foils. 2013 , 7, 5199-206	182
1672	Synthesis of boron-doped graphene monolayers using the sole solid feedstock by chemical vapor deposition. 2013 , 9, 1316-20	157

(2013-2013)

1671	A platform for large-scale graphene electronicsCVD growth of single-layer graphene on CVD-grown hexagonal boron nitride. 2013 , 25, 2746-52	196
1670	Covalent electron transfer chemistry of graphene with diazonium salts. 2013 , 46, 160-70	231
1669	Chemical vapor deposition and characterization of aligned and incommensurate graphene/hexagonal boron nitride heterostack on Cu(111). 2013 , 13, 2668-75	98
1668	Interaction between hydrogen flux and carbon monolayer on SiC(0001): graphene formation kinetics. 2013 , 5, 671-80	16
1667	Hofstadter's butterfly and the fractal quantum Hall effect in moir superlattices. 2013, 497, 598-602	1084
1666	Cloning of Dirac fermions in graphene superlattices. 2013 , 497, 594-7	884
1665	Inverse relationship between carrier mobility and bandgap in graphene. 2013 , 138, 084701	94
1664	Ultrasensitive photodetectors based on monolayer MoS2. <i>Nature Nanotechnology</i> , 2013 , 8, 497-501 28.7	3412
1663	Solvated graphenes: an emerging class of functional soft materials. 2013 , 25, 13-30	192
1662	Competing topological phases in few-layer graphene. 2013 , 12, 175-187	1
1661	Atomic layer deposition of dielectrics for carbon-based electronics. 2013 , 546, 85-93	15
1660	Precisely aligned graphene grown on hexagonal boron nitride by catalyst free chemical vapor deposition. 2013 , 3, 2666	184
1659	Heterogeneous integration of hexagonal boron nitride on bilayer quasi-free-standing epitaxial graphene and its impact on electrical transport properties. 2013 , 210, 1062-1070	14
1658	Electron tunneling in a vertical graphene heterostructure. 2013 , 86, 1	3
1657	Ferromagnetic two-dimensional crystals: Single layers of K2CuF4. 2013 , 88,	71
1656	Robust Superlubricity in Graphene/h-BN Heterojunctions. 2013 , 4, 115-20	131
1655	Multiple excitation of confined graphene plasmons by single free electrons. 2013, 7, 11409-19	67
1654	The selective transfer of patterned graphene. 2013 , 3, 3216	17

1653	A facile chemical exfoliation method to obtain large size boron nitride nanosheets. 2013 , 15, 1782	140
1652	Moir Buperstructures of silicene on hexagonal boron nitride: A first-principles study. 2013, 377, 2628-2632	48
1651	Uncovering the dominant scattering mechanism in graphene system. 2013 , 377, 1649-1654	4
1650	One-dimensional half-metallic interfaces of two-dimensional honeycomb insulators. 2013, 88,	25
1649	Quasi free-standing silicene in a superlattice with hexagonal boron nitride. 2013 , 3, 3192	97
1648	Characterization of Interfaces between Graphene Films and Support Substrates by Observation of Lipid Membrane Formation. 2013 , 117, 18913-18918	10
1647	Enhanced absorption of graphene in the visible region by use of plasmonic nanostructures. 2013 , 15, 055003	54
1646	Ultraclean freestanding graphene by platinum-metal catalysis. 2013 , 31, 020605	40
1645	Hyperspectral imaging of structure and composition in atomically thin heterostructures. 2013 , 13, 3942-6	37
1644	Possibility of a field effect transistor based on Dirac particles in semiconducting anatase-TiO2 nanowires. 2013 , 13, 1073-9	10
1643	Efficient gate-tunable light-emitting device made of defective boron nitride nanotubes: from ultraviolet to the visible. 2013 , 3, 2698	20
1642	Dimensional dependence of phonon transport in freestanding atomic layer systems. 2013 , 5, 11870-5	5
1641	Electrical Spin Injection into Graphene through Monolayer Hexagonal Boron Nitride. 2013, 6, 073001	80
1640	Diamond as an inert substrate of graphene. 2013 , 138, 054701	38
1639	A ballistic pn junction in suspended graphene with split bottom gates. 2013 , 102, 223102	72
1638	Plane wave excitation-detection of non-resonant plasmons along finite-width graphene strips. 2013 , 21, 24856-72	68
1637	Optoelectronic properties of graphene-MoS2 hybrid. 2013 , 1505, 1	2
1636	Dependence of Field-Effect Mobility of Graphene Grown by Thermal Chemical Vapor Deposition on Its Grain Size. 2013 , 52, 110106	7

1635	Unidirectional surface plasmons in nonreciprocal graphene. 2013 , 15, 113003	33
1634	Josephson Coupling Realized in Graphite-Based Vertical Junction. 2013, 6, 025102	3
1633	High Performance of the Thermal Transport in Graphene Supported on Hexagonal Boron Nitride. 2013 , 6, 075202	7
1632	Simulating analogue holography in flexible Dirac metals. 2013 , 104, 47002	10
1631	Contact resistance in graphene channel transistors. 2013 , 14, 162-170	30
1630	Fabrication and Characterization of High-Mobility Graphene pflp Junctions Encapsulated by Hexagonal Boron Nitride. 2013 , 52, 110105	19
1629	Flexible graphene-PZT ferroelectric nonvolatile memory. 2013 , 24, 475202	57
1628	Atomic and Electronic Structure of Multilayer Graphene on a Monolayer Hexagonal Boron Nitride. 2013 , 1549, 65-70	
1627	Boron Nitride Nanosheets: novel Syntheses and Applications in polymeric Composites. 2013 , 471, 012003	40
1626	High frequency performance limits of nanointerconnects based on CVD-grown graphene films transferred on SiO2-substrate. 2013 ,	1
1625	Performance modeling for interconnects for conventional and emerging switches. 2013,	
1624	Integer quantum Hall effect in single-layer graphene with tilted magnetic field. 2013 , 114, 073705	2
1623	Insulating behavior at the neutrality point in single-layer graphene. 2013 , 110, 216601	93
1622	Magnetotunneling spectroscopy of chiral two-dimensional electron systems. 2013 , 88,	7
1621	First-principles study of graphene adsorbed on WS2 monolayer. 2013 , 114, 183709	21
1620	Optical thickness determination of hexagonal boron nitride flakes. 2013 , 102, 161906	57
1619	Top oxide thickness dependence of remote phonon and charged impurity scattering in top-gated graphene. 2013 , 102, 183506	11
1618	Two-dimensional excitons in three-dimensional hexagonal boron nitride. 2013 , 103, 191106	63

1617	Graphene on boron nitride microwave transistors driven by graphene nanoribbon back-gates. 2013 , 102, 033505	9
1616	Theory of substrate, Zeeman, and electron-phonon interaction effects on the quantum capacitance in graphene. 2013 , 114, 223711	3
1615	Investigation of ripple-limited low-field mobility in large-scale graphene nanoribbons. 2013 , 102, 253506	4
1614	Modulation of Fermi velocities of Dirac electrons in single layer graphene by moir uperlattice. 2013 , 103, 113106	5
1613	Fine structure of the lowest Landau level in suspended trilayer graphene. 2013, 88,	11
1612	Graphene-based non-Boolean logic circuits. 2013 , 114, 154310	47
1611		26
1610	Topography, complex refractive index, and conductivity of graphene layers measured by correlation of optical interference contrast, atomic force, and back scattered electron microscopy. 2013 , 114, 183107	3
1609	Gate-tunable carbon nanotube-MoS2 heterojunction p-n diode. 2013 , 110, 18076-80	304
1608	Edge and substrate-induced bandgap in zigzag graphene nanoribbons on the hexagonal nitride boron 8-ZGNR/h-BN(0001). 2013 , 3, 092105	18
1607	Quantum Hall ferromagnetic phases in the Landau level N=0 of a graphene bilayer. 2013 , 87,	29
1606	Selective charge doping of chemical vapor deposition-grown graphene by interface modification. 2013 , 103, 253116	14
1605	Bandgap engineering of rippled MoS2 monolayer under external electric field. 2013 , 102, 173112	90
1604	Electronic properties of Mn-decorated silicene on hexagonal boron nitride. 2013, 88,	60
1603	Stress-enhanced chemical vapor deposited graphene NEMS RF resonators. 2013,	2
1602	Self-Healing of StoneWales Defects in Boron Nitride Monolayer by Irradiation: Ab Initio Molecular Dynamics Simulations. 2013 , 30, 103102	4
1601	The registry index: a quantitative measure of materials' interfacial commensurability. 2013 , 14, 2376-91	47
1600	Fluorescence quenching of CdSe quantum dots on graphene. 2013 , 103, 201909	16

1599	Controlling the spontaneous emission rate of monolayer MoS in a photonic crystal nanocavity. 2013 , 103, 181119	155
1598	Probing built-in strain in freestanding graphene monolayers by Raman spectroscopy. 2013 , 250, 2681-2686	16
1597	Screening and interlayer coupling in multilayer MoS2. 2013 , 7, 268-273	122
1596	Van der Waals epitaxial double heterostructure: InAs/single-layer graphene/InAs. 2013 , 25, 6847-53	61
1595	Etched graphene single electron transistors on hexagonal boron nitride in high magnetic fields. 2013 , 250, 2692-2696	8
1594	Nanolithography on graphene by using scanning tunneling microscopy in a methanol environment. 2013 , 19, 1569-74	1
1593	Fringe structures and tunable bandgap width of 2D boron nitride nanosheets. 2014 , 5, 1186-92	13
1592	Bibliography. 2014 , 105-118	
1591	. 2014,	2
1590	Tunneling transport in a few monolayer-thick WS2/graphene heterojunction. 2014 , 105, 223109	27
1589	First-principles study on the currentWoltage characteristics of B24N24 fullerene-like nanocage. 2014 , 40, 275-284	2
1588	Criticality of surface topology for charge-carrier transport characteristics in two-dimensional borocarbonitrides: design principles for an efficient electronic material. 2014 , 6, 13430-4	14
1587	Effect of biaxial strain on structural and electronic properties of graphene / boron nitride hetero bi-layer structure. 2014 ,	1
1586	One-Step Exfoliation and Fluorination of Boron Nitride Nanosheets and a Study of Their Magnetic Properties. 2014 , 126, 3719-3723	29
1585	High-Frequency Devices. 2014 , 111-148	
1584	Thermal Transient Analysis of High-Power Green LED Fixed on BN Coated Al Substrates as Heatsink. 2014 , 61, 3213-3216	9
1583	Role of defects in the process of graphene growth on hexagonal boron nitride from atomic carbon. 2014 , 105, 191610	23
1582	A micro-magneto-Raman scattering study of graphene on a bulk graphite substrate. 2014 , 108, 27011	5

1581	Controlled construction of nanostructures in graphene. 2014 , 23, 028102	4
1580	Side-gate modulation effects on high-quality BN-Graphene-BN nanoribbon capacitors. 2014 , 105, 243507	6
1579	Deterministic transfer of two-dimensional materials by all-dry viscoelastic stamping. 2014 , 1, 011002	986
1578	Growth of graphene from SiC{0001} surfaces and its mechanisms. 2014 , 29, 064009	25
1577	Prospects of direct growth boron nitride films as substrates for graphene electronics. 2014 , 29, 459-471	40
1576	Graphene on nanoscale gratings for the generation of terahertz Smith-Purcell radiation. 2014 , 105, 241102	20
1575	Inelastic carrier lifetime in a coupled graphene/electron-phonon system: Role of plasmon-phonon coupling. 2014 , 90,	9
1574	Magneto-transport properties of a random distribution of few-layer graphene patches. 2014 , 116, 193705	O
1573	Synthesis of wafer-scale hexagonal boron nitride monolayers free of aminoborane nanoparticles by chemical vapor deposition. 2014 , 25, 145604	44
1572	Room Temperature Electroluminescence from Mechanically Formed van der Waals III V I Homojunctions and Heterojunctions. 2014 , 2, 1064-1069	61
1571	Stability and electronic properties of hexagonal boron nitride monolayer with irregular graphene domains embedded. 2014 , 28, 1450144	4
1570	Architectured van der Waals epitaxy of ZnO nanostructures on hexagonal BN. 2014 , 6, e145-e145	37
1569	Recent experimental progress of fractional quantum Hall effect: 5/2 filling state and graphene. 2014 , 1, 564-579	28
1568	Wafer bonding solution to epitaxial grapheneBilicon integration. 2014 , 47, 094001	11
1567	Contact resistance and overlapping capacitance in flexible sub-micron long oxide thin-film transistors for above 100 MHz operation. 2014 , 105, 263504	47
1566	Graphene transport properties upon exposure to PMMA processing and heat treatments. 2014 , 1, 035005	56
1565	Extraction of carrier transport properties in graphene from microwave measurements. 2014,	
1564	Photo-patternable ion gel-gated graphene transistors and inverters on plastic. 2014 , 25, 014002	48

1563	Free-space carpet cloak using transformation optics and graphene. 2014 , 39, 6739-42	6
1562	Photon emission rate engineering using graphene nanodisc cavities. 2014 , 22, 6400-15	7
1561	Tuning photoinduced terahertz conductivity in monolayer graphene: Optical-pump terahertz-probe spectroscopy. 2014 , 90,	33
1560	Symmetry-dependent band gap opening in graphene induced by g-C3N4 substrates. 2014 , 4, 64577-64582	7
1559	Effects of boron-nitride substrates on Stone-Wales defect formation in graphene: An ab initio molecular dynamics study. 2014 , 104, 203106	5
1558	Improvement of graphene field-effect transistors by hexamethyldisilazane surface treatment. 2014 , 105, 033117	16
1557	Generation and morphing of plasmons in graphene superlattices. 2014 , 90,	22
1556	Dual-probe spectroscopic fingerprints of defects in graphene. 2014 , 90,	9
1555	Stable path to ferromagnetic hydrogenated graphene growth. 2014 , 90,	19
1554	Reconfigurable p-n junction diodes and the photovoltaic effect in exfoliated MoS2 films. 2014 , 104, 122104	47
1554 1553	Reconfigurable p-n junction diodes and the photovoltaic effect in exfoliated MoS2 films. 2014 , 104, 122104 Carbon nanotube quantum dots on hexagonal boron nitride. 2014 , 105, 023111	12
1553	Carbon nanotube quantum dots on hexagonal boron nitride. 2014 , 105, 023111 Critical point for the canted antiferromagnetic to ferromagnetic phase transition at charge	12
1553 1552	Carbon nanotube quantum dots on hexagonal boron nitride. 2014 , 105, 023111 Critical point for the canted antiferromagnetic to ferromagnetic phase transition at charge neutrality in bilayer graphene. 2014 , 90, Revealing origin of quasi-one dimensional current transport in defect rich two dimensional	12 6
1553 1552 1551	Carbon nanotube quantum dots on hexagonal boron nitride. 2014 , 105, 023111 Critical point for the canted antiferromagnetic to ferromagnetic phase transition at charge neutrality in bilayer graphene. 2014 , 90, Revealing origin of quasi-one dimensional current transport in defect rich two dimensional materials. 2014 , 105, 053115 Friction force microscopy studies on SiO2 supported pristine and hydrogenated graphene. 2014 ,	12 6 10
1553 1552 1551 1550	Carbon nanotube quantum dots on hexagonal boron nitride. 2014, 105, 023111 Critical point for the canted antiferromagnetic to ferromagnetic phase transition at charge neutrality in bilayer graphene. 2014, 90, Revealing origin of quasi-one dimensional current transport in defect rich two dimensional materials. 2014, 105, 053115 Friction force microscopy studies on SiO2 supported pristine and hydrogenated graphene. 2014, 104, 041910 Thickness determination of few-layer hexagonal boron nitride films by scanning electron	12 6 10 24
1553 1552 1551 1550 1549	Carbon nanotube quantum dots on hexagonal boron nitride. 2014, 105, 023111 Critical point for the canted antiferromagnetic to ferromagnetic phase transition at charge neutrality in bilayer graphene. 2014, 90, Revealing origin of quasi-one dimensional current transport in defect rich two dimensional materials. 2014, 105, 053115 Friction force microscopy studies on SiO2 supported pristine and hydrogenated graphene. 2014, 104, 041910 Thickness determination of few-layer hexagonal boron nitride films by scanning electron microscopy and Auger electron spectroscopy. 2014, 2, 092502	12 6 10 24 20

1545	Pure valley current generation in graphene with a Dirac gap by quantum pumping. 2014 , 7, 125102	12
1544	Half-metallicity modulation of hybrid BN-C nanotubes by external electric fields: a first-principles study. 2014 , 140, 234702	5
1543	Fast pick up technique for high quality heterostructures of bilayer graphene and hexagonal boron nitride. 2014 , 105, 013101	208
1542	Extreme sub-threshold swing in tunnelling relays. 2014 , 104, 013509	6
1541	Generating electric current based on the solvent-dependent charging effects of defective boron nitride nanosheets. 2014 , 6, 19752-7	8
1540	Investigation of plasmonic whispering-gallery mode characteristics for graphene monolayer coated dielectric nanodisks. 2014 , 39, 5527-30	15
1539	Two-dimensional quasi-freestanding molecular crystals for high-performance organic field-effect transistors. 2014 , 5, 5162	270
1538	Intrinsic carrier mobility of Dirac cones: the limitations of deformation potential theory. 2014 , 141, 144107	28
1537	Field effect in the quantum Hall regime of a high mobility graphene wire. 2014 , 116, 073705	7
1536	Electronic properties of graphene/hexagonal-boron-nitride moir uperlattice. 2014, 90,	131
1535	Single-layer MoS2 roughness and sliding friction quenching by interaction with atomically flat substrates. 2014 , 105, 053111	51
1534	Terahertz Frequency-Dependent Carrier Scattering Rate and Mobility of Monolayer and AA-Stacked Multilayer Graphene. 2014 , 20, 122-129	8
1533	Ground state of graphene heterostructures in the presence of random charged impurities. 2014 , 90,	19
1532	Nanocrystalline-graphene-tailored hexagonal boron nitride thin films. 2014 , 53, 11493-7	21
1531	Total Ionizing Dose Effects on hBN Encapsulated Graphene Devices. 2014 , 61, 2868-2873	24
1530	Introduction. 2014 , 1-18	
1529	Moir[patterns as a probe of interplanar interactions for graphene on h-BN. 2014 , 113, 135504	105

1527	Electronic structure of spontaneously strained graphene on hexagonal boron nitride. 2014 , 90,	37
1526	A cohesive law for interfaces in graphene/hexagonal boron nitride heterostructure. 2014 , 115, 144308	13
1525	Graphene on hexagonal lattice substrate: Stress and pseudo-magnetic field. 2014 , 104, 173106	16
1524	Band structure mapping of bilayer graphene via quasiparticle scattering. 2014 , 2, 092503	18
1523	Charge carrier transport properties in layer structured hexagonal boron nitride. 2014, 4, 107126	21
1522	Graphene quantum dot on boron nitride: Dirac cone replica and Hofstadter butterfly. 2014 , 90,	34
1521	Layer-structured hexagonal (BN)C semiconductor alloys with tunable optical and electrical properties. 2014 , 115, 093509	30
1520	Epitaxial hexagonal boron nitride on Ir(111): A work function template. 2014 , 89,	72
1519	Schottky barriers at hexagonal boron nitride/metal interfaces: A first-principles study. 2014 , 90,	62
1518	Graphene-enabled low-control quantum gates between static and mobile spins. 2014, 89,	19
1517	Nanocrystalline-Graphene-Tailored Hexagonal Boron Nitride Thin Films. 2014 , 126, 11677-11681	4
1516	Two-dimensional material nanophotonics. 2014 , 8, 899-907	1805
1515	In Situ Observations during Chemical Vapor Deposition of Hexagonal Boron Nitride on Polycrystalline Copper. 2014 , 26, 6380-6392	147
1514	Chiral symmetry breaking and the quantum Hall effect in monolayer graphene. 2014 , 90,	38
1513	Electron transfer and coupling in graphene-tungsten disulfide van der Waals heterostructures. 2014 , 5, 5622	170
1512	Spin-valley filtering in strained graphene structures with artificially induced carrier mass and spin-orbit coupling. 2014 , 113, 046601	84
1511	Wafer-scale solution-derived molecular gate dielectrics for low-voltage graphene electronics. 2014 , 104, 083503	22
1510	Field emission characteristics from graphene on hexagonal boron nitride. 2014, 104, 221603	19

1509 Synthesis of few-layer, large area hexagonal-boron nitride by pulsed laser deposition. 2014 , 572, 245-250	67
1508 Wigner localization in a graphene quantum dot with a mass gap. 2014 , 90,	11
1507 Terahertz-frequency electronic transport in graphene. 2014 , 90,	20
Large on/off current ratio in hybrid graphene/BN nanoribbons by transverse electric field-induced control of bandgap. 2014 , 105, 073114	19
Optical characterization of electron-phonon interactions at the saddle point in graphene. 2014 , 112, 187401	14
Valence and conduction band offsets at amorphous hexagonal boron nitride interfaces with silicon network dielectrics. 2014 , 104, 102901	18
1503 Vertical heterojunction of MoS2 and WSe2. 2014 ,	3
1502 Percolation transitions in bilayer graphene encapsulated by hexagonal boron nitride. 2014 , 90,	5
1501 Emergence of bound states in ballistic magnetotransport of graphene antidots. 2014 , 90,	10
1500 Contact-induced spin polarization of monolayer hexagonal boron nitride on Ni(111). 2014 , 104, 051604	10
Enhancing the Electrochemical and Electronic Performance of CVD-Grown Graphene by Minimizing Trace Metal Impurities. 2014 , 1, 2070-2074	28
Effects of temperature and strain rate on the mechanical properties of hexagonal boron nitride nanosheets. 2014 , 47, 025303	78
Spectroscopic study of graphene nanoribbons formed by crystallographic etching of highly oriented pyrolytic graphite. 2014 , 105, 123116	2
1496 On-chip graphene optoelectronic devices for high-speed modulation and photodetection. 2014 ,	1
Effects of hydrogen intercalation on transport properties of quasi-free-standing monolayer graphene. 2014 , 53, 04EN01	16
Graphene interlayer for current spreading enhancement by engineering of barrier height in GaN-based light-emitting diodes. 2014 , 22 Suppl 4, A1040-50	14
Frequency-tunable circular polarization beam splitter using a graphene-dielectric sub-wavelength film. 2014 , 22, 19748-57	11
1492 Growth of 2D heterostructures of graphene/BN. 2014 ,	o

	Large potential steps at weakly interacting metal-insulator interfaces. 2014 , 90,	16
1490	Self-terminating growth in hexagonal boron nitride by metal organic chemical vapor deposition. 2014 , 7, 071004	32
1489	Theory of carrier transport in graphene double-layer structure with carrier imbalance. 2014 , 53, 06JD07	2
1488	Focused ion beam as a tool for graphene technology: Structural study of processing sequence by electron microscopy. 2014 , 53, 02BC22	1
1487	Transport properties of rippled graphene. 2014 , 26, 135303	12
1486	Experimental Manifestation of Berry Phase in Graphene. 2014 , 3-27	1
1485	Probing Dirac Fermions in Graphene by Scanning Tunneling Microscopy and Spectroscopy. 2014 , 29-63	2
1484	Graphene Constrictions. 2014 , 141-169	2
1483	Encapsulation of graphene interconnects with 2D Layered Insulator for improved performance. 2014 , 1658, 47	
~ . O a	Transition from Tubes to SheetsA Comparison of the Properties and Applications of Carbon	
1482	Nanotubes and Graphene. 2014 , 519-568	2
		13
1481	Nanotubes and Graphene. 2014, 519-568	
1481	Nanotubes and Graphene. 2014, 519-568 Graphene-photonic crystal switch. 2014, 321, 150-156	13
1481 1480	Nanotubes and Graphene. 2014, 519-568 Graphene-photonic crystal switch. 2014, 321, 150-156 Large Scale Graphene/Hexagonal Boron Nitride Heterostructure for Tunable Plasmonics. 2014, 24, 731-738 One-step exfoliation and fluorination of boron nitride nanosheets and a study of their magnetic properties. 2014, 53, 3645-9	13
1481 1480 1479	Nanotubes and Graphene. 2014, 519-568 Graphene-photonic crystal switch. 2014, 321, 150-156 Large Scale Graphene/Hexagonal Boron Nitride Heterostructure for Tunable Plasmonics. 2014, 24, 731-738 One-step exfoliation and fluorination of boron nitride nanosheets and a study of their magnetic properties. 2014, 53, 3645-9	13 48 105
1481 1480 1479 1478	Nanotubes and Graphene. 2014, 519-568 Graphene-photonic crystal switch. 2014, 321, 150-156 Large Scale Graphene/Hexagonal Boron Nitride Heterostructure for Tunable Plasmonics. 2014, 24, 731-738 One-step exfoliation and fluorination of boron nitride nanosheets and a study of their magnetic properties. 2014, 53, 3645-9 25th anniversary article: hybrid nanostructures based on two-dimensional nanomaterials. 2014, 26, 2185-204	13 48 105 514
1481 1480 1479 1478	Nanotubes and Graphene. 2014, 519-568 Graphene-photonic crystal switch. 2014, 321, 150-156 Large Scale Graphene/Hexagonal Boron Nitride Heterostructure for Tunable Plasmonics. 2014, 24, 731-738 One-step exfoliation and fluorination of boron nitride nanosheets and a study of their magnetic properties. 2014, 53, 3645-9 25th anniversary article: hybrid nanostructures based on two-dimensional nanomaterials. 2014, 26, 2185-204 Reducing disorder in graphene nanoribbons by chemical edge modification. 2014, 104, 083105 The electronic transport behavior of hybridized zigzag graphene and boron nitride nanoribbons.	13 48 105 514

1473	Is graphene a promising nano-material for promoting surface modification of implants or scaffold materials in bone tissue engineering?. 2014 , 20, 477-91	81
1472	Wiedemann-Franz relation and thermal-transistor effect in suspended graphene. 2014 , 14, 289-93	37
1471	Rebar graphene. 2014 , 8, 5061-8	155
1470	Will a graphitic-like ZnO single-layer be an ideal substrate for graphene?. 2014 , 4, 17478	13
1469	GrapheneBoron nitride superlattices: the role of point defects at the BN layer. 2014 , 25, 165705	14
1468	Graphene Plasmonics: Challenges and Opportunities. 2014 , 1, 135-152	817
1467	Synthesis of metal nanoparticle@graphene hydrogel composites by substrate-enhanced electroless deposition and their application in electrochemical sensors. 2014 , 4, 9133	27
1466	Epitaxial graphene on SiC{0001}: advances and perspectives. 2014 , 16, 3501-11	117
1465	Magnetic breakdown in twisted bilayer graphene. 2014 , 89,	11
1464	Centered Honeycomb NiSe2 Nanoribbons: Structure and Electronic Properties. 2014 , 118, 3295-3304	27
1463	Graphene versus ohmic metal as source-drain electrode for MoSIhanosheet transistor channel. 2014 , 10, 2356-61	79
1462	Performance Analysis of Graphene Nanoribbon Field Effect Transistors in the Presence of Surface Roughness. 2014 , 61, 1193-1198	21
1461	Band gap tunning in BN-doped graphene systems with high carrier mobility. 2014 , 104, 073116	65
1460	Clustered impurities and carrier transport in supported graphene. 2014 , 89,	14
1459	Spin-orbit interaction and isotropic electronic transport in graphene. 2014 , 112, 136602	32
1458	Direct laser fabrication of large-area and patterned graphene at room temperature. 2014 , 68, 784-790	40
1457	Thermal conductivity of ultra-thin chemical vapor deposited hexagonal boron nitride films. 2014 , 104, 013113	33
1456	High performance vertical tunneling diodes using graphene/hexagonal boron nitride/graphene hetero-structure. 2014 , 104, 053103	30

1455	Lattice matching and electronic structure of finite-layer graphene/h-BN thin films. 2014 , 89,	18
1454	Direct synthesis of van der Waals solids. 2014 , 8, 3715-23	218
1453	Charge transport mechanisms of graphene/semiconductor Schottky barriers: A theoretical and experimental study. 2014 , 115, 013701	52
1452	van der Waals trilayers and superlattices: modification of electronic structures of MoS2 by intercalation. 2014 , 6, 4566-71	92
1451	Nanomechanical and Charge Transport Properties of Two-Dimensional Atomic Sheets. 2014 , 1, 1300089	28
1450	Rapid reductions in North Atlantic Deep Water during the peak of the last interglacial period. 2014 , 343, 1129-32	82
1449	Magnetism and transport properties of zigzag graphene nanoribbons/hexagonal boron nitride heterostructures. 2014 , 115, 053708	27
1448	Controlling graphene ultrafast hot carrier response from metal-like to semiconductor-like by electrostatic gating. 2014 , 14, 1578-82	105
1447	Resistive switching in manganite/graphene hybrid planar nanostructures. 2014 , 104, 102408	6
1446	Synthesis, Properties, and Applications of 2-D Materials: A Comprehensive Review. 2014 , 39, 231-252	97
1445	Monolayer hexagonal boron nitride films with large domain size and clean interface for enhancing the mobility of graphene-based field-effect transistors. 2014 , 26, 1559-64	178
1444	Strong interlayer coupling in van der Waals heterostructures built from single-layer chalcogenides. 2014 , 111, 6198-202	803
1443	Fabrication and characterization of solid-state thermal neutron detectors based on hexagonal boron nitride epilayers. 2014 , 748, 84-90	43
1442	Hybrid functional with semi-empirical van der Waals study of native defects in hexagonal BN. 2014 , 177, 74-79	16
1441	Theoretical analysis of a dual-probe scanning tunneling microscope setup on graphene. 2014 , 112, 096801	24
1440	Large Fermi energy modulation in graphene transistors with high-pressure O2-annealed Y2O3 topgate insulators. 2014 , 104, 083519	18
1439	CommensurateIncommensurate transition in graphene on hexagonal boron nitride. 2014 , 10, 451-456	582
1438	Growth of large single-crystalline two-dimensional boron nitride hexagons on electropolished copper. 2014 , 14, 839-46	226

1437	The effect of the substrate on the Raman and photoluminescence emission of single-layer MoS2. 2014 , 7, 561-571	392
1436	Interlayer coupling enhancement in graphene/hexagonal boron nitride heterostructures by intercalated defects or vacancies. 2014 , 140, 134706	42
1435	Field-effect transistors built from all two-dimensional material components. 2014 , 8, 6259-64	496
1434	25th anniversary article: label-free electrical biodetection using carbon nanostructures. 2014 , 26, 1154-75	68
1433	Controllable co-segregation synthesis of wafer-scale hexagonal boron nitride thin films. 2014 , 26, 1776-81	73
1432	Structural and elastic properties of hybrid bilayer graphene/h-BN with different interlayer distances using DFT. 2014 , 72, 230-237	21
1431	Electronic properties of graphene encapsulated with different two-dimensional atomic crystals. 2014 , 14, 3270-6	345
1430	High performance graphene field effect transistors on an aluminum nitride substrate with high surface phonon energy. 2014 , 104, 193112	15
1429	Thermal interface conductance across a graphene/hexagonal boron nitride heterojunction. 2014 , 104, 081908	61
1428	Thermal expansion, anharmonicity and temperature-dependent Raman spectra of single- and few-layer MoSeland WSell 2014 , 15, 1592-8	193
1427	Graphene/MoS2 hybrid technology for large-scale two-dimensional electronics. 2014 , 14, 3055-63	472
1426	Boron nitride-graphene nanocapacitor and the origins of anomalous size-dependent increase of capacitance. 2014 , 14, 1739-44	100
1425	All two-dimensional, flexible, transparent, and thinnest thin film transistor. 2014 , 14, 2861-6	289
1424	Graphene and graphene-like two-dimensional materials in photodetection: mechanisms and methodology. 2014 , 8, 4133-56	412
1423	Highly thermally conductive papers with percolative layered boron nitride nanosheets. 2014, 8, 3606-13	337
1422	Efficient coupling of light to graphene plasmons by compressing surface polaritons with tapered bulk materials. 2014 , 14, 2896-901	65
1421	Coupling graphene mechanical resonators to superconducting microwave cavities. 2014 , 14, 2854-60	109
1420	Efficient transfer of carbon nanotubes for device fabrication using an LOR resist sacrificial layer. 2014 , 208, 152-158	5

1419	Electronic transport in graphene-based heterostructures. 2014 , 104, 183504	58
1418	Band offset and negative compressibility in graphene-MoS2 heterostructures. 2014 , 14, 2039-45	117
1417	Epitaxial growth of molecular crystals on van der waals substrates for high-performance organic electronics. 2014 , 26, 2812-7	103
1416	Intrinsic device-to-device variation in graphene field-effect transistors on a Si/SiO2 substrate as a platform for discriminative gas sensing. 2014 , 104, 013114	24
1415	Sinusoidally Modulated Graphene Leaky-Wave Antenna for Electronic Beamscanning at THz. 2014 , 4, 116-122	169
1414	Ballistic transport in graphene grown by chemical vapor deposition. 2014 , 104, 023103	52
1413	Chemical vapor deposition of graphene single crystals. 2014 , 47, 1327-37	170
1412	Beyond graphene: stable elemental monolayers of silicene and germanene. 2014 , 6, 7743-50	193
1411	Selective equilibration of spin-polarized quantum Hall edge states in graphene. 2014 , 112, 196601	58
1410	Active tunable absorption enhancement with graphene nanodisk arrays. 2014 , 14, 299-304	477
1409	Bandgap opening in silicene: Effect of substrates. 2014 , 592, 222-226	85
1408	Electrical and optical characterization of atomically thin WSII2014, 43, 10388-91	43
1407	Electrolyte gate dependent high-frequency measurement of graphene field-effect transistor for sensing applications. 2014 , 104, 013102	14
1406	Band structure engineering of monolayer MoS2 on h-BN: first-principles calculations. 2014 , 47, 075301	77
1405	Direct chemical conversion of graphene to boron- and nitrogen- and carbon-containing atomic layers. 2014 , 5, 3193	169
1404	Role of the seeding promoter in MoS2 growth by chemical vapor deposition. 2014 , 14, 464-72	534
1403	Excitonic recombinations in hBN: From bulk to exfoliated layers. 2014 , 89,	52
1402	Mechanical properties of silicene. 2014 , 82, 50-55	77

1401	Graphene plasmonics for terahertz to mid-infrared applications. 2014 , 8, 1086-101	909
1400	Graphene/g-C3N4 bilayer: considerable band gap opening and effective band structure engineering. 2014 , 16, 4230-5	119
1399	Tunable symmetry breaking and helical edge transport in a graphene quantum spin Hall state. 2014 , 505, 528-32	188
1398	Strong oxidation resistance of atomically thin boron nitride nanosheets. 2014 , 8, 1457-62	490
1397	Interface properties of CVD grown graphene transferred onto MoS2(0001). 2014 , 6, 1071-8	82
1396	Nano boron nitride flatland. 2014 , 43, 934-59	499
1395	Superlattice assembly of graphene oxide (GO) and titania nanosheets: fabrication, in situ photocatalytic reduction of GO and highly improved carrier transport. 2014 , 6, 14419-27	22
1394	Mid-infrared polaritonic coupling between boron nitride nanotubes and graphene. 2014 , 8, 11305-12	35
1393	Three-dimensional spirals of atomic layered MoS2. 2014 , 14, 6418-23	136
1392	Novel hybrid carbon nanofiber/highly branched graphene nanosheet for anode materials in lithium-ion batteries. 2014 , 6, 18590-6	18
1391	Graphene-Based Plasmonic Tunable Low-Pass Filters in the Terahertz Band. 2014 , 13, 1145-1153	87
1390	Solid state theory. Quantum spin Hall effect in two-dimensional transition metal dichalcogenides. 2014 , 346, 1344-7	1150
1389	High energy and power density capacitors from solution-processed ternary ferroelectric polymer nanocomposites. 2014 , 26, 6244-9	352
1388	. 2014 , 23, 298-307	14
1387	Giant enhancement in vertical conductivity of stacked CVD graphene sheets by self-assembled molecular layers. 2014 , 5, 5461	61
1386	Controlled synthesis of single-crystalline graphene. 2014 , 4, 031314	4
1385	Large current modulation in exfoliated-graphene/MoS2/metal vertical heterostructures. 2014 , 105, 083119	91
1384	Heterostructures based on inorganic and organic van der Waals systems. 2014 , 2, 092511	52

1383	Large-scale synthesis of hexagonal boron nitride nanosheets and their improvement in thermal properties of epoxy composites. 2014 , 35, 1707-1715	24
1382	Temperature-dependent electrical characterization of exfoliated EGa2O3 micro flakes. 2014 , 211, 543-549	20
1381	Phonons and electron-phonon coupling in graphene-h-BN heterostructures. 2014 , 526, 381-386	31
1380	Low-temperature compatible electrostatic comb-drive actuators with integrated graphene. 2014,	2
1379	Point defect weakened thermal contraction in monolayer graphene. 2014 , 141, 064705	11
1378	Electrostatic coupling between two surfaces of a topological insulator nanodevice. 2014 , 113, 206801	32
1377	Cyclic chlorine trap-doping for transparent, conductive, thermally stable and damage-free graphene. 2014 , 6, 15301-8	28
1376	Tunable magnetic and electronic properties of BN nanosheets with triangular defects: a first-principles study. 2014 , 26, 435302	6
1375	Synthesis and microwave absorption property of flexible magnetic film based on graphene oxide/carbon nanotubes and Fe3O4 nanoparticles. 2014 , 2, 14940	254
1374	Sublattice-induced symmetry breaking and band-gap formation in graphene. 2014 , 1, 563-571	38
1373	Bimolecular porous supramolecular networks deposited from solution on layered materials: graphite, boron nitride and molybdenum disulphide. 2014 , 50, 8882-5	23
1372	Raman modes of MoS2 used as fingerprint of van der Waals interactions in 2-D crystal-based heterostructures. 2014 , 8, 9914-24	142
1371	Preparation of Graphene with Large Area. 2014 , 39-76	2
1370	Insulating to metallic transition of an oxidized boron nitride nanosheet coating by tuning surface oxygen adsorption. 2014 , 6, 3731-6	12
1369	Cyclotrimerization of arylalkynes on Au(111). 2014 , 50, 11200-3	96
1368	Conditioning of graphene surface by CO2 cluster jet. 2014 , 4, 41922-41926	5
1367	Spiers Memorial Lecture. Advances of carbon nanomaterials. 2014 , 173, 9-46	20
1366	Epitaxial growth of a single-domain hexagonal boron nitride monolayer. 2014 , 8, 12063-70	49

1365	A systematic study of the atmospheric pressure growth of large-area hexagonal crystalline boron nitride film. 2014 , 2, 1650	60
1364	Realizing semiconductor-half-metal transition in zigzag graphene nanoribbons supported on hybrid fluorographene-graphane nanoribbons. 2014 , 16, 23214-23	22
1363	Non-conformal decoration of semiconductor nanowire surfaces with boron nitride (BN) molecules for stability enhancement: degradation-resistant Zn3P2, ZnO and Mg2Si nanowires. 2014 , 16, 16150-7	7
1362	Structure stability and high-temperature distortion resistance of trilayer complexes formed from graphenes and boron nitride nanosheets. 2014 , 16, 88-94	14
1361	Single-charge transport in graphene. 2014 , 292-323	
1360	Electronic decoupling by h-BN layer between silicene and Cu(111): A DFT-based analysis. 2014 , 16, 105019	19
1359	Polaron coupling in graphene field effect transistors on patterned self-assembled monolayer. 2014 , 16, 4313-9	5
1358	Boron-nitrogen substituted perylene obtained through photocyclisation. 2014 , 50, 7821-3	40
1357	Two-dimensional heterostructures: fabrication, characterization, and application. 2014 , 6, 12250-72	266
1356	Phonon-limited resistivity of graphene by first-principles calculations: Electron-phonon interactions, strain-induced gauge field, and Boltzmann equation. 2014 , 90,	76
1355	Tunable terahertz radiation from graphene induced by moving electrons. 2014, 89,	44
1354	Giant spin Hall effect in graphene grown by chemical vapour deposition. 2014 , 5, 4748	143
1353	Control of two-dimensional excitonic light emission via photonic crystal. 2014 , 1, 011001	124
1352	Metal-insulator transition in graphene on boron nitride. 2014 , 113, 096801	29
1351	Silicene on substrates: interaction mechanism and growth behavior. 2014 , 491, 012007	16
1350	Photovoltaic and photothermoelectric effect in a double-gated WSe2 device. 2014 , 14, 5846-52	186
1349	Graphene spintronics: Spin injection and proximity effects from first principles. 2014 , 90,	35
1348	Synthesis of wafer-scale uniform molybdenum disulfide films with control over the layer number using a gas phase sulfur precursor. 2014 , 6, 2821-6	153

1347	High gain, low noise, fully complementary logic inverter based on bi-layer WSe2 field effect transistors. 2014 , 105, 083511	72
1346	Control of molecular organization and energy level alignment by an electronically nanopatterned boron nitride template. 2014 , 8, 430-42	68
1345	A universal, rapid method for clean transfer of nanostructures onto various substrates. 2014 , 8, 6563-70	170
1344	High quality and large-scale manually operated monolayer graphene pasters. 2014 , 25, 275704	4
1343	Periodic buckling patterns of graphene/hexagonal boron nitride heterostructure. 2014 , 25, 445401	7
1342	Graphene field effect transistors with mica as gate dielectric layers. 2014 , 10, 4213-8	17
1341	Spontaneous strains and gap in graphene on boron nitride. 2014 , 90,	74
1340	Tuning the band structure, magnetic and transport properties of the zigzag graphene nanoribbons/hexagonal boron nitride heterostructures by transverse electric field. 2014 , 141, 014708	34
1339	Aqueous gating of van der Waals materials on bilayer nanopaper. 2014 , 8, 10606-12	30
1338	Interface thermal conductance and rectification in hybrid graphene/silicene monolayer. 2014 , 79, 236-244	93
1337	Superior characteristics of graphene field effect transistor enclosed by chemical-vapor-deposition-grown hexagonal boron nitride. 2014 , 2, 7776-7784	17
1336	Biomass-directed synthesis of 20 g high-quality boron nitride nanosheets for thermoconductive polymeric composites. 2014 , 8, 9081-8	114
1335	Hot carriers in epitaxial graphene sheets with and without hydrogen intercalation: role of substrate coupling. 2014 , 6, 10562-8	4
1334	All-CVD graphene field-effect transistors with h-BN gate dielectric and local back gate. 2014 ,	
1333	Electrical characteristics of multilayer MoS2 FET's with MoS2/graphene heterojunction contacts. 2014 , 14, 4511-6	142
1332	Directional Control of the Electronic and Transport Properties of Graphynes. 2014 , 118, 18793-18798	16
1331	Theoretical exploration of the half-metallicity of graphene nanoribbons/boron nitride bilayer system. 2014 , 95, 384-392	3
1330	Bilayer graphene. Chemical potential and quantum Hall ferromagnetism in bilayer graphene. 2014 , 345, 58-61	97

1329	Low-Temperature Deposition of Hexagonal Boron Nitride via Sequential Injection of Triethylboron and N2/H2 Plasma. 2014 , 97, 4052-4059	28
1328	Interface engineering for CVD graphene: current status and progress. 2014 , 10, 4443-54	25
1327	The effect of H adsorption on the electronic and magnetic states in the hybrid structure of graphene and BN. 2014 , 93, 50-55	6
1326	Crystal growth of hexagonal boron nitride (hBN) from MgBN solvent system under high pressure. 2014 , 402, 308-311	32
1325	What's Next for Low-Dimensional Materials?. 2014 , 2, 1-9	13
1324	Rediscovering black phosphorus as an anisotropic layered material for optoelectronics and electronics. 2014 , 5, 4458	2389
1323	Contact properties to CVD-graphene on GaAs substrates for optoelectronic applications. 2014 , 25, 335707	16
1322	Colloquium: Graphene spectroscopy. 2014 , 86, 959-994	184
1321	Band gaps in incommensurable graphene on hexagonal boron nitride. 2014 , 89,	81
1320	Dirac materials. 2014 , 63, 1-76	589
		J29
1319	Surface-induced hybridization between graphene and titanium. 2014 , 8, 7704-13	33
1319 1318		
		33
1318	Dispersed CuD octahedrons on h-BN nanosheets for p-nitrophenol reduction. 2014 , 6, 14469-76 Graphene on hexagonal boron nitride. 2014 , 26, 303201	33
1318	Dispersed CuD octahedrons on h-BN nanosheets for p-nitrophenol reduction. 2014 , 6, 14469-76 Graphene on hexagonal boron nitride. 2014 , 26, 303201	33 201 61
1318 1317 1316	Dispersed CuD octahedrons on h-BN nanosheets for p-nitrophenol reduction. 2014, 6, 14469-76 Graphene on hexagonal boron nitride. 2014, 26, 303201 Graphene nanotransistors for RF charge detection. 2014, 47, 094004	33201615
1318 1317 1316 1315	Dispersed Cu® octahedrons on h-BN nanosheets for p-nitrophenol reduction. 2014, 6, 14469-76 Graphene on hexagonal boron nitride. 2014, 26, 303201 Graphene nanotransistors for RF charge detection. 2014, 47, 094004 Graphene digital phase shifter based on Defected Ground Structure for THz applications. 2014,	33 201 61 5

1311	Photovoltaic effect in an electrically tunable van der Waals heterojunction. 2014 , 14, 4785-91	759
1310	Photovoltaic effect in few-layer black phosphorus PN junctions defined by local electrostatic gating. 2014 , 5, 4651	555
1309	Selective deposition of graphene sheets on a flexible substrate by a nonuniform electric field. 2014 , 32, 020602	3
1308	Graphene: electrons en masse. <i>Nature Nanotechnology</i> , 2014 , 9, 575-6	6
1307	Graphene on boron-nitride: Moir[pattern in the van der Waals energy. 2014 , 104, 041909	60
1306	Stacking of Two-Dimensional Materials in Lateral and Vertical Directions. 2014 , 26, 4891-4903	84
1305	Structures, Energetics, and Electronic Properties of Multifarious Stacking Patterns for High-Buckled and Low-Buckled Silicene on the MoS2 Substrate. 2014 , 118, 19129-19138	67
1304	Proximity effect in graphene-topological-insulator heterostructures. 2014 , 112, 096802	83
1303	Analytical study of the energy levels in bilayer graphene quantum dots. 2014 , 78, 392-400	29
1302	Direct chemical vapor deposition growth of WS2 atomic layers on hexagonal boron nitride. 2014 , 8, 8273-7	234
1301	Band gap and effective mass of multilayer BN/graphene/BN: van der Waals density functional approach. 2014 , 115, 194304	7
1300	Observation of an intrinsic bandgap and Landau level renormalization in graphene/boron-nitride heterostructures. 2014 , 5, 4461	122
1299	Twist-controlled resonant tunnelling in graphene/boron nitride/graphene heterostructures. <i>Nature Nanotechnology</i> , 2014 , 9, 808-13	341
1298	Wafer-size free-standing single-crystalline graphene device arrays. 2014 , 105, 083118	3
1297	Impact of copper overpressure on the synthesis of hexagonal boron nitride atomic layers. 2014 , 6, 16755-62	15
1296	Anomalous sequence of quantum Hall liquids revealing a tunable Lifshitz transition in bilayer graphene. 2014 , 113, 116602	52
1295	Ultrathin Chemical Vapor Deposition (CVD)-Grown Hexagonal Boron Nitride as a High-Quality Dielectric for Tunneling Devices on Rigid and Flexible Substrates. 2014 , 118, 3340-3346	23
1294	Plasmon losses due to electron-phonon scattering: The case of graphene encapsulated in hexagonal boron nitride. 2014 , 90,	68

1293	Exceptional charge transport properties of graphene on germanium. 2014 , 8, 10237-45	31
1292	Vertical and in-plane heterostructures from WS2/MoS2 monolayers. 2014 , 13, 1135-42	1580
1291	Perfect mismatch. 2014 , 10, 709-711	1
1290	MoS 2 MoS2: choice substrate for accessing and tuning the electronic properties of graphene. 2014 , 113, 156804	65
1289	Piezoelectricity of single-atomic-layer MoS2 for energy conversion and piezotronics. 2014 , 514, 470-4	1360
1288	Gate-dependent pseudospin mixing in graphene/boron nitride moir uperlattices. 2014, 10, 743-747	53
1287	High thermal conductivity of suspended few-layer hexagonal boron nitride sheets. 2014 , 7, 1232-1240	157
1286	Van der Waals epitaxy and characterization of hexagonal boron nitride nanosheets on graphene. 2014 , 9, 367	20
1285	Indirect doping effects from impurities in MoS2/h-BN heterostructures. 2014 , 90,	36
1284	INVERSION OF THE ELECTRICAL AND OPTICAL PROPERTIES OF PARTIALLY OXIDIZED HEXAGONAL BORON NITRIDE. 2014 , 09, 1450002	6
1283	Configurable three-dimensional boron nitride-carbon architecture and its tunable electronic behavior with stable thermal performances. 2014 , 10, 2992-9	43
1282	Charge transport and rectification in molecular junctions formed with carbon-based electrodes. 2014 , 111, 10928-32	74
1281	Antenna-integrated 0.6 THz FET direct detectors based on CVD graphene. 2014 , 14, 5834-8	137
1280	Limitations to carrier mobility and phase-coherent transport in bilayer graphene. 2014 , 113, 126801	43
1279	Fabrication of ballistic suspended graphene with local-gating. 2014 , 79, 486-492	20
1278	Electronics based on two-dimensional materials. <i>Nature Nanotechnology</i> , 2014 , 9, 768-79 28.7	1953
1277	Boron Nitride Quasi-Nanoscale Fibers: Controlled Synthesis and Improvement on Thermal Properties of PHA Polymer. 2014 , 63, 794-799	6
1276	Reduced stability of copper interconnects due to wrinkles and steps on hexagonal boron nitride substrates. 2014 , 105, 123108	11

1275	Large-area monolayer hexagonal boron nitride on Pt foil. 2014 , 8, 8520-8	160
1274	Van der Waals Epitaxial Growth of Transition Metal Dichalcogenides on Pristine and N-Doped Graphene. 2014 , 14, 4920-4928	15
1273	Theoretical prediction of the mechanisms for defect healing or oxygen doping in a hexagonal boron nitride (h-BN) sheet with nitrogen vacancies by NO2 molecules. 2014 , 20, 2307	5
1272	Physical adsorption and charge transfer of molecular Br2 on graphene. 2014 , 8, 2943-50	54
1271	Transition Metal Embedded Two-Dimensional C3N4@raphene Nanocomposite: A Multifunctional Material. 2014 , 118, 15487-15494	81
1270	Coherent Tunneling and Negative Differential Conductivity in a Graphene/h-BN/Graphene Heterostructure. 2014 , 2,	38
1269	Phenomenological theory of second-harmonic generation from hexagonal centrosymmetric crystals. 2014 , 31, 607	2
1268	The Non-Equilibrium Green's Function Method for Nanoscale Device Simulation. 2014,	22
1267	Carbon nanotubes and graphene towards soft electronics. 2014 , 1, 15	81
1266	Surface effects on electronic transport of 2D chalcogenide thin films and nanostructures. 2014 , 1, 18	23
1265	A new horizon for hexagonal boron nitride film. 2014 , 64, 1605-1616	19
1264	Metallic behavior and enhanced adsorption energy of graphene on BN layer induced by Cu(111) substrate. 2014 , 64, 900-903	3
1263	Organic Field Effect Transistors Based on Graphene and Hexagonal Boron Nitride Heterostructures. 2014 , 24, 5157-5163	57
1262	Electronic transport in graphene: towards high mobility. 2014 , 199-227	17
1261	Electric field control of soliton motion and stacking in trilayer graphene. 2014 , 13, 786-9	71
1260	Monolayer Graphene on a hBN Underlay. 2014 , 19-32	
1259	Extrinsic origins of electronic disorder in 2D organic crystals. 2014 , 32, 030601	5
1258	Postgrowth tuning of the bandgap of single-layer molybdenum disulfide films by sulfur/selenium exchange. 2014 , 8, 4672-7	88

1257	Controlled LightMatter Interaction in Graphene Electrooptic Devices Using Nanophotonic Cavities and Waveguides. 2014 , 20, 95-105	16
1256	Optimization of Ni©r flux growth for hexagonal boron nitride single crystals. 2014 , 393, 114-118	42
1255	Multi-wall effects on the thermal transport properties of nanotube structures. 2014 , 25, 245703	3
1254	Electron mobility calculation for graphene on substrates. 2014 , 116, 083703	63
1253	Evolution of the Raman spectrum of graphene grown on copper upon oxidation of the substrate. 2014 , 7, 1613-1622	45
1252	Characterizing mechanical behavior of atomically thin films: A review. 2014 , 29, 338-347	31
1251	Lateral MoS2 p-n junction formed by chemical doping for use in high-performance optoelectronics. 2014 , 8, 9332-40	419
1250	Tailoring the electronic structure in bilayer molybdenum disulfide via interlayer twist. 2014 , 14, 3869-75	213
1249	Towards superlattices: Lateral bipolar multibarriers in graphene. 2014 , 89,	18
1248	Substrate dielectric effects on graphene field effect transistors. 2014 , 115, 194507	21
1247	Spin-orbit proximity effect in graphene. 2014 , 5, 4875	321
1246	Bilayer graphene. Tunable fractional quantum Hall phases in bilayer graphene. 2014 , 345, 61-4	113
1245	Measurement of collective dynamical mass of Dirac fermions in graphene. <i>Nature Nanotechnology</i> , 2014 , 9, 594-9	45
1244	Lattice-Contraction-Induced Moir[Patterns in Direction-Controlled Epitaxial Graphene on Cu(111). 2014 , 1, 1300080	10
1243	Fabry-PEot interference in gapped bilayer graphene with broken anti-Klein tunneling. 2014, 113, 116601	63
1242	Time resolved terahertz spectroscopy of low frequency electronic resonances and optical pump-induced terahertz photoconductivity in reduced graphene oxide membrane. 2014 , 80, 762-770	17
1241	Buried triple-gate structures for advanced field-effect transistor devices. 2014 , 119, 95-99	10
1240	Tuning on-off current ratio and field-effect mobility in a MoS(2)-graphene heterostructure via Schottky barrier modulation. 2014 , 8, 5790-8	207

1239	Ab initio study of structural and electronic properties of zigzag graphene nanoribbons on hexagonal boron nitride. 2014 , 55, 191-200	9
1238	Large scale thermal exfoliation and functionalization of boron nitride. 2014 , 10, 2352-5	148
1237	Catalytic transparency of hexagonal boron nitride on copper for chemical vapor deposition growth of large-area and high-quality graphene. 2014 , 8, 5478-83	43
1236	Transport fingerprints at graphene superlattice Dirac points induced by a boron nitride substrate. 2014 , 89,	8
1235	Structural and electronic properties of germanene/MoS2 monolayer and silicene/MoS2 monolayer superlattices. 2014 , 9, 110	61
1234	Strain tuning of magnetism in Mn doped MoS2 monolayer. 2014 , 26, 256003	23
1233	Effects of sulfur doping on graphene-based nanosheets for use as anode materials in lithium-ion batteries. 2014 , 262, 79-85	183
1232	Tunable phonon polaritons in atomically thin van der Waals crystals of boron nitride. 2014 , 343, 1125-9	695
1231	The effect of oxygen functional groups on the electrical transport behavior of a single piece multi-layered graphene oxide. 2014 , 191, 1-5	21
1230	Electron Beam Induced Deposition on graphene on silicon oxide and hexagonal boron nitride: A comparison of substrates. 2014 , 121, 122-126	3
1229	Bilayer graphene with long-range scatterers: Diamagnetism and weak-field Hall effect. 2014 , 58, 6-15	12
1228	Comparative study of metal atom adsorption on free-standing h-BN and h-BN/Ni (111) surfaces. 2014 , 299, 29-34	28
1227	Electronic and magnetic properties of 3d-metal trioxides superhalogen cluster-doped monolayer MoS2: A first-principles study. 2014 , 378, 1651-1656	18
1226	Raman study of damage extent in graphene nanostructures carved by high energy helium ion beam. 2014 , 72, 233-241	46
1225	Two-dimensional layered materials: Structure, properties, and prospects for device applications. 2014 , 29, 348-361	143
1224	Low-voltage graphene field-effect transistors based on octadecylphosphonic acid modified solution-processed high-k dielectrics. 2014 , 25, 265201	4
1223	Vertical heterostructures of layered metal chalcogenides by van der Waals epitaxy. 2014 , 14, 3047-54	118
1222	Persistent topological surface state at the interface of Bi2Se3 film grown on patterned graphene. 2014 , 8, 1154-60	30

1221	Field-Induced Superconductivity in Electric Double Layer Transistors. 2014 , 83, 032001	121
1220	Controlling the nanoscale rippling of graphene with SiO2 nanoparticles. 2014 , 6, 6030-6	17
1219	Graphene for Electron Devices: The Panorama of a Decade. 2014 , 2, 77-104	13
1218	Photoinduced doping in heterostructures of graphene and boron nitride. <i>Nature Nanotechnology</i> , 2014 , 9, 348-52	221
1217	Heterostructures produced from nanosheet-based inks. 2014 , 14, 3987-92	147
1216	Ab initio theory of moir superlattice bands in layered two-dimensional materials. 2014, 89,	155
1215	Probing substrate-dependent long-range surface structure of single-layer and multilayer MoS2 by low-energy electron microscopy and microprobe diffraction. 2014 , 89,	15
1214	Extraction and scattering analyses of 2D and bulk carriers in epitaxial graphene-on-SiC structure. 2014 , 63, 87-92	5
1213	Characterization of bulk hexagonal boron nitride single crystals grown by the metal flux technique. 2014 , 403, 110-113	24
1212	High mobility WSe2 p- and n-type field-effect transistors contacted by highly doped graphene for low-resistance contacts. 2014 , 14, 3594-601	341
1211	Analysis of vibrational properties of C-doped hexagonal boron nitride (h-BN). 2014 , 94, 225-233	6
1210	Emerging challenges and materials for thermal management of electronics. 2014 , 17, 163-174	897
1209	Numerical investigation of the effect of substrate surface roughness on the performance of zigzag graphene nanoribbon field effect transistors symmetrically doped with BN. 2014 , 5, 1569-74	13
1208	Terahertz Optoelectronic Property of Graphene: Substrate-Induced Effects on Plasmonic Characteristics. 2014 , 4, 28-41	21
1207	Quantitative analysis of interfacial reactions at a graphene/SiO2 interface using the discharge current analysis method. 2014 , 104, 151604	6
1206	Graphene-based Mid-infrared Photodetectors and Spin Transport Devices. 2014 , 57, 451-456	
1205	Colloidal and Epitaxial Quantum Dot Infrared Photodetectors: Growth, Performance, and Comparison. 2014 , 1-26	2
1204	Impact of thermal annealing on graphene devices encapsulated in hexagonal boron nitride. 2014 , 251, 2545-2550	12

Low-Temperature Scanning Capacitance Probe for Imaging Electron Motion. 2014 , 568, 032005	2
Thickness and rotational effects in simulated HRTEM images of graphene on hexagonal boron nitride. 2014 , 20, 1753-63	2
1201 Improvement of Wrinkles in Roll-to-Roll Microwave Plasma CVD Graphene. 2015 , 1761, 1	
1200 Flexible 2D FETs using hBN dielectrics. 2015 ,	7
Moir uperlattice effects in graphene/boron-nitride van der Waals heterostructures. 2015 , 527, 359-376	57
1198 Chemistry of Boron Nitride Nanosheets. 2015 , 386-427	1
Finding the right substrate support for magnetic superatom assembly from density functional calculations. 2015 , 91,	3
1196 Persistent current states in bilayer graphene. 2015 , 91,	7
Electronic response of graphene to linelike charge perturbations. 2015 , 91,	3
Physics of a disordered Dirac point in epitaxial graphene from temperature-dependent magnetotransport measurements. 2015 , 92,	8
Excitons in one-dimensional van der Waals materials: Sb2S3 nanoribbons. 2015 , 92,	21
1192 Magneto-optical response of graphene: Probing substrate interactions. 2015 , 92,	14
1191 Terahertz conductivity of graphene on boron nitride. 2015 , 92,	6
Local spectroscopy of moirfinduced electronic structure in gate-tunable twisted bilayer graphene. 2015, 92,	86
van der Waals bilayer energetics: Generalized stacking-fault energy of graphene, boron nitride, and graphene/boron nitride bilayers. 2015 , 92,	74
1188 Degenerate epitaxy-driven defects in monolayer silicon oxide on ruthenium. 2015 , 92,	10
Nonlocal transport and the hydrodynamic shear viscosity in graphene. 2015 , 92,	139
1186 Hot electron cooling in graphite: Supercollision versus hot phonon decay. 2015 , 92,	25

1185	Ballistic transport in graphene antidot lattices. 2015 , 92,	23
1184	Drift-induced modifications to the dynamical polarization of graphene. 2015 , 92,	20
1183	Lifting of the Landau level degeneracy in graphene devices in a tilted magnetic field. 2015, 92,	13
1182	Edge-state transport in graphene pfi junctions in the quantum Hall regime. 2015 , 92,	30
1181	Interaction-induced conductance from zero modes in a clean magnetic graphene waveguide. 2015 , 92,	4
1180	Infrared absorption of closely aligned heterostructures of monolayer and bilayer graphene with hexagonal boron nitride. 2015 , 92,	9
1179	Temperature-induced strain and doping in monolayer and bilayer isotopically labeled graphene. 2015 , 92,	41
1178	Tunneling in graphene E opological insulator hybrid devices. 2015 , 92,	13
1177	Oxygen-stabilized triangular defects in hexagonal boron nitride. 2015 , 92,	19
1176	Coherent and Tunable Terahertz Radiation from Graphene Surface Plasmon Polarirons Excited by Cyclotron Electron Beam. 2015 , 5, 16059	24
1175	Atomically Sharp Interface in an h-BN-epitaxial graphene van der Waals Heterostructure. 2015 , 5, 16465	50
1174	Fractal butterflies of Dirac fermions in monolayer and bilayer graphene. 2015 , 9, 19-29	4
1173	Vertical transport in graphene-hexagonal boron nitride heterostructure devices. 2015 , 5, 14519	25
1172	Low-temperature-grown continuous graphene films from benzene by chemical vapor deposition at ambient pressure. 2015 , 5, 17955	88
1171	Single Crystalline Film of Hexagonal Boron Nitride Atomic Monolayer by Controlling Nucleation Seeds and Domains. 2015 , 5, 16159	60
1170	Edge-Channel Transport of Dirac Fermions in Graphene Quantum Hall Junctions. 2015 , 84, 121007	3
1169	Scattering-type scanning near-field optical microscopy with reconstruction of vertical interaction. 2015 , 6, 8973	40
1168	Graphene Plasmonic Metasurfaces to Steer Infrared Light. 2015 , 5, 12423	165

1167	Bistability and pH Hysteresis of Graphene Oxide Solution in Circle AcidBase Titration. 2015 , 44, 454-456	O
1166	Growth and Features of Epitaxial Graphene on SiC. 2015 , 84, 121014	17
1165	Graphene circular polarization analyzer based on unidirectional excitation of plasmons. 2015 , 23, 32420-8	10
1164	Observation of reduced 1/f noise in graphene field effect transistors on boron nitride substrates. 2015 , 107, 113101	41
1163	Direct growth of graphene on in situ epitaxial hexagonal boron nitride flakes by plasma-assisted molecular beam epitaxy. 2015 , 107, 213103	33
1162	Suppression of 1/f noise in near-ballistic h-BN-graphene-h-BN heterostructure field-effect transistors. 2015 , 107, 023106	74
1161	Growth kinetics of white graphene (h-BN) on a planarised Ni foil surface. 2015 , 5, 11985	35
1160	Mobility enhancement in graphene transistors on low temperature pulsed laser deposited boron nitride. 2015 , 107, 203110	22
1159	Reexamination of basal plane thermal conductivity of suspended graphene samples measured by electro-thermal micro-bridge methods. 2015 , 5, 053206	32
1158	Capacitive coupling in hybrid graphene/GaAs nanostructures. 2015 , 107, 023105	2
1157	A van der Waals pn heterojunction with organic/inorganic semiconductors. 2015 , 107, 183103	62
1156	Atomically precise semiconductor-graphene and hBN interfaces by Ge intercalation. 2015 , 5, 17700	19
1155	Vibrational Properties of h-BN and h-BN-Graphene Heterostructures Probed by Inelastic Electron Tunneling Spectroscopy. 2015 , 5, 16642	52
1154	In-situ epitaxial growth of graphene/h-BN van der Waals heterostructures by molecular beam epitaxy. 2015 , 5, 14760	65
1153	Point contacts in encapsulated graphene. 2015 , 107, 183108	4
1152	Visibility of two-dimensional layered materials on various substrates. 2015 , 118, 145305	14
1151	Cooling of levitated graphene nanoplatelets in high vacuum. 2015 , 106, 244102	25
1150	Electrical level of defects in single-layer two-dimensional TiO2. 2015 , 5, 15989	8

1149	Imaging ballistic carrier trajectories in graphene using scanning gate microscopy. 2015 , 107, 243102	23
1148	A two-dimensional analytical model for short channel junctionless double-gate MOSFETs. 2015 , 5, 057122	25
1147	Imaging interfacial electrical transport in graphene-MoS heterostructures with electron-beam-induced-currents. 2015 , 107, 223104	17
1146	Thermal transport across few-layer boron nitride encased by silica. 2015 , 107, 031603	23
1145	Tunable positive and negative refraction of infrared radiation in graphene-dielectric multilayers. 2015 , 107, 191112	16
1144	Twist-controlled resonant tunnelling between monolayer and bilayer graphene. 2015 , 107, 203506	17
1143	Fabrication of Gate-tunable Graphene Devices for Scanning Tunneling Microscopy Studies with Coulomb Impurities. 2015 , e52711	6
1142	Individual Mo Dopant Atoms in WS2 Monolayers: Atomic Structure and Induced Strain. 2015 , 21, 435-436	3
1141	Tight-binding model for amine-terminated oligophenyl molecular junctions formed with carbon electrodes. 2015 , 66, 1499-1502	
1140	Self-Aligned Single-Crystalline Hexagonal Boron Nitride Arrays: Toward Higher Integrated Electronic Devices. 2015 , 1, 1500223	38
1139	Synthesis of Large-Sized Single-Crystal Hexagonal Boron Nitride Domains on Nickel Foils by Ion Beam Sputtering Deposition. 2015 , 27, 8109-15	60
1138	Highly Crumpled Boron Nitride Nanosheets as Adsorbents: Scalable Solvent-Less Production. 2015 , 2, 1400529	92
1137	BN-Enabled Epitaxy of Pb(1-x)Sn(x)Se Nanoplates on SiO//Si for High-Performance Mid-Infrared Detection. 2015 , 11, 5388-94	34
1136	Position-Controlled Selective Growth of ZnO Nanostructures and Their Heterostructures. 2015 , 173-229	2
1135	Nonvolatile Floating-Gate Memories Based on Stacked Black Phosphorus B oron Nitride M oS2 Heterostructures. 2015 , 25, 7360-7365	95
1134	High-Performance Monolayer WS2 Field-Effect Transistors on High-Dielectrics. 2015 , 27, 5230-4	177
1133	Two-Dimensional Layered Heterostructures Synthesized from Core-Shell Nanowires. 2015 , 54, 8957-60	64
1132	Band renormalization and spin polarization of MoS2 in graphene/MoS2 heterostructures. 2015 , 9, 701-706	12

1131	graphene and beyond. 2015 , 46, 217-230	13
1130	Graphen auf dem Weg zur Anwendung. 2015 , 46, 269-270	
1129	Large Single-Crystal Hexagonal Boron Nitride Monolayer Domains with Controlled Morphology and Straight Merging Boundaries. 2015 , 11, 4497-502	55
1128	Innovation and discovery of graphene-like materials via density-functional theory computations. 2015 , 5, 360-379	172
1127	Canted antiferromagnetic to ferromagnetic phase transition in bilayer graphene. 2015, 647, 012044	1
1126	Electronic Properties of Incommensurate Atomic Layers. 2015 , 84, 121001	23
1125	Two-Dimensional Layered Heterostructures Synthesized from CoreBhell Nanowires. 2015 , 127, 9085-9088	5
1124	Plasmonic mass and Johnson-Nyquist noise. 2015 , 26, 354002	1
1123	Controlled Synthesis of Organic/Inorganic van der Waals Solid for Tunable Light-Matter Interactions. 2015 , 27, 7800-8	94
1122	Integration of High-k Oxide on MoS2 by Using Ozone Pretreatment for High-Performance MoS2 Top-Gated Transistor with Thickness-Dependent Carrier Scattering Investigation. 2015 , 11, 5932-8	48
1121	Aligned Growth of Hexagonal Boron Nitride Monolayer on Germanium. 2015, 11, 5375-80	45
1120	Formation and thermal decomposition of oxynitride germanium compounds. 2015 , 50, 769-772	О
1119	A Van Der Waals Homojunction: Ideal p-n Diode Behavior in MoSe2. 2015 , 27, 5534-40	162
1118	A Self-Aligned High-Mobility Graphene Transistor: Decoupling the Channel with Fluorographene to Reduce Scattering. 2015 , 27, 6519-25	40
1117	Carrier Accumulation in Graphene with Electron Donor/Acceptor Molecules. 2015, 1, 1500073	10
1116	Evolution of temperature-induced strain and doping of double-layer graphene: An in situ Raman spectral mapping study. 2015 , 252, 2401-2406	9
1115	Photocurrent generation of a single-gate graphene p-n junction fabricated by interfacial modification. 2015 , 26, 385203	13
1114	Attenuation, dispersion and nonlinearity effects in graphene-based waveguides. 2015 , 6, 1221-8	4

1113	Review of Graphene Technology and Its Applications for Electronic Devices. 2015,	5
1112	Synthesis of Ternary Borocarbonitrides by High Temperature Pyrolysis of Ethane 1,2-Diamineborane. 2015 , 8, 5974-5985	10
1111	Recent Progress in the Growth and Applications of Graphene as a Smart Material: A Review. 2015 , 2,	63
1110	Tuning Electronic Structures of BN and C Double-Wall Hetero-Nanotubes. 2015 , 2015, 1-9	2
1109	Catalyst-Free Bottom-Up Synthesis of Few-Layer Hexagonal Boron Nitride Nanosheets. 2015 , 2015, 1-8	4
1108	The rare two-dimensional materials with Dirac cones. 2015 , 2, 22-39	243
1107	Thickness-dependent mobility in two-dimensional MoSIL ransistors. 2015, 7, 6255-60	54
1106	High-speed electro-optic modulator integrated with graphene-boron nitride heterostructure and photonic crystal nanocavity. 2015 , 15, 2001-5	111
1105	Persistent hysteresis in graphene-mica van der Waals heterostructures. 2015 , 26, 015202	17
1104	Gate-controlled mid-infrared light bending with aperiodic graphene nanoribbons array. 2015 , 26, 134002	41
1103	Electric field and substrateInduced modulation of spin-polarized transport in graphene nanoribbons on A3B5 semiconductors. 2015 , 117, 174309	28
1102	Development of high frequency and wide bandwidth Johnson noise thermometry. 2015 , 106, 023121	23
1101	Effect of WO3 precursor and sulfurization process on WS2 crystals growth by atmospheric pressure CVD. 2015 , 156, 156-160	28
1100	Atomic layer deposition of Y2O3 on h-BN for a gate stack in graphene FETs. 2015 , 26, 175708	12
1099	Modulation of Schottky barrier height in graphene/MoS2/metal vertical heterostructure with large current ONDFF ratio. 2015 , 54, 04DJ04	22
1098	Electronic, structural, and substrate effect properties of single-layer covalent organic frameworks. 2015 , 142, 184708	15
1097	Ultrafast Lateral Photo-Dember Effect in Graphene Induced by Nonequilibrium Hot Carrier Dynamics. 2015 , 15, 4234-9	26
1096	Epitaxial growth of a single-crystal hybridized boron nitride and graphene layer on a wide-band gap semiconductor. 2015 , 137, 6897-905	43

1095	Local doping of graphene devices by selective hydrogen adsorption. 2015 , 5, 017120	9
1094	Efficient photoinduced charge accumulation in reduced graphene oxide coupled with titania nanosheets to show highly enhanced and persistent conductance. 2015 , 7, 11436-43	19
1093	Indirect Band Gap Emission by Hot Electron Injection in Metal/MoSland Metal/WSell Heterojunctions. 2015 , 15, 3977-82	46
1092	Negative differential resistance in boron nitride graphene heterostructures: physical mechanisms and size scaling analysis. 2015 , 5, 10712	31
1091	Simulated scanning tunneling microscopy images of few-layer phosphorus capped by graphene and hexagonal boron nitride monolayers. 2015 , 91,	27
1090	Ultrasensitive graphene far-infrared power detectors. 2015 , 27, 164203	9
1089	Electrical Control of near-Field Energy Transfer between Quantum Dots and Two-Dimensional Semiconductors. 2015 , 15, 4374-80	81
1088	High Photoresponsivity and Short Photoresponse Times in Few-Layered WSe2 Transistors. 2015 , 7, 12080-8	87
1087	High carrier mobility in Si-MOSFETs with a hexagonal boron nitride buffer layer. 2015 , 209-210, 1-4	6
1086	Chlorine Radical Doping of a Few Layer Graphene with Low Damage. 2015 , 4, N5095-N5097	15
1085	Charge Transfer Excitons at van der Waals Interfaces. 2015 , 137, 8313-20	201
1084	Graphene/h-BN plasmon-phonon coupling and plasmon delocalization observed by infrared nano-spectroscopy. 2015 , 7, 11620-5	48
1083	Thermoelectric effects in graphene nanostructures. 2015 , 27, 133204	90
1082	Nanophotonics. 2015 , 351-370	
1081	Graphene transfer in vacuum yielding a high quality graphene. 2015 , 93, 286-294	24
1080	Quantized magneto-thermoelectric transport in low-dimensional junctions. 2015 , 109, 68003	2
1079	Towards intrinsic graphene biosensor: A label-free, suspended single crystalline graphene sensor for multiplex lung cancer tumor markers detection. 2015 , 72, 168-74	54
1078	Mechanical Control of Graphene on Engineered Pyramidal Strain Arrays. 2015 , 9, 5799-806	27

1077	High mobility flexible graphene field-effect transistors and ambipolar radio-frequency circuits. 2015 , 7, 10954-62	46
1076	Gate-modulated conductance of few-layer WSe2 field-effect transistors in the subgap regime: Schottky barrier transistor and subgap impurity states. 2015 , 106, 152104	27
1075	Band Gap Engineering of Boron Nitride by Graphene and Its Application as Positive Electrode Material in Asymmetric Supercapacitor Device. 2015 , 7, 14211-22	100
1074	Structures, stabilities, and electronic properties of defects in monolayer black phosphorus. 2015 , 5, 10848	72
1073	Fatigue Properties of ITO and Graphene on Flexible Substrates. 2015 , 15, 423-428	3
1072	Coherent phonon dynamics in single-layer and multilayer graphene. 2015 ,	1
1071	2D materials via liquid exfoliation: a review on fabrication and applications. 2015 , 60, 1994-2008	180
1070	Vertical field effect tunneling transistor based on graphene-ultrathin Si nanomembrane heterostructures. 2015 , 2, 044006	8
1069	Bandgap-tunable lateral and vertical heterostructures based on monolayer Mo1-x W x S2 alloys. 2015 , 8, 3261-3271	46
1068	Chemical Vapor Deposition Growth of Graphene and Related Materials. 2015 , 84, 121013	18
1067	Synthesis of Hexagonal Boron Nitride Monolayer: Control of Nucleation and Crystal Morphology. 2015 , 27, 8041-8047	153
1066	Proximity Effect Induced Electronic Properties of Graphene on BilleBe. 2015 , 9, 10861-6	31
1065	Arrayed liquid crystal microlens based on graphene electrode for imaging application. 2015,	1
1064	Radio-frequency transport Electromagnetic Properties of chemical vapour deposition graphene from direct current to 110 MHz. 2015 , 9, 46-51	2
1063	Graphene-based liquid crystal microlens arrays. 2015,	1
1062	Interface engineering of electronic properties of graphene/boron nitride lateral heterostructures. 2015 , 2, 041001	34
1061	High-Tc Layered Ferrielectric Crystals by Coherent Spinodal Decomposition. 2015 , 9, 12365-73	39
1060	Robust intrinsic ferromagnetism and half semiconductivity in stable two-dimensional single-layer chromium trihalides. 2015 , 3, 12457-12468	388

(2015-2015)

1059	Bandgap engineering in van der Waals heterostructures of blue phosphorene and MoS2: A first principles calculation. 2015 , 231, 64-69	48
1058	Quantification of misalignment in e-beam lithography due to height map error on optically non-uniform substrates for plasmonic nanoantennas. 2015 ,	
1057	Origin of 1/f noise in graphene produced for large-scale applications in electronics. 2015 , 9, 52-58	6
1056	Spotting 2D atomic layers on aluminum nitride thin films. 2015 , 26, 425202	6
1055	Bilayer graphene: physics and application outlook in photonics. 2015 , 4, 115-127	15
1054	Performance Improvement in SC-MLGNRs Interconnects Using Interlayer Dielectric Insertion. 2015 , 3, 470-482	14
1053	Controllable Schottky barriers between MoS2 and permalloy. 2014 , 4, 6928	56
1052	Composite fermions and broken symmetries in graphene. 2015 , 6, 5838	61
1051	Proximity-induced ferromagnetism in graphene revealed by the anomalous Hall effect. 2015 , 114, 016603	336
1050	Gate tunable quantum oscillations in air-stable and high mobility few-layer phosphorene heterostructures. 2015 , 2, 011001	172
1049	Layer-by-layer dielectric breakdown of hexagonal boron nitride. 2015 , 9, 916-21	120
1048	Magnetoresistance and charge transport in graphene governed by nitrogen dopants. 2015 , 9, 1360-6	46
1047	Electronic structure, phase stability and resistivity of hybrid hexagonal Cx(BN)1 two-dimensional nanomaterial: A first-principles study. 2015 , 69, 138-144	10
1046	Electronic transport of encapsulated graphene and WSe2 devices fabricated by pick-up of prepatterned hBN. 2015 , 15, 1898-903	98
1045	Intrinsic disorder in graphene on transition metal dichalcogenide heterostructures. 2015 , 15, 1925-9	33
1044	Development of solid-state nanopore fabrication technologies. 2015 , 60, 304-319	47
1043	Experimental and theoretical investigations of monolayer and few-layer talc. 2015 , 2, 015004	24
1042	A facile process to achieve hysteresis-free and fully stabilized graphene field-effect transistors. 2015 , 7, 4013-9	21

1041	Conductance oscillations induced by ballistic snake states in a graphene heterojunction. 2015 , 6, 6093	66
1040	Luminescent properties of a water-soluble conjugated polymer incorporating graphene-oxide quantum dots. 2015 , 16, 1258-62	18
1039	Microwave and hydrothermal syntheses of WSe2 micro/nanorods and their application in supercapacitors. 2015 , 5, 21700-21709	59
1038	Suppressed Thermal Conductivity of Bilayer Graphene with Vacancy-Initiated Linkages. 2015 , 119, 1748-1752	24
1037	Polytype Pure sp2-BN Thin Films As Dictated by the Substrate Crystal Structure. 2015 , 27, 1640-1645	24
1036	Extraction of the Interface State Density of Top-Gate Graphene Field-Effect Transistors. 2015 , 36, 408-410	13
1035	Ultimately short ballistic vertical graphene Josephson junctions. 2015 , 6, 6181	73
1034	Alkyl-chain-grafted hexagonal boron nitride nanoplatelets as oil-dispersible additives for friction and wear reduction. 2015 , 7, 3708-16	124
1033	Direct observation of interlayer hybridization and Dirac relativistic carriers in graphene/MoSDan der Waals heterostructures. 2015 , 15, 1135-40	142
1032	Scalable exfoliation process for highly soluble boron nitride nanoplatelets by hydroxide-assisted ball milling. 2015 , 15, 1238-44	379
1031	Optical phonons in twisted bilayer graphene with gate-induced asymmetric doping. 2015 , 15, 1203-10	18
1030	Interface-induced warping in hybrid two-dimensional materials. 2015 , 8, 2015-2023	13
1029	Progress in Large-Scale Production of Graphene. Part 2: Vapor Methods. 2015 , 67, 44-52	26
1028	Van der Waals heterostructures: Stacked 2D materials shed light. 2015 , 14, 264-5	167
1027	Organization of Artificial Superlattices Utilizing Nanosheets as a Building Block and Exploration of Their Advanced Functions. 2015 , 45, 111-127	33
1026	Ultrabroad Band Rainbow Capture and Releasing in Graded Chemical Potential Distributed Graphene Monolayer. 2015 , 10, 1023-1028	6
1025	Polymorphic Behavior and Enzymatic Degradation of Poly(butylene adipate) in the Presence of Hexagonal Boron Nitride Nanosheets. 2015 , 54, 1832-1841	34
1024	Is hexagonal boron nitride always good as a substrate for carbon nanotube-based devices?. 2015 , 17, 5072-7	6

1023	Scalable tight-binding model for graphene. 2015 , 114, 036601	58
1022	MoS2 Quantum Dot: Effects of Passivation, Additional Layer, and h-BN Substrate on Its Stability and Electronic Properties. 2015 , 119, 1565-1574	19
1021	First-Principles Study of Dislocation Slips in Impurity-Doped Graphene. 2015 , 119, 3418-3427	8
1020	Freestanding ZnO nanorod/graphene/ZnO nanorod epitaxial double heterostructure for improved piezoelectric nanogenerators. 2015 , 12, 268-277	56
1019	Atomically thin nonreciprocal optical isolation. 2014 , 4, 4190	32
1018	Ferroelectric-like SrTiO3 surface dipoles probed by graphene. 2014 , 4, 3657	28
1017	Photoluminescence quenching and charge transfer in artificial heterostacks of monolayer transition metal dichalcogenides and few-layer black phosphorus. 2015 , 9, 555-63	145
1016	Ferroelectric polymer nanocomposites for room-temperature electrocaloric refrigeration. 2015 , 27, 1450-4	157
1015	Probing the electron states and metal-insulator transition mechanisms in molybdenum disulphide vertical heterostructures. 2015 , 6, 6088	151
1014	Effect of Annealing in Ar/H2 Environment on Chemical Vapor Deposition-Grown Graphene Transferred With Poly (Methyl Methacrylate). 2015 , 14, 70-74	25
1013	Screening-induced surface polar optical phonon scattering in dual-gated graphene field effect transistors. 2015 , 461, 118-121	2
1012	Few-atomic-layer boron nitride nanosheets synthesized in solid thermal waves. 2015 , 5, 8579-8584	16
1011	van der Waals epitaxial ultrathin two-dimensional nonlayered semiconductor for highly efficient flexible optoelectronic devices. 2015 , 15, 1183-9	116
1010	Synthesis of large single-crystal hexagonal boron nitride grains on Cu-Ni alloy. 2015 , 6, 6160	258
1009	Controlled synthesis of single-crystal SnSe nanoplates. 2015 , 8, 288-295	170
1008	Growth and spectroscopic characterization of monolayer and few-layer hexagonal boron nitride on metal substrates. 2015 , 7, 3694-702	23
1007	Graphene for nanoelectronics. 2015 , 54, 040102	26
1006	Direct growth of large-area graphene and boron nitride heterostructures by a co-segregation method. 2015 , 6, 6519	173

1005	On-chip picosecond pulse detection and generation using graphene photoconductive switches. 2015 , 15, 1591-6	20
1004	Hexagonal boron nitride thin film thermal neutron detectors with high energy resolution of the reaction products. 2015 , 783, 121-127	43
1003	Origin of band gaps in graphene on hexagonal boron nitride. 2015 , 6, 6308	192
1002	Terahertz generation from surface plasmon polaritons in graphene induced by a moving electron beam. 2015 , 346, 149-153	3
1001	Multifunctional oxides for integrated manufacturing of efficient graphene electrodes for organic electronics. 2015 , 106, 063304	13
1000	Use of Terahertz Photoconductive Sources to Characterize Tunable Graphene RF Plasmonic Antennas. 2015 , 14, 390-396	45
999	Observation of long-lived interlayer excitons in monolayer MoSe2-WSe2 heterostructures. 2015 , 6, 6242	896
998	Waveguide-integrated black phosphorus photodetector with high responsivity and low dark current. 2015 , 9, 247-252	600
997	Strain tunable electronic and magnetic properties of pristine and semihydrogenated hexagonal boron phosphide. 2015 , 106, 043107	24
996	Tunnel magnetoresistance with atomically thin two-dimensional hexagonal boron nitride barriers. 2015 , 8, 1357-1364	72
995	Transport and particle-hole asymmetry in graphene on boron nitride. 2015 , 91,	27
994	Amplitude- and Phase-Resolved Nanospectral Imaging of Phonon Polaritons in Hexagonal Boron Nitride. 2015 , 2, 790-796	102
993	Interface Coupling in Twisted Multilayer Graphene by Resonant Raman Spectroscopy of Layer Breathing Modes. 2015 , 9, 7440-9	105
992	Destruction of anti-Klein tunneling induced by resonant states in bilayer graphene. 2015 , 48, 285102	5
991	Amphiphilic graphene oxide stabilisation of hexagonal BN and MoS2 sheets. 2015 , 51, 11709-12	26
990	Hyperbolic Plasmons and Topological Transitions Over Uniaxial Metasurfaces. 2015 , 114, 233901	193
989	Large optical anisotropy for terahertz light of stacked graphene ribbons with slight asymmetry. 2015 , 117, 174302	2
988	Electronic transport properties of transition metal dichalcogenide field-effect devices: surface and interface effects. 2015 , 44, 7715-36	282

(2015-2015)

987	Van der Waals Epitaxial Growth of Two-Dimensional Single-Crystalline GaSe Domains on Graphene. 2015 , 9, 8078-88	87
986	Interaction of BN- and BP-doped graphene nanoflakes with some representative neutral molecules and anions. 2015 , 113, 2916-2929	
985	Flexible high-temperature dielectric materials from polymer nanocomposites. 2015 , 523, 576-9	1017
984	Grain Boundary Structures and Electronic Properties of Hexagonal Boron Nitride on Cu(111). 2015 , 15, 5804-10	100
983	Two-Step Growth of Two-Dimensional WSe2/MoSe2 Heterostructures. 2015 , 15, 6135-41	401
982	Modelling of stacked 2D materials and devices. 2015 , 2, 032003	51
981	Revealing the planar chemistry of two-dimensional heterostructures at the atomic level. 2015 , 6, 7482	54
980	Ultrahigh-mobility graphene devices from chemical vapor deposition on reusable copper. 2015 , 1, e1500222	491
979	Aqueous dispersions of few-layer-thick chemically modified magnesium diboride nanosheets by ultrasonication assisted exfoliation. 2015 , 5, 10522	54
978	Interfacial Interactions in 1D and 2D Nanostructure-Based Material Systems. 2015 , 379-424	1
977	Large area CVD growth of graphene. 2015 , 210, 95-108	140
976	Ballistic Josephson junctions in edge-contacted graphene. <i>Nature Nanotechnology</i> , 2015 , 10, 761-4 28.7	151
975	Spin and charge transport in graphene-based spin transport devices with Co/MgO spin injection and spin detection electrodes. 2015 , 210, 42-55	9
974	Recent developments in black phosphorus transistors. 2015 , 3, 8760-8775	128
973	Uniaxial Strain Redistribution in Corrugated Graphene: Clamping, Sliding, Friction, and 2D Band Splitting. 2015 , 15, 5969-75	24
972	A Thermally Conductive Separator for Stable Li Metal Anodes. 2015 , 15, 6149-54	262
971	Synthesis and Development of Graphene-Inorganic Semiconductor Nanocomposites. 2015 , 115, 8294-343	199
970	Boron Nitride Surface Activity as Route to Composite Dielectric Films. 2015 , 7, 16913-6	20

969	Switching Behaviors of Graphene-Boron Nitride Nanotube Heterojunctions. 2015 , 5, 12238	16
968	Enhanced photovoltaic performances of graphene/Si solar cells by insertion of a MoSIthin film. 2015 , 7, 14476-82	93
967	Quality Heterostructures from Two-Dimensional Crystals Unstable in Air by Their Assembly in Inert Atmosphere. 2015 , 15, 4914-21	289
966	Graphene-like two-dimensional layered nanomaterials: applications in biosensors and nanomedicine. 2015 , 7, 14217-31	180
965	A molecular dynamics study of nanofracture in monolayer boron nitride. 2015 , 641, 225-230	31
964	Ultraclean and large-area monolayer hexagonal boron nitride on Cu foil using chemical vapor deposition. 2015 , 26, 275601	22
963	Raman shift and electrical properties of MoS2 bilayer on boron nitride substrate. 2015 , 26, 295702	13
962	Opening of triangular hole in triangular-shaped chemical vapor deposited hexagonal boron nitride crystal. 2015 , 5, 10426	36
961	Interplay of donor-acceptor interactions in stabilizing boron nitride compounds: insights from theory. 2015 , 17, 16525-35	11
960	CVD synthesis of $Mo((1-x))W(x)S2$ and $MoS(2(1-x))Se(2x)$ alloy monolayers aimed at tuning the bandgap of molybdenum disulfide. 2015 , 7, 13554-60	72
959	Interlayer interaction in general incommensurate atomic layers. 2015 , 17, 015014	60
958	Landau level spectroscopy of electron-electron interactions in graphene. 2015 , 114, 126804	49
957	Three-Dimensional Integration of Graphene via Swelling, Shrinking, and Adaptation. 2015, 15, 4525-31	39
956	High-mobility and air-stable single-layer WS2 field-effect transistors sandwiched between chemical vapor deposition-grown hexagonal BN films. 2015 , 5, 10699	187
955	A Cu(111) supported h-BN nanosheet: a potential low-cost and high-performance catalyst for CO oxidation. 2015 , 17, 22097-105	41
954	Elastic Deformations in 2D van der waals Heterostructures and their Impact on Optoelectronic Properties: Predictions from a Multiscale Computational Approach. 2015 , 5, 10872	65
953	First-principles study on electronic and magnetic properties of MnO3superhalogen cluster-doped bilayer graphene. 2015 , 48, 325002	1
952	Strain engineering in semiconducting two-dimensional crystals. 2015 , 27, 313201	266

951	Two-Photon Absorption in Graphene Enhanced by the Excitonic Fano Resonance. 2015 , 119, 16954-16961	18
950	Temperature dependent structural properties and bending rigidity of pristine and defective hexagonal boron nitride. 2015 , 27, 315302	32
949	Dual-gated BN-sandwiched multilayer graphene field-effect transistor fabricated by stamping transfer method and self-aligned contact. 2015 , 15, 1184-1187	5
948	A first principles approach to magnetic and optical properties in single-layer graphene sandwiched between boron nitride monolayers. 2015 , 2, 075601	3
947	Scalable Transfer of Suspended Two-Dimensional Single Crystals. 2015 , 15, 5089-97	33
946	Passivation of CdSe Quantum Dots by Graphene and MoS2 Monolayer Encapsulation. 2015 , 27, 5032-5039	13
945	Hamiltonian Optics of Hyperbolic Polaritons in Nanogranules. 2015 , 15, 4455-60	26
944	Highly Stable, Dual-Gated MoS2 Transistors Encapsulated by Hexagonal Boron Nitride with Gate-Controllable Contact, Resistance, and Threshold Voltage. 2015 , 9, 7019-26	256
943	Silane-catalysed fast growth of large single-crystalline graphene on hexagonal boron nitride. 2015 , 6, 6499	141
942	Versatile Single-Layer Sodium Phosphidostannate(II): Strain-Tunable Electronic Structure, Excellent Mechanical Flexibility, and an Ideal Gap for Photovoltaics. 2015 , 6, 2682-7	48
941	Synthesis, properties and applications of 2D non-graphene materials. 2015 , 26, 292001	82
940	Transmission Through Graphene Junctions with Rashba Spin-Orbit Coupling. 2015 , 127, 481-483	
939	CVD-Enabled Graphene Manufacture and Technology. 2015 , 6, 2714-21	89
938	Modifying the interlayer interaction in layered materials with an intense IR laser. 2015 , 114, 116102	17
937	Supercritical fluid processing: a rapid, one-pot exfoliation process for the production of surfactant-free hexagonal boron nitride nanosheets. 2015 , 17, 5895-5899	61
936	Interface engineering for high performance graphene electronic devices. 2015 , 2, 11	15
935	Suppressing bacterial interaction with copper surfaces through graphene and hexagonal-boron nitride coatings. 2015 , 7, 6430-7	48
934	Electrically configurable graphene field-effect transistors with a graded-potential gate. 2015 , 15, 3212-6	15

933	Photocurrent generation with two-dimensional van der Waals semiconductors. 2015 , 44, 3691-718	608
932	High Mobility of Graphene-Based Flexible Transparent Field Effect Transistors Doped with TiO2 and Nitrogen-Doped TiO2. 2015 , 7, 9453-61	27
931	Technology/circuit co-optimization and benchmarking for graphene interconnects at Sub-10nm technology node. 2015 ,	
930	Plasmon-induced optical anisotropy in hybrid graphene-metal nanoparticle systems. 2015 , 15, 3458-64	40
929	Iron-embedded boron nitride nanosheet as a promising electrocatalyst for the oxygen reduction reaction (ORR): A density functional theory (DFT) study. 2015 , 287, 431-438	83
928	Geometry, stability and thermal transport of hydrogenated graphene nanoquilts. 2015 , 213-214, 31-36	5
927	Hybrid structures of organic dye and graphene for ultrahigh gain photodetectors. 2015 , 88, 165-172	48
926	A grapheneBoron nitride lateral heterostructure has first-principles study of its growth, electronic properties, and chemical topology. 2015 , 3, 5918-5932	26
925	Scaling of graphene integrated circuits. 2015 , 7, 8076-83	14
924	All Chemical Vapor Deposition Growth of MoS2:h-BN Vertical van der Waals Heterostructures. 2015 , 9, 5246-54	285
924 923		
	, 9, 5246-54	
923	, 9, 5246-54 Crystal-oriented wrinkles with origami-type junctions in few-layer hexagonal boron nitride. 2015 , 8, 1680-1688	832
923 922	Crystal-oriented wrinkles with origami-type junctions in few-layer hexagonal boron nitride. 2015 , 8, 1680-1688 Directional excitation of graphene surface plasmons. 2015 , 23, 2383-91 Freestanding van der Waals heterostructures of graphene and transition metal dichalcogenides.	32
923 922 921	Crystal-oriented wrinkles with origami-type junctions in few-layer hexagonal boron nitride. 2015, 8, 1680-1688 Directional excitation of graphene surface plasmons. 2015, 23, 2383-91 Freestanding van der Waals heterostructures of graphene and transition metal dichalcogenides. 2015, 9, 4882-90 Defect Control and n-Doping of Encapsulated Graphene by Helium-Ion-Beam Irradiation. 2015, 15, 4006-12	32 132
923 922 921 920	Crystal-oriented wrinkles with origami-type junctions in few-layer hexagonal boron nitride. 2015, 8, 1680-1688 Directional excitation of graphene surface plasmons. 2015, 23, 2383-91 Freestanding van der Waals heterostructures of graphene and transition metal dichalcogenides. 2015, 9, 4882-90 Defect Control and n-Doping of Encapsulated Graphene by Helium-Ion-Beam Irradiation. 2015, 15, 4006-12	32 132 52
923 922 921 920 919	Crystal-oriented wrinkles with origami-type junctions in few-layer hexagonal boron nitride. 2015, 8, 1680-1688 Directional excitation of graphene surface plasmons. 2015, 23, 2383-91 Freestanding van der Waals heterostructures of graphene and transition metal dichalcogenides. 2015, 9, 4882-90 Defect Control and n-Doping of Encapsulated Graphene by Helium-Ion-Beam Irradiation. 2015, 15, 4006-12 Sharp Switching by Field-Effect Bandgap Modulation in All-Graphene Side-Gate Transistors. 2015, 3, 144-148 Technology/Circuit/System Co-Optimization and Benchmarking for Multilayer Graphene	32 132 52

(2015-2015)

915	Ultimate thin vertical p-n junction composed of two-dimensional layered molybdenum disulfide. 2015 , 6, 6564	231
914	Band Alignment in WSe2-Graphene Heterostructures. 2015 , 9, 4527-32	105
913	Single-step deposition of high-mobility graphene at reduced temperatures. 2015 , 6, 6620	153
912	Effects of dielectric material properties on graphene transistor performance. 2015 , 109, 8-11	17
911	Air-stable transport in graphene-contacted, fully encapsulated ultrathin black phosphorus-based field-effect transistors. 2015 , 9, 4138-45	393
910	Wetting of mono and few-layered WS2 and MoS2 films supported on Si/SiO2 substrates. 2015 , 9, 3023-31	156
909	Electron-beam induced nano-etching of suspended graphene. 2015 , 5, 7781	52
908	A graphene field-effect transistor as a molecule-specific probe of DNA nucleobases. 2015 , 6, 6563	73
907	Nanobiosensors and Nanobioanalyses. 2015 ,	7
906	Van der Waals heterostructures: Mid-infrared nanophotonics. 2015 , 14, 364-6	48
905	Thermal conductivity of boron nitride nanoribbons: Anisotropic effects and boundary scattering. 2015 , 94, 72-78	28
904	A predictive approach to CVD of crystalline layers of TMDs: the case of MoS2. 2015 , 7, 7802-10	93
903	Polyethylene-Assisted Exfoliation of Hexagonal Boron Nitride in Composite Fibers: A Combined Experimental and Computational Study. 2015 , 216, 847-855	18
902	Enhanced anode performance of micro/meso-porous reduced graphene oxide prepared from carbide-derived carbon for energy storage devices. 2015 , 91, 241-251	17
902		17 6
	carbide-derived carbon for energy storage devices. 2015 , 91, 241-251	
901	carbide-derived carbon for energy storage devices. 2015 , 91, 241-251 CVD Growth of High-Quality Single-Layer Graphene. 2015 , 3-20	6

897	Deterministic Two-Dimensional Polymorphism Growth of Hexagonal n-Type SnSIand Orthorhombic p-Type SnS Crystals. 2015 , 15, 3703-8	231
896	Towards Wafer-Scale Monocrystalline Graphene Growth and Characterization. 2015 , 11, 3512-28	46
895	Improving performance of armchair graphene nanoribbon field effect transistors via boron nitride doping. 2015 , 85, 522-529	12
894	Direct growth of nanocrystalline hexagonal boron nitride films on dielectric substrates. 2015 , 106, 101901	47
893	Tunable Light-Matter Interaction and the Role of Hyperbolicity in Graphene-hBN System. 2015 , 15, 3172-80	194
892	Transport properties of ultrathin black phosphorus on hexagonal boron nitride. 2015 , 106, 083505	77
891	van der Waals epitaxial growth of atomically thin Bißeland thickness-dependent topological phase transition. 2015 , 15, 2645-51	45
890	In situ synthesis of a large area boron nitride/graphene monolayer/boron nitride film by chemical vapor deposition. 2015 , 7, 7574-9	48
889	Recent Progress on Fabrications and Applications of Boron Nitride Nanomaterials: A Review. 2015 , 31, 589-598	199
888	Resonant Visible Light Modulation with Graphene. 2015 , 2, 550-558	61
887	Transport properties of pristine few-layer black phosphorus by van der Waals passivation in an inert atmosphere. 2015 , 6, 6647	394
886	Tunable graphene/indium phosphide heterostructure solar cells. 2015 , 13, 509-517	43
885	Corrosion resistance of graphene directly and locally grown on bulk nickel substrate by laser irradiation. 2015 , 5, 35384-35390	25
884	Adsorption of carbon monoxide, carbon dioxide and methane on hexagonal boron nitride with high titanium coverage. 2015 , 637-638, 48-52	5
883	Electron-transfer transparency of graphene: Fast reduction of metal ions on graphene-covered donor surfaces. 2015 , 9, 180-186	12
882	Graphene diamond-like carbon films heterostructure. 2015 , 106, 102108	7
881	Topological Winding Number Change and Broken Inversion Symmetry in a Hofstadter's Butterfly. 2015 , 15, 6395-9	18
880	Electrically and Magnetically Biased Graphene-Based Cylindrical Waveguides: Analysis and Applications as Reconfigurable Antennas. 2015 , 5, 951-960	69

(2015-2015)

879	Z-scan measurement of the nonlinear refractive index of monolayer WS(2). 2015, 23, 15616-23	92
878	Hyperbolic metasurfaces: surface plasmons, light-matter interactions, and physical implementation using graphene strips [Invited]. 2015 , 5, 2313	85
877	Strong interface-induced spin-orbit interaction in graphene on WS2. 2015 , 6, 8339	233
876	Suspended graphene devices with local gate control on an insulating substrate. 2015 , 26, 405201	5
875	Study on adsorption and desorption of ammonia on graphene. 2015 , 10, 359	32
874	Extremely large magnetoresistance in few-layer graphene/boron-nitride heterostructures. 2015, 6, 8337	70
873	Raman spectroscopy measurement of bilayer graphene's twist angle to boron nitride. 2015, 107, 033101	5
872	Interface effect on structural and electronic properties of graphdiyne adsorbed on SiO 2 and h-BN substrates: A first-principles study. 2015 , 24, 096806	
871	Z-scan measurement of nonlinear optical properties of BiOCl nanosheets. 2015 , 54, 6592-7	4
870	Large-Area, Transfer-Free, Oxide-Assisted Synthesis of Hexagonal Boron Nitride Films and Their Heterostructures with MoS2 and WS2. 2015 , 137, 13060-5	95
869	Characterization of nonlinear properties of black phosphorus nanoplatelets with femtosecond pulsed Z-scan measurements. 2015 , 40, 3480-3	80
868	Synthesis and Application of Monolayer Semiconductors (June 2015). 2015 , 51, 1-10	10
867	Superior Current Carrying Capacity of Boron Nitride Encapsulated Carbon Nanotubes with Zero-Dimensional Contacts. 2015 , 15, 6836-40	20
866	Ultrathin Two-Dimensional Nanomaterials. 2015 , 9, 9451-69	1342
865	Cleaning of pyrolytic hexagonal boron nitride surfaces. 2015 , 47, 798-803	9
864	Mid-infrared hyperbolic metamaterial based on graphene-dielectric multilayers. 2015,	3
863	Measurement of Lateral and Interfacial Thermal Conductivity of Single- and Bilayer MoS2 and MoSe2 Using Refined Optothermal Raman Technique. 2015 , 7, 25923-9	195
862	Thermal properties of graphene and few-layer graphene: applications in electronics. 2015 , 9, 4-12	64

861	First-Principles Study on Graphene/Hexagonal Boron Nitride Heterostructures. 2015, 84, 121002	19
860	Self-screened high performance multi-layer MoSII ransistor formed by using a bottom graphene electrode. 2015 , 7, 19273-81	27
859	Ferroelectric Single-Crystal Gated Graphene/Hexagonal-BN/Ferroelectric Field-Effect Transistor. 2015 , 9, 10729-36	46
858	Electronic Transport of Graphene Subjected to Periodic Structure Modulation. 2015 , 84, 121008	
857	Evidence for Defect-Mediated Tunneling in Hexagonal Boron Nitride-Based Junctions. 2015 , 15, 7329-33	62
856	Recent Advances in Two-Dimensional Materials beyond Graphene. 2015 , 9, 11509-39	1581
855	Exploration of sensitivity limit for graphene magnetic sensors. 2015 , 94, 585-589	24
854	Synthesis of large-area multilayer hexagonal boron nitride for high material performance. 2015 , 6, 8662	298
853	Pressure evolution of the potential barriers for transformations of layered BN to dense structures. 2015 , 5, 87550-87555	2
852	Striped nanoscale friction and edge rigidity of MoS2 layers. 2015 , 5, 92165-92173	13
851	Electronic and Mechanical Properties of Graphene-Germanium Interfaces Grown by Chemical Vapor Deposition. 2015 , 15, 7414-20	83
850	Tunable Fermi surface topology and Lifshitz transition in bilayer graphene. 2015 , 210, 19-31	18
849	Synthesis of atomically thin hexagonal boron nitride films on nickel foils by molecular beam epitaxy. 2015 , 106, 213108	68
848	Measuring the local quantum capacitance of graphene using a strongly coupled graphene nanoribbon. 2015 , 91,	12
847	Electric field modulation of Schottky barrier height in graphene/MoSe2 van der Waals heterointerface. 2015 , 107, 023109	66
846	Quantum Transport Detected by Strong Proximity Interaction at a Graphene-WS2 van der Waals Interface. 2015 , 15, 5682-8	16
845	Near-field radiation between graphene-covered carbon nanotube arrays. 2015 , 5, 053501	14
844	Electrostatically transparent graphene quantum-dot trap layers for efficient nonvolatile memory. 2015 , 106, 103105	11

843	Edge-channel interferometer at the graphene quantum Hall pn junction. 2015 , 106, 183101	22
842	Quantum Hall conductance of graphene combined with charge-trap memory operation. 2015 , 26, 345202	4
841	Two-Dimensional Atomic Crystals: Paving New Ways for Nanoelectronics. 2015 , 44, 4080-4097	5
840	Overview of carbon-based circuits and systems. 2015 ,	1
839	Localized charge carriers in graphene nanodevices. 2015 , 2, 031301	62
838	Fractional Quantum Hall States in Bilayer Graphene Probed by Transconductance Fluctuations. 2015 , 15, 7445-51	24
837	Laser Controllable Growth of Graphene via Ni-Cu Alloy Composition Modulation. 2015 , 2, 219-230	4
836	Properties of Self-Aligned Short-Channel Graphene Field-Effect Transistors Based on Boron-Nitride-Dielectric Encapsulation and Edge Contacts. 2015 , 62, 4322-4326	15
835	Anisotropic in-plane thermal conductivity observed in few-layer black phosphorus. 2015 , 6, 8572	426
834	Functionalized boron nitride porous solids. 2015 , 5, 93964-93968	59
833	Tunable GaTe-MoS2 van der Waals p-n Junctions with Novel Optoelectronic Performance. 2015 , 15, 7558-66	303
832	Creating a Nanospace under an h-BN Cover for Adlayer Growth on Nickel(111). 2015 , 9, 11589-98	32
831	Exciton-polaritons in van der Waals heterostructures embedded in tunable microcavities. 2015 , 6, 8579	275
830	Whispering-gallery mode quantum resonators in graphene. 2015 , 7, e218-e218	2
829	Noise in Graphene Superlattices Grown on Hexagonal Boron Nitride. 2015 , 9, 11382-8	13
828	Two-dimensional transition metal dichalcogenide alloys: preparation, characterization and applications. 2015 , 7, 18392-401	157
827	Graphene-Based Thermopile for Thermal Imaging Applications. 2015 , 15, 7211-6	57
826	Chemically Modulated Band Gap in Bilayer Graphene Memory Transistors with High On/Off Ratio. 2015 , 9, 9034-42	46

825	Fabrication and electrical properties of single wall carbon nanotube channel and graphene electrode based transistors arrays. 2015 , 107, 033103	4
824	Growth mechanism and modification of electronic and magnetic properties of silicene. 2015 , 24, 087303	5
823	Characterization and manipulation of individual defects in insulating hexagonal boron nitride using scanning tunnelling microscopy. <i>Nature Nanotechnology</i> , 2015 , 10, 949-53	148
822	Dynamical conductivity of gated AA-stacking multilayer graphene with spinBrbital coupling. 2015 , 5, 32511-32519	
821	Electronic structure and ultrafast charge transfer dynamics of phosphorous doped graphene layers on a copper substrate: a combined spectroscopic study. 2015 , 5, 74189-74197	17
820	Strain induced mobility modulation in single-layer MoS2. 2015 , 48, 375104	31
819	Chemical vapor deposition growth of large-scale hexagonal boron nitride with controllable orientation. 2015 , 8, 3164-3176	131
818	Measurement Back-Action in Stacked Graphene Quantum Dots. 2015 , 15, 6003-8	30
817	Substrates and coating for graphene based devices. 2015,	
816	I-V characteristics of in-plane and out-of-plane strained edge-hydrogenated armchair graphene nanoribbons. 2015 , 117, 244504	1
815	Direct Growth of Single- and Few-Layer MoS2 on h-BN with Preferred Relative Rotation Angles. 2015 , 15, 6324-31	152
814	Vertical heterostructures of MoS2 and graphene nanoribbons grown by two-step chemical vapor deposition for high-gain photodetectors. 2015 , 17, 25210-5	19
813	Growth of Large-Area Graphene Single Crystals in Confined Reaction Space with Diffusion-Driven Chemical Vapor Deposition. 2015 , 27, 6249-6258	48
812	Topological Bloch bands in graphene superlattices. 2015 , 112, 10879-83	61
811	Wettability of water droplet on misoriented graphene bilayer sructure: A molecular dynamics study. 2015 , 5, 067150	10
810	Cooling hot spots by hexagonal boron nitride heat spreaders. 2015,	4
809	Triplet excitations in graphene-based systems. 2015 , 109, 47005	1
808	In-Plane Anisotropy in Mono- and Few-Layer ReS2 Probed by Raman Spectroscopy and Scanning Transmission Electron Microscopy. 2015 , 15, 5667-72	327

807	Flexible Graphene Field-Effect Transistors Encapsulated in Hexagonal Boron Nitride. 2015, 9, 8953-9	87
806	Structural, electronic and optical properties of a hybrid triazine-based graphitic carbon nitride and graphene nanocomposite. 2015 , 17, 23613-8	22
805	Single layer lead iodide: computational exploration of structural, electronic and optical properties, strain induced band modulation and the role of spin-orbital-coupling. 2015 , 7, 15168-74	67
804	Synthesis of in-plane and stacked graphene/hexagonal boron nitride heterostructures by combining with ion beam sputtering deposition and chemical vapor deposition. 2015 , 7, 16046-53	56
803	Broadband silicon optical modulator using a graphene-integrated hybrid plasmonic waveguide. 2015 , 26, 365201	32
802	Design of ultra-broadband graphene absorber using circuit theory. 2015 , 32, 1941	90
801	Electric Field Tunable Band Gap in Bi-Axially Strained Graphene/Hexagonal Boron Nitride Super-Lattice. 2015 , 66, 1-10	1
800	Nanoelectromechanical Sensors Based on Suspended 2D Materials. 2020 , 2020, 8748602	39
799	Measuring the Thickness of Flakes of Hexagonal Boron Nitride Using the Change in Zero-Contrast Wavelength of Optical Contrast. 2015 , 19, 503-507	2
798	Transferring Few-Layer Graphene Sheets on Hexagonal Boron Nitride Substrates for Fabrication of Graphene Devices. 2014 , 03, 25-35	18
797	Quantum Field Theory of Graphene with Dynamical Partial Symmetry Breaking. 2014, 05, 984-994	4
796	Thermal Modulation of Photoluminescence from Single-Layer MoS2. 2014 , 35, 3077-3080	9
795	Toward Charge Neutralization of CVD Graphene. 2015 , 24, 268-272	2
794	Structural, Optical, and Electrical Characterization of p-type Graphene for Various AuCl3Doping Concentrations. 2013 , 22, 270-275	1
793	Significance of Boron Nitride in Composites and Its Applications.	3
792	Polyvilylidenefluoride-based Nanocomposite Films Induced-by Exfoliated Boron Nitride Nanosheets with Controlled Orientation. 2015 , 28, 270-276	1
791	Graphene/h-BN Moiré superlattice. 2015 , 64, 077305	5
790	Novel p-n junctions based on ambipolar two-dimensional crystals. 2017 , 66, 217302	2

7 ⁸ 9	Synthesis and characterization of graphene nanoribbons on hexagonal boron nitride. 2019 , 68, 168102	1
788	Carrier Transport Properties of the Field Effect Transistors with Graphene Channel Prepared by Chemical Vapor Deposition. 2012 , 51, 06FD03	12
787	Electronic Structure Modulation of Graphene by Metal Electrodes. 2012, 51, 085102	7
786	Hole Defects on Two-Dimensional Materials Formed by Electron Beam Irradiation: Toward Nanopore Devices. 2015 , 45, 107-114	32
785	Raman Spectroscopic Studies on Two-Dimensional Materials. 2015 , 45, 126-130	24
784	Probing the Atomic Structures of Synthetic Monolayer and Bilayer Hexagonal Boron Nitride Using Electron Microscopy. 2016 , 46, 217-226	2
783	Experimental Technicalities. 2021 , 71-84	
782	First-principles study on the electronic structures and contact properties of graphene/XC (X = P, As, Sb, and Bi) van der Waals heterostructures. 2021 , 23, 25136-25142	1
781	Review of Rhombohedral Graphite. 2021 , 1-40	
780	2D material hybrid heterostructures: achievements and challenges towards high throughput fabrication.	1
779	Quantum transport study in three-dimensional topological insulator BiSbTeSe2. 2021 , 108, 73-124	
778	Proximity Effect of Epitaxial Iron Phthalocyanine Molecules on High-Quality Graphene Devices. 2021 , 38, 087201	1
777	2D Materials for Solar Cell Applications. 2021 , 227-267	
776	Correlated Insulating States and Transport Signature of Superconductivity in Twisted Trilayer Graphene Superlattices. 2021 , 127, 166802	4
775	Visualization of Transition Metal Decoration on h-BN Surface. 2021,	1
774	Synthesis of emerging two-dimensional (2D) materials [Advances, challenges and prospects. 2021 , 30, 100305	5
773	Fabrication of thermally conductive polymer composites based on hexagonal boron nitride: recent progresses and prospects. 2021 , 2, 042002	0
772	Steering on Degrees of Freedom of 2D Van der Waals Heterostructures. 2100033	4

(2015-2021)

771	Visualization of a hexagonal born nitride monolayer on an ultra-thin gold film via reflected light microscopy. 2021 , 33,	О
770	Gas-Phase Fluorination of Hexagonal Boron Nitride. 2021 , e2106084	2
769	Thin-film electronics based on all-2D van der Waals heterostructures. 1-15	О
768	Constructing a new 2D Janus black phosphorus/SMoSe heterostructure for spontaneous wide-spectral-responsive photocatalytic overall water splitting. 2021 ,	3
767	Printed Flexible Thin-Film Transistors. 2022 , 257-345	О
766	Tunable contacts and device performances in graphene/group-III monochalcogenides MX (M = In, Ga; X = S, Se) van der Waals heterostructures. 2021 , 130, 144303	2
765	Nonlinear intensity dependence of edge photocurrents in graphene induced by terahertz radiation. 2021 , 104,	1
764	High Field Quantum Hall Effect in Disordered Graphene Near the Dirac Point. 2012, 61-73	
763	Tunable Magnetic Properties of Rhombohedral Graphite Thin Films: Effects of Insulating Substrate on Magnetic Properties. 2012 , 51, 02BN04	
762	Anisotropic Electronic Transport of Graphene on a Nano-Patterned Substrate. 2012 , 21, 279-285	1
761	Electronic Transport in Graphene. 2012 , 59-94	
760	Structural and Optical Characterizations of VO2Film on Graphene/Sapphire Substrate by Post-annealing after Sputtering. 2013 , 22, 98-104	
759	Nanosession: Carbon-Based Molecular Systems. 461-469	
758	INDUCED BANDGAP AND MAGNETIC BEHAVIOR IN ZIGZAG GRAPHENE NANORIBBONS ON HEXAGONAL NITRIDE BORON: EDGE AND SUBSTRATE EFFECTS. 2013 , 13, 75-87	1
757	Optical Spectroscopy of Graphene/Boron Nitride Hetrostructures. 2014 ,	1
756	Applications to Terahertz and Infrared Detectors with Graphene. 2014 , 42, 645	
755	Device Architecture and Biosensing Applications for Attractive One- and Two-Dimensional Nanostructures. 2015 , 41-70	
754	Beyond graphene. 2015 , 2015, 11-20	

753	Nanoboron Nitrides. 2015, 3-32	1
75 ²	Graphene-Based Ultra-Broadband Slow-Light System and Plamonic Whispering-Gallery-Mode Nanoresonators. 2016 , 169-190	
751	Scanning tunneling microscopy study of h-BN thin films grown on Cu foils. 2016 , 65, 116801	
750	First-principles study on the structure stability and doping performance of double layer h-BN/Graphene. 2016 , 65, 136101	1
749	Encyclopedia of Nanotechnology. 2016 , 1346-1357	
748	12 Current Topics in Graphene and Carbon Nanotube Research. 2016 , 223-246	
747	Structure, Stabilities, and Electronic Properties of Smart Ceramic Composites. 2017 , 113-131	
746	Introduction. 2017 , 1-15	
745	Logical integration device for two-dimensional semiconductor transition metal sulfide. 2017 , 66, 218503	4
744	Design of Optical and Radiative Properties of Surfaces. 2017 , 1-46	
743	Defect Characterization and Metrology. 2017 , 631-678	
742	Chapter 11: Perspective. 2017 , 177-186	
741	Background. 2018 , 7-36	
740	Two-dimensional graphene electronics: current status and prospects. 2018 , 188, 1249-1287	1
739	Reliable and High Spatial Resolution Method to Identify the Number of MoS2 Layers Using a Scanning Electron Microscopy. 2017 , 27, 705-709	1
738	Structure and band structure of epitaxial graphene on hexagonal silicon carbide. 2018 , 689-715	
737	Electronic transport properties of epigraphene. 2018 , 716-722	
736	Tuning the electronic and magnetic property of semihydrogenated graphene and monolayer boron nitride heterostructure. 2018 . 67. 167101	1

Nanomechanical Electro-Optical Modulator Based on Atomic Heterostructures. 2018, 65-82 735 Direct Synthesis of van der Waals Solids. 2018, 73-87 734 Energy band and Hall resistivity, longitudinal resistivity and Shubnikov-de Haas oscillation in 1 733 graphenes (II). **2018**, 2018, 60-79 Ultra-compact optical switch based on Fano resonance in graphene-functionalized plasmonic 732 nano-cavity. 2018, A broadband graphene absorber based on alternating structure of MgF2 and SiO2. 2018, 731 Josephson Effect in Graphene and 3D Topological Insulators. 2019, 529-553 730 Fabrication and Characterisation Techniques. 2019, 33-51 729 728 Studying Superlattice Kinks via Electronic Transport. **2019**, 53-70 Stability and electronic structure of hydrogenated two-dimensional transition metal 727 3 dichalcogenides: First-principles study. 2019, 68, 037102 Interfacial interaction and Schottky contact of two-dimensional WS2/graphene heterostructure. 6 726 2019, 68, 097101 Nanoscale Thermal Transport in Low Dimensional Materials. 2019, 101-118 725 First-principles study of metal-graphene edge contact for ballistic Josephson junction. 2019, 3, 724 Modal properties of a cylindrical graphene-coated nanowire deposited on a hexagonal boron 2 nitride substrate. 2019, 58, 6666-6671 Growth of Two-dimensional Materials and Their In-plane Heterostructures by Thermal Chemical 722 Vapor Deposition. **2019**, 62, 593-598 Electronic and Optical Properties of Sn Doped Hexagonal BN Monolayer: A First-principles Study. 721 1 2020, Hafnene on Ir(111). **2020**, 37-46 720 Two-Dimensional Hexagonal Boron Nitride and Borophenes. 2020, 303-336 719 1 Signature of pseudodiffusive transport in mesoscopic topological insulators. 2020, 2, 718

717	Theoretical prediction of superconductivity in monolayer h-BN doped with alkaline-earth metals (Ca, Sr, Ba). 2020 , 32, 435002	2
716	Imaging the flow of holes from a collimating contact in graphene. 2020 , 35, 09LT02	
715	Recent advances in 2D materials-based UV photodetectors: A Review.	2
714	Optical pulse modulators based on layered vanadium diselenide nanosheets. 2021 , 33,	
713	Comprehensive search for buckled honeycomb binary compounds based on noble metals (Cu, Ag, and Au). 2021 , 5,	1
712	Optical Inspection of 2D Materials: From Mechanical Exfoliation to Wafer-Scale Growth and Beyond. 2021 , e2102128	2
711	Radiative lifetime of free excitons in hexagonal boron nitride. 2021 , 104,	1
710	Van der Waals Heterostructures in Photocatalytic Energy Conversion. 2022 , 225-274	
709	Recent Advances in Structural Engineering of 2D Hexagonal Boron Nitride Electrocatalysts. 2021 , 91, 106661	6
708	Observation of metallic electronic structure in a single-atomic-layer oxide. 2021 , 12, 6171	5
707	Direct growth of hexagonal boron nitride on non-metallic substrates and its heterostructures with graphene. 2021 , 24, 103374	5
706	Design of high extinction ratio silicon electro optic modulator based on coupled hybrid plasmonic waveguide using graphene. 2021 , 160, 107061	O
705	Interlayer Interactions in Low-Dimensional Layered Hetero-structures: Modeling and Applications. 2020 , 635-659	
704	Layer-Dependent Band Structure of Ternary Metal Chalcogenides: Thickness-Controlled Hexagonal FeIn2S4. 2021 , 33, 164-176	O
703	Thermoelectric transport in coupled double layers with interlayer excitons and exciton condensation. 2020 , 102, 235304	1
702	Progress on band structure engineering of twisted bilayer and two-dimensional moir heterostructures. 2020 , 29, 127304	4
701	Band gap variation in bi, tri and few-layered 2D graphene/hBN heterostructures. 2022 , 341, 114553	1
700	A comprehensive review on planar boron nitride nanomaterials: From 2D nanosheets towards 0D quantum dots. 2022 , 124, 100884	8

699	Effects of spin-orbit coupling on the electronic properties of the buckled IIIIV monolayers. 2022 , 543, 168638	O
698	Mechanical and electronic properties of boron nitride nanosheets with graphene domains under strain 2021 , 11, 35127-35140	
697	Introduction. 2020 , 1-11	
696	Tuning Schottky barrier in graphene/InSe van der Waals heterostructures by electric field. 2020 , 69, 157302	1
695	On the Ballistic Motion of Electrons in PdCoO(_text {2}). 2020 , 35-98	
694	Introduction. 2020 , 1-26	
693	Synthesis of photonic crystal fiber based on graphene directly grown on air-hole by chemical vapor deposition. 2020 , 69, 194202	O
692	Theoretical study on Schottky regulation of WSe2/graphene heterostructure doped with nonmetallic elements. 2020 , 69, 117101	2
691	Dynamics of excited interlayer states in hexagonal boron nitride monolayers. 2020, 53, 203001	3
690	Recent progress in the CVD growth of 2D vertical heterostructures based on transition-metal dichalcogenides.	1
689	Interactions in stanene centred van der Waals trilayers structures of boron-nitride and graphene: effect of mirror symmetry on electronic interactions. 2020 , 32, 265001	1
688	Ion-Selective Membrane-Coated Graphene-Hexagonal Boron Nitride Heterostructures for Field-Effect Ion Sensing. 2021 , 6, 30281-30291	O
687	Twist the doorknob to open the electronic properties of graphene-based van der Waals structure. 2021 , 4, 3444-3482	3
686	Role of metal contacts on the electric and thermoelectric response of hBN/WSe2 based transistors. 2021 , 130, 185102	О
685	A Facile Liquid-Phase, Solvent-Dependent Exfoliation of Large Scale MoS2 Nanosheets and Study of Their Photoconductive Behaviour for UV-Photodetector Application. 2021 , 6, 11285-11292	3
684	Subatomic species transport through atomically thin membranes: Present and future applications. 2021 , 374, eabd7687	10
683	Distinguishing viscous, ballistic, and diffusive current flows in anisotropic metals. 2021 , 104,	0
682	Recent Advances on 2D Materials towards 3D Printing. 2021 , 3, 1314-1343	3

681	Scalably Nanomanufactured Atomically Thin Materials-Based Wearable Health Sensors. 2100120	3
680	In-memory computing with emerging nonvolatile memory devices. 2021 , 64, 1	6
679	Direct growth of hexagonal boron nitride films on dielectric sapphire substrates by pulsed laser deposition for optoelectronic applications. 2021 ,	3
678	Analytical method for designing tunable terahertz absorbers with the desired frequency and bandwidth. 2021 , 29, 39777-39787	3
677	Recent Progress in the Transfer of Graphene Films and Nanostructures 2021 , 5, e2100771	3
676	Structural and Magnetic Behavior of MoS2 on Doping of Transition Metals: a DFT Study. 2021 , 34, 3441	O
675	Metallihsulator transition in few-layered GaTe transistors. 2020 , 41, 072902	0
674	Twistronics in graphene-based van der Waals structures. 2020 , 29, 117303	7
673	Low field hall effect for differentiating between the single- and double-layer graphenes. 2021 , 54, 015306	
672	Role of defects and grain boundaries in the thermal response of wafer-scale hBN films. 2021 , 32, 075702	1
671	Photoresist-enabled assembly of BN/graphene/BN heterostructure and fabrication of one-dimensional contact electrode. 2020 , 7, 116405	
670	Sensitive detection of water/oxygen molecule adsorption and reaction on a titanium oxide nanosheet with a graphene field effect transistor. 2020 , 1, 030022	
669	Mechanical removal of surface residues on graphene for TEM characterizations. 2020 , 50, 28	4
668	Graphene Field-Effect Transistor on a Calcium Fluoride Substrate. 2020 , 77, 879-883	O
667	Feasibility of a Dual-Gate Graphene Transistor to Test Various Gate Dielectrics for Two-Dimensional Device Application. 2020 , 77, 888-892	
666	Electron-Enhanced Atomic Layer Deposition of Boron Nitride Thin Films at Room Temperature and 100 °C. 2018 , 122,	1
665	Tuning single-electron charging and interactions between compressible Landau level islands in graphene. 2020 , 101,	2
664	Synthesis, characterization, properties and applications of two-dimensional magnetic materials. 2022 , 42, 101338	8

Photocurrent generation in graphene/h-BN heterostructures under solar illumination. **2022**, 276, 115540

662	Graphene-enabled wearable sensors for healthcare monitoring. 2022 , 197, 113777	14
661	Superatoms as Building Blocks of 2D Materials. 2021 , 209-255	
660	Orbital gating driven by giant Stark effect in tunneling phototransistors. 2021 , e2106625	1
659	Effect of electric field on two-dimensional honeycomb structures from group (Ⅲ☑). 2021 , 162, 110507	1
658	Flexible and quasi-isotropically thermoconductive polyimide films by guided assembly of boron nitride nanoplate/boron nitride flakes for microelectronic application. 2021 , 431, 133740	5
657	2½ Type PVDF-Based Composites Interlayered by Epitaxial (111)-Oriented BTO Films for High Energy Storage Density. 2108496	8
656	Characterization of RF magnetron-sputtered a-BOxNy/ZnO MIS structures for transparent electronics. 1	
655	An investigation of the coupling of phonon-polaritons with plasmon-polaritons in hBN/nanopatterned Au layered devices. 2021 , 130, 193101	О
654	Theoretical study of SnS2 encapsulated in Graphene as a promising anode material for K-ion batteries. 2021 ,	
653	Using graphene conductors to enhance the functionality of atom chips. 2021 , 104,	0
652	Quasistationary near-gate plasmons in van der Waals heterostructures. 2021 , 104,	1
651	Optical and dielectric properties of MoO3 nanosheets for van der Waals heterostructures. 2021 , 119, 223104	2
650	Determination of the Spin Axis in Quantum Spin Hall Insulator Candidate Monolayer WTe2. 2021 , 11,	2
649	Van der Waals Heterostructure of Hexagonal Boron Nitride with an AlGaN/GaN Epitaxial Wafer for High-Performance Radio Frequency Applications. 2021 ,	3
648	Room-temperature non-Dirac quantum anomalous Hall states, half semiconductors, and strain-tuned half metals in monolayer zirconium trihalide. 2021 , 104,	O
647	Recent Developments in van der Waals Antiferromagnetic 2D Materials: Synthesis, Characterization, and Device Implementation. 2021 ,	9
646	Anomalous electrical transport in orientationally controlled trinary hybrids of graphene and twisted bilayer molybdenum disulphide. 2021 , 44, 1	

645	In situ microscopy techniques for characterizing the mechanical properties and deformation behavior of two-dimensional (2D) materials. 2021 , 51, 247-247	2
644	Thickness-dependent enhanced optoelectronic performance of surface charge transfer-doped ReS2 photodetectors. 1	3
643	Experimental and Simulation Research on the Preparation of Carbon Nano-Materials by Chemical Vapor Deposition. 2021 , 14,	1
642	A Comprehensive Review on Recent Advances in Two-Dimensional (2D) Hexagonal Boron Nitride.	3
641	Approaching the intrinsic exciton physics limit in two-dimensional semiconductor diodes. 2021 , 599, 404-410	7
640	Hot carrier dynamics and electron-optical phonon coupling in photoexcited graphene via time-resolved ultrabroadband terahertz spectroscopy. 2021 , 3,	1
639	Spin-orbit coupling and interactions in quantum Hall states of graphene/WSe2 heterobilayers. 2021 , 104,	
638	Molecular Approach to Engineer Two-Dimensional Devices for CMOS and beyond-CMOS Applications. 2021 ,	7
637	Multiterminal Inverse AC Josephson Effect. 2021 , 21, 9668-9674	1
636	Tailoring Dirac Plasmons via Anisotropic Dielectric Environment by Design. 2021 , 16,	О
635	Interlayer Interactions in 1D Van der Waals Moir (Superlattices. 2021, e2103460	5
634	Optimum design for the ballistic diode based on graphene field-effect transistors. 2021 , 5,	1
633	Synthesis of Large Area Graphitic Carbon Nitride Nanosheet by Chemical Vapor Deposition.	
632	Surface adsorption of nitrosourea on pristine and doped (Al, Ga and In) boron nitride nanosheets as anticancer drug carriers: the DFT and COSMO insights 2021 , 11, 36866-36883	4
631	Mechanical Strain and Electric Field Tunable Electronic Structure of Black/Violet Phosphorene Van Der Waals Heterostructure: From Type I to Z-Scheme System.	
630	Mixed magnetic edge states in graphene quantum dots. 2022 , 5, 014001	
629	Electrical Characterization of Individual Boron Nitride Nanowall Structures. 2022, 17-23	
628	Enhanced terahertz detection of multigate graphene nanostructures. 2021,	2

627	Analysis of hybrid plasmon-phonon-polariton modes in hBN/graphene/hBN stacks for mid-infrared waveguiding 2022 , 30, 2863-2876	О
626	Facile synthesis of an organic/inorganic hybrid 2D structure tincone film by molecular layer deposition 2022 ,	1
625	Magnetron co-sputtered th-thick Mollu films as structural material with low heat extension for key parts of high-power millimeter-band vacuum microelectronic devices. 2022 , 40, 014201	0
624	Apparent Colors of 2D Materials. 2100221	2
623	Geometric interference in a high-mobility graphene annulus p-n junction device. 2022 , 105,	0
622	Turbostratic stacked graphene-based high-responsivity mid-wavelength infrared detector using an enhanced photogating effect. 2022 , 12, 458	1
621	Optimization of Mechanically Assembled Van Der Waals Heterostructure Based On Solution Immersion and Hot Plate Heating. 2022 , 2152, 012007	0
620	Self-energy corrected band-gap tuning induced by strain in the hexagonal boron phosphide monolayer. 2022 , 203, 111144	O
619	Field-induced semiconductorEnetal transition of hybrid ZnO and graphene nanocomposites. 2022 , 203, 111138	
618	Phonon-assisted Interfacial Charge Transfer Excitons in Graphene/h-BN van der Waals Heterostructures. 2022 , 76, 110-120	1
617	First-principles calculations of molecular adsorption on the surface of two-dimensional BCOH. 2022 , 555, 111442	0
616	Preparation of ZnO/Ti3C2Tx/Nafion/Au electrode. 2022 , 175, 107068	O
615	Synthesis of large area graphitic carbon nitride nanosheet by chemical vapor deposition. 2022 , 900, 163310	0
614	Superconductivity in the calcium-decorated hexagonal boron nitride monolayer. 2022 , 548, 168927	1
613	Thermal Conductivities and Interfacial Thermal Conductance of 2D WSe2. 2020 ,	1
612	Continuous orientated growth of scaled single-crystal 2D monolayer films. 2021 , 3, 6545-6567	O
611	Optical and Electrical Properties of Graphene, Few Layer Graphene, and Boron Nitride. 2021, 229-294	
610	The Interaction of Light with Solids: An Overview of Optical Characterization. 2021 , 1-60	

609	Highly-anisotropic carrier transport and optical properties of two-dimensional titanium trisulfide. 2022 , 57, 3486-3496	3
608	All About the Interface: Do Residual Contaminants at A High-Quality h-BN Monolayer Perylene Diimide Interface Cause Charge Trapping?. 2101701	O
607	Effect of Strain on Excitons in Van Der Waals Solids. 2022 ,	
606	ReviewRecent Advances in Graphene-Based Field-Effect-Transistor Biosensors: A Review on Biosensor Designing Strategy.	O
605	Self-aligned stitching growth of centimeter-scale quasi-single-crystalline hexagonal boron nitride monolayers on liquid copper 2022 ,	0
604	Correlation between morphology and local mechanical and electrical properties of van der Waals heterostructures 2021 ,	O
603	Topological invariants in two-dimensional quasicrystals. 2022 , 4,	O
602	Porous monolith of few-layered boron nitride for effective water cleanup. 2022 , 10, 846-854	2
601	Intervalley Excitonic Hybridization, Optical Selection Rules, and Imperfect Circular Dichroism in Monolayer h-BN 2022 , 128, 047402	O
600	Vertical 1D/2D Heterojunction Architectures for Self-Powered Photodetection Application: GaN Nanorods Grown on Transition Metal Dichalcogenides 2022 ,	5
599	Theoretical study of anisotropy and ultra-low thermal conductance of porous graphene nanoribbons. 2022 , 71, 027803	O
598	Microscopic understanding of exceptional orientation-dependent tensile and fracture responses of two-dimensional transition-metal carbides. 2022 , 585, 152557	O
597	van der Waals graphene/MoS2 heterostructures: tuning the electronic properties and Schottky barrier by applying a biaxial strain. 2022 , 3, 624-631	3
596	Fabrication Technologies for the On-Chip Integration of 2D Materials 2022 , e2101435	8
595	Design and fabrication of a large-range graphene/hexagonal boron nitride heterostructure based pressure sensor with poly(methyl methacrylate) substrate 2022 , 93, 015009	Ο
594	First principles studies on infrared band structure and absorption of As/Sb lateral heterostructures. 2022 , 131, 023101	O
593	Effect of Interlayer Coupling and Symmetry on High-Order Harmonic Generation from Monolayer and Bilayer Hexagonal Boron Nitride. 2022 , 14, 84	1
592	Trions in MoS2 are quantum superpositions of intra- and intervalley spin states. 2022 , 105,	O

591 Magnetoconductance modulations due to interlayer tunneling in radial superlattices.. **2022**,

590	Electronically Tunable Transparent Conductive Thin Films for Scalable Integration of 2D Materials with Passive 2DBD Interfaces. 2111343	O
589	Influence of h-BN on electronic properties of GeS/InSe heterojunction. 2022, 128, 1	
588	Perspective on 2D material polaritons and innovative fabrication techniques. 2022 , 120, 040501	2
587	A BN monolayer: a direct band gap semiconductor with high and highly anisotropic carrier mobility 2022 ,	О
586	Synthesis of layered nanomaterials. 2022,	
585	Ferroelectric polymer composites for capacitive energy storage. 2022 , 477-502	
584	A van der Waals Integrated Damage-Free Memristor Based on Layered 2D Hexagonal Boron Nitride 2022 , e2106253	2
583	Recent Progress in Improving the Performance of Infrared Photodetectors via Optical Field Manipulations 2022 , 22,	4
582	Reconfigurable InSe Electronics with van der Waals Integration. 2101176	1
581	Influence of the hBN Dielectric Layers on the Quantum Transport Properties of MoS Transistors 2022 , 15,	1
580	Two-Dimensional Materials for Future Terahertz Wireless Communications. 2022 , 3, 217-228	4
579	Experimental and theoretical characterization of the interfacial adhesion of 2D heterogeneous materials: A review. 1-18	О
578	The thermal oxidation of hexagonal boron nitride single crystals: Dry and ambient air compared. 1	O
577	First-principles investigation of copper diffusion barrier performance in defective 2D layered materials 2022 ,	0
576	Universal co-existence of photovoltaics and ferroelectricity from a two-dimensional 3R bilayer BX (X = P, As, Sb). 2022 , 10, 1048-1061	O
575	Two-dimensional reconfigurable electronics enabled by asymmetric floating gate. 1	1
574	Introduction. 2022, 1-21	

573	Facile fabrication of 2D material multilayers and vdW heterostructures with multimodal microscopy and AFM characterization. 2022 ,	0
572	Recent Advances on Tuning the Interlayer Coupling and Properties in van der Waals Heterostructures 2022 , e2105877	4
57 ¹	Novel transport phenomena in graphene induced by strong spin-orbit interaction. 2021 , 22, 1-18	Ο
57°	Revealing Dielectric Screening in Twisted Graphene Devices. 2022 , 19,	
569	Excitonic devices with van der Waals heterostructures: valleytronics meets twistronics.	15
568	A Review of Recent Progress in Molecular Dynamics and Coarse-Grain Simulations Assisted Understanding of Wettability. 1	2
567	Positron charge sensing using a double-gated graphene field effect transistor 2022 , 93, 015002	
566	Recent Advances in Growth of Transition Metal Carbides and Nitrides (MXenes) Crystals. 2111357	7
565	Transfer Printing of Perovskite Whispering Gallery Mode Laser Cavities by Thermal Release Tape 2022 , 17, 8	1
564	A bright future for engineering piezoelectric 2D crystals 2021 ,	3
563	Interfacial charge and energy transfer in van der Waals heterojunctions.	6
563 562	Interfacial charge and energy transfer in van der Waals heterojunctions. Epitaxy of 2D Materials toward Single Crystals 2022 , e2105201	6
562	Epitaxy of 2D Materials toward Single Crystals 2022 , e2105201	1
562 561	Epitaxy of 2D Materials toward Single Crystals 2022, e2105201 Dielectric permittivity, conductivity and breakdown 🗄 d of hexagonal boron nitride.	2
562 561 560	Epitaxy of 2D Materials toward Single Crystals 2022, e2105201 Dielectric permittivity, conductivity and breakdown Bld of hexagonal boron nitride. Flexible 2D Materials beyond Graphene: Synthesis, Properties, and Applications 2022, e2105383 Direct band gap and anisotropic transport of ZnSb monolayers tuned by hydrogenation and strain	1 2 13
562 561 560 559	Epitaxy of 2D Materials toward Single Crystals 2022, e2105201 Dielectric permittivity, conductivity and breakdown Bld of hexagonal boron nitride. Flexible 2D Materials beyond Graphene: Synthesis, Properties, and Applications 2022, e2105383 Direct band gap and anisotropic transport of ZnSb monolayers tuned by hydrogenation and strain 2022, 12, 2693-2700	1 2 13 0

555	Aligned Stacking of Nanopatterned 2D Materials for High-Resolution 3D Device Fabrication 2022,	О
554	Field-Effect Transistor Based on MoSi2N4 and WSi2N4 Monolayers Under Biaxial Strain: A Computational Study of the Electronic Properties. 2022 , 69, 863-869	3
553	Raman spectra of twisted bilayer graphene close to the magic angle. 2022 , 9, 025007	3
552	Vibrational Properties in Highly Strained Hexagonal Boron Nitride Bubbles 2022,	2
551	Giant Magnetoresistance in a Chemical Vapor Deposition Graphene Constriction 2022,	
550	Plasmonic nanostructure integrated two - dimensional materials for optoelectronic devices.	1
549	Stability and Bandgap Engineering of InGaSe Monolayer 2022 , 12,	
548	Robust type-I band alignment in ZnS nanowire/MoTe2 nanotube van der Waals heterostructures. 2022 , 791, 139370	О
547	2D materials for organic and perovskite photovoltaics. 2022 , 94, 106833	1
546	Interfacial polarization regulation of ultrathin 2D nanosheets inducing high energy storage density of polymer-based nanocomposite with opposite gradient architecture. 2022 , 46, 503-511	3
545	Growth of wafer-scale graphene-hexagonal boron nitride vertical heterostructures with clear interfaces for obtaining atomically thin electrical analogs 2022 ,	2
544	Graphene moir uperlattices with giant quantum nonlinearity of chiral Bloch electrons <i>Nature Nanotechnology</i> , 2022 ,	3
543	2D Heterostructures for Ubiquitous Electronics and Optoelectronics: Principles, Opportunities, and Challenges 2022 ,	28
542	All Solution-Processed van der Waals Heterostructures for Wafer-Scale Electronics 2021 , e2106110	10
541	Thermal currents obtained and mutually switched by a modified Haldane model in graphene.	О
540	Directional etching for high aspect ratio nano-trenches on hexagonal boron nitride by catalytic metal particles.	1
539	Mechanical Behavior of Blisters Spontaneously Formed by Multilayer 2D Materials. 2101939	1
538	Homogeneous Palladium Diselenide pn-Junction Diodes for Reconfigurable Circuit Applications. 2101282	Ο

537	Layered 2D Nanomaterials to Tailor Friction and Wear in Machine Elements A Review. 2022, 9, 2101622	15
536	Crossover from Linear Chains to a Honeycomb Network for the Nucleation of Hexagonal Boron Nitride Grown on the Ni(111) Surface. 2021 , 125, 26542-26551	21
535	Few-Layer WS-WSe Lateral Heterostructures: Influence of the Gas Precursor Selenium/Tungsten Ratio on the Number of Layers 2021 ,	2
534	Realization of electronic-grade two-dimensional transition metal dichalcogenides by thin-film deposition techniques. 2022 , 159-193	
533	High-Performance All-Optical Modulator Based on Graphene-hBN Heterostructures. 2022, 1-1	O
532	Introduction. 2022 , 1-5	
531	Novel charm of 2D materials engineering in memristor: when electronics encounter layered morphology 2022 ,	8
530	Nonvolatile MOX RRAM assisted by graphene and 2D materials. 2022 , 399-443	
529	Doping effects on the antibonding states and carriers of two-dimensional PC 2022,	0
528	A DFT Study on the Potential Application of Graphene-Like Pure and Doped Boron Phosphide Monolayer in Li- and Na-Ion Batteries. 2022 , 96, 125-134	
527	Devices and defects in two-dimensional materials: outlook and perspectives. 2022, 339-401	
526	Construction and physical properties of low-dimensional structures for nanoscale electronic devices 2022 ,	1
525	Prediction of high Curie-temperature intrinsic ferromagnetic semiconductors and quantum anomalous Hall states in XBr3 (X = Cu, Ag, Au) monolayers.	1
524	2D material based heterostructures for solar light driven photocatalytic H2 production.	4
523	Challenges in synthesis of heterostructures.	O
522	???????????. 2022,	1
521	Broadband and high-performance SnS2/FePS3/graphene van der Waals heterojunction photodetector. 2022 , 120, 081101	1
520	Low-threshold single-mode laser in perovskite microdiscs direct-synthesized into planar microcavity. 2022 , 120, 071110	1

519	Two-dimensional Materials for all-solid-state Lithium Batteries 2021, e2108079	8
518	Structural, electronic, and transport properties of 1D Ta2Ni3Se8 semiconducting material. 2022 , 120, 073101	Ο
517	Photodetection Tuning with High Absorptivity Using Stacked 2D Heterostructure Films 2022, 12,	1
516	Nanometer-Scale Lateral p-n Junctions in Graphene/RuCl Heterostructures 2022,	2
515	Spatiotemporally controlled room-temperature exciton transport under dynamic strain. 2022 , 16, 242-247	2
514	Phonon Lifetimes in Boron-Isotope-Enriched Graphene- Hexagonal Boron Nitride Devices. 2200030	
513	Electric fields and substrates dramatically accelerate spin relaxation in graphene. 2022, 105,	O
512	Graphene-based SiC Van der Waals heterostructures: nonequilibrium molecular dynamics simulation study 2022 , 28, 88	
511	2D Materials for Wearable Energy Harvesting. 2101623	1
510	Rectifying Effect in a High-Performance Ballistic Diode Bridge Based on Encapsulated Graphene with a Unique Design.	O
509	An In Situ Spectral Monitoring Scheme for Advanced Manufacturing of Novel Nanodevices. 2022 , 2022, 1-10	
508	Two-dimensional weak topological insulators in inversion-symmetric crystals. 2022, 105,	1
507	Two-dimensional ferromagnetism detected by proximity-coupled quantum Hall effect of graphene. 2022 , 7,	1
506	Challenges and opportunities in 2D heterostructures for electronic and optoelectronic devices 2022 , 25, 103942	4
505	Fluorinated Graphene Contacts and Passivation Layer for MoS 2 Field Effect Transistors. 2101370	
504	Hyperbolic phonon polaritons with positive and negative phase velocities in suspended M oO3. 2022 , 120, 113101	5
503	2D Ultrawide Bandgap Semiconductors: Odyssey and Challenges 2022 , e2101348	2
502	Interior and Edge Magnetization in Thin Exfoliated CrGeTe Films 2022,	2

501	Dry Transfer Process of Single-Layer Graphene on Multi-Layer Hexagonal Boron Nitride for High Quality Heterostructure. 1055, 171-178	
500	Edge State Quantum Interference in Twisted Graphitic Interfaces 2022 , e2102261	
499	Synthesis of transition metal dichalcogenide van der Waals heterostructures through chemical vapor deposition 2022 ,	О
498	Wrinkle-Free Graphene Films on Fluorinated Self-Assembled Monolayer-Modified Substrates for Enhancing the Electrical Performance of Transistors.	O
497	Spatial Control of Graphene Functionalization by Patterning a 2D Substrate: Implications for Graphene Based van-der-Waals Heterostructures.	O
496	Electronic structure of 2D van der Waals crystals and heterostructures investigated by spatially-and angle-resolved photoemission. 2021 , 22, 107-131	
495	A conductive AFM study of carbon-rich hexagonal (BN)C semiconductor alloys. 1	
494	2D materials shrink superconducting qubits 2022 , 21, 381-382	O
493	Highly accurate, reliable, and non-contaminating two-dimensional material transfer system. 2022 , 9, 011419	О
492	Constructing van der Waals heterostructures by dry-transfer assembly for novel optoelectronic device 2022 ,	O
491	Nanoscale graphene plasmonics logic gate based on the plasma dispersion effect. 2022 , 54, 1	
490	A green and facile method to fabricate multifunctional and highly thermally conductive boron nitride-based polymer composites. 52307	O
489	Excitonic response of AA? and AB stacked hBN bilayers. 2022 , 105,	2
488	Existence of BeCN and Its First-Principles Phase Diagram: Be and C Introducing Structural Diversity 2022 ,	3
487	First-principles Study of a New BP2 Two-dimensional Material.	
486	Effect of fully functionalization on carrier mobility of two-dimensional BN. 2022 , 346, 114698	
485	Growth and characterization of uniformly distributed triangular single-crystalline hexagonal boron nitride grains on liquid copper surface.	
484	Science of 2.5 dimensional materials: paradigm shift of materials science toward future social innovation 2022 , 23, 275-299	4

483	Mechanisms of Interface Cleaning in Heterostructures Made from Polymer-Contaminated Graphene 2022 , e2201248	2
482	Tungsten nanoparticle anchoring on boron nitride nanosheet-based polymer nanocomposites for complex radiation shielding. 2022 , 221, 109353	4
481	Dynamics of Interfacial Bubble Controls Adhesion Mechanics in Van der Waals Heterostructure 2022 ,	0
480	Revealing the superlative electrochemical properties of o-B2N2 monolayer in Lithium/Sodium-ion batteries. 2022 , 96, 107066	6
479	Hexagonal boron nitride film on sapphire substrate grown by low-pressure and high-temperature halide vapor phase epitaxy. 2022 , 588, 126655	
478	Experimental evidence of a mixed amorphous-crystalline graphene/SiC interface due to oxygen-intercalation. 2022 , 30, 101906	
477	Tunable electronic and magnetic properties of two-dimensional magnetic semiconductor VIBr2. 2022 , 209, 111319	3
476	Hierarchical ZnO/MXene (Nb2C and V2C) heterostructure with efficient electron transfer for enhanced photocatalytic activity. 2022 , 590, 153095	3
475	Enhanced magnetic anisotropy in two-dimensional 2HIIaS2 by self-intercalation: A DFT study. 2022 , 553, 168988	0
474	Modulation of strain on electronic structure and contact type of BP/SnS van der waals heterostructure. 2022 , 55, 125102	1
473	Synthesis of Nanostructured Boron Nitride Aerogels by Rapid Pyrolysis of Melamine Diborate Aerogels via Induction Heating: From Composition Adjustment to Property Studies. 2021 , 4, 13788-13797	2
472	Role of the Spatial Distribution of Gas Flow for Tuning the Vertical/Planar Growth of Nonlayered Two-Dimensional Nanoplates. 2022 , 22, 763-771	Ο
471	Synthesis of Atomically Thin h-BN Layers Using BCl and NH by Sequential-Pulsed Chemical Vapor Deposition on Cu Foil 2021 , 12,	1
470	Band Structure Engineering of WSe 2 Homo-Junction Interfaces via Thickness Control. 2022 , 9, 2101763	1
469	Enhanced catalysis through structurally modified hybrid 2-D boron nitride nanosheets comprising of complexed 2-hydroxy-4-methoxybenzophenone motif 2021 , 11, 24429	Ο
468	Emergence and Tuning of Multiple Flat Bands in Twisted Bilayer EGraphyne 2021 , 12, 12283-12291	Ο
467	Optical Imaging of Redox and Molecular Diffusion in 2D van der Waals Space 2021 ,	1
466	Efficient Suppression of Charge Recombination in Self-Powered Photodetectors with Band-Aligned Transferred van der Waals Metal Electrodes 2021 , 13, 61799-61808	3

465	Plasmon excitation in \$\$hbox {MoS}_{2}/\$\$graphene van der waals heterostructures. 2022 , 96, 1	
464	A wafer-scale van der Waals dielectric made from an inorganic molecular crystal film. 2021 , 4, 906-913	16
463	Colloidal PbS QDs heterostructure photodetector based on high-quality graphene. 2021,	
462	Coulomb Drag between a Carbon Nanotube and Monolayer Graphene 2021 , 127, 257701	О
461	Perspectives of 2D Materials for Optoelectronic Integration. 2022 , 32, 2110119	9
460	Free Trions with Near-Unity Quantum Yield in Monolayer MoSe 2021,	2
459	Broadband high-efficiency near-infrared graphene phase modulators enabled by metallianoribbon integrated hybrid plasmonic waveguides. 2022 , 11, 613-623	0
458	Two-dimensional noble transition-metal dichalcogenides for nanophotonics and optoelectronics: Status and prospects. 2022 , 15, 3675-3694	4
457	Bidirectional switchable beam splitter/filter based graphene loaded Si ring resonators. 2021 , 96, 125536	О
456	New van der Waals Heterostructures Based on Borophene and Rhenium Sulfide/Selenide for Photovoltaics: An Ab Initio Study. 2021 , 11, 11636	
455	Quantum Oscillations in Two-Dimensional Insulators Induced by Graphite Gates 2021 , 127, 247702	4
454	Broadband Optical Constants and Nonlinear Properties of SnS and SnSe 2021 , 12,	1
453	Excitonic effects in graphene-like C3N. 2022 , 6,	0
452	Two-Dimensional Field-Effect Transistor Sensors: The Road toward Commercialization 2022,	9
451	Adsorption of Water Molecule in Graphene/MoS2 Heterostructure with Vacancy Defects in Mo Sites. 2022 , 2022, 1-18	
450	Potential Anodic Application of 2D h-AlC for Li and Na-ions Batteries. 2022 , 153424	5
449	Preparation and photoelectric characterization of p-GeSe/p-WS2 heterojunction devices.	0
448	Full 2ltunable phase modulation using avoided crossing of resonances 2022 , 13, 2103	1

447	Dissipation-enabled hydrodynamic conductivity in a tunable bandgap semiconductor 2022 , 8, eabi8481	1
446	Gate-Controlled Quantum Dots Based on 2D Materials. 2100162	2
445	Entangled two-plasmon generation in carbon nanotubes and graphene-coated wires. 2022, 105,	
444	Performance Enhancement of SnS/-BN Heterostructure p-Type FET via the Thermodynamically Predicted Surface Oxide Conversion Method 2022 ,	O
443	Crystal Orientation Control of Hexagonal Boron Nitride/Graphene Heterostructure. 2022, 65, 190-195	
442	Fundamentals of Chemical Vapor Deposition of Atomic Layer Materials. 2022 , 65, 169-176	
441	Substrate roughness and crystal orientation-controlled growth of ultra-thin BN films deposited on Cu foils. 2022 , 128,	1
440	The Magnetic Genome of Two-Dimensional van der Waals Materials 2022,	10
439	An atomistic approach for the structural and electronic properties of twisted bilayer graphene-boron nitride heterostructures. 2022 , 8,	O
438	Anomalies at the Dirac Point in Graphene and Its Hole-Doped Compositions 2022 , 128, 166401	O
437	Strain engineering in optoelectronic properties of MoSi2N4 monolayer: ultrahigh tunability.	О
436	2D materials-enabled optical modulators: From visible to terahertz spectral range. 2022 , 9, 021302	2
435	Presentation_1.pdf. 2018 ,	
434	Quantum Engineered Devices Based on Two-Dimensional Materials for Next-Generation Information Processing and Storage 2022 , e2109894	2
433	Dirac Fermion Cloning, Moir[Flat Bands and Magic Lattice Constants in Epitaxial Monolayer Graphene 2022 , e2200625	1
432	Transition Metal Dichalcogenides (TMDCs) Heterostructures: Synthesis, Excitons and Photoelectric Properties 2022 , e202100313	1
431	Dissociation of ammonia borane and its subsequent nucleation on the Ru(0001) surface revealed by density functional theoretical simulations 2022 ,	1
430	Consumer Applications of Graphene and Its Composites. 2022 , 471-500	O

429	Recent progress in 2D material van der Waals heterostructure-based luminescence devices towards the infrared wavelength range.	1
428	Exploring the emerging applications of the advanced 2-dimensional material borophene with its unique properties 2022 , 12, 12166-12192	O
427	Magneto-Optical Properties of Gapped-Graphene.	
426	Quantum Coupled Borophene Based Heterolayers for Excitonic and Molecular Sensing Applications.	2
425	Finding Suitable Gate Insulators for Reliable 2D FETs. 2022 ,	1
424	??????????????????. 2022 ,	
423	Moir[Modulation of Van Der Waals Potential in Twisted Hexagonal Boron Nitride 2022,	О
422	All-Optical Reconfigurable Electronic Memory in a Graphene/SrTiO Heterostructure 2022 , 7, 15841-15845	
421	Terahertz radiation induced circular Hall effect in graphene. 2022 , 105,	О
420	Fabrication and characterization of InSb nanosheet/hBN/graphite heterostructure devices 2022 , 33,	Ο
419	A Review of Ultrawide Bandgap Materials: Properties, Synthesis, and Devices.	1
418	Light emission properties of mechanical exfoliation induced extended defects in hexagonal boron nitride flakes.	1
417	Revisiting Solution-Based Processing of van der Waals Layered Materials for Electronics.	0
416	Benchmarking Noise and Dephasing in Emerging Electrical Materials for Quantum Technologies 2022 , e2109671	1
415	Engineering tunable terahertz radiation from anelectron bunch using graphene metasurfaces.	1
414	Activation of magnetic moments by annealing in chemical vapor deposited graphene. 2022, 105,	
413	Nanoscale Electronic Transparency of Wafer-Scale Hexagonal Boron Nitride 2022,	1
412	Imaging of Submicroampere Currents in Bilayer Graphene Using a Scanning Diamond Magnetometer. 2022 , 17,	4

411	Recent advances of amorphous-phase-engineered metal-based catalysts for boosted electrocatalysis. 2022 , 127, 1-18	1
410	Revealing initial nucleation of hexagonal boron nitride on Ru(0001) and Rh(111) surfaces by density functional theoretical simulations.	2
409	Toward batch synthesis of high-quality graphene by cold-wall chemical vapor deposition approach. 1	0
408	Mechanics of Biosurfactant Aided Liquid Phase Exfoliation of 2D Materials. 2022, 100098	
407	Compact modeling technology for the simulation of integrated circuits based on graphene field-effect transistors 2022 , e2201691	3
406	Recent progress in 1D contacts for 2D material-based devices 2022 , e2202408	1
405	Emergent Multifunctional Magnetic Proximity in van der Waals Layered Heterostructures. 2200186	2
404	Phonon-Limited Mobility in h -BN Encapsulated AB -Stacked Bilayer Graphene. 2022 , 128,	O
403	Low-Temperature Synthesis of Boron Nitride as a Large-Scale Passivation and Protection Layer for Two-Dimensional Materials and High-Performance Devices.	1
402	Insights into controllable electronic properties of 2D type-II Twin-Graphene/g-CN43 and type-I Twin-Graphene/hBN vertical heterojunctions via external electric field and strain engineering. 2022 , 128216	
401	Electronic and thermoelectric properties of group IVI/I van der Waals heterostructures.	
400	Theoretical Prediction of the Carrier Mobilities for MII2MIII-Cl-Layered Double Hydroxides in the Three-Dimensional Directions.	
399	Intralayer Phonons in Multilayer Graphene Moir Superlattices. 2022, 2022, 1-11	1
398	Evidence for 4e charge of Cooper quartets in a biased multi-terminal graphene-based Josephson junction. 2022 , 13,	1
397	Few-Layered MnAl2S4 Dielectrics for High-Performance van der Waals Stacked Transistors.	3
396	WaferBcale Growth of FeDoped Hexagonal Boron Nitride (hBN) Films via CoBputtering. 2022 , 12, 777	
395	Nontrivial effect of out-of-plane acoustic phonon mode on limiting room temperature conductivity of ABA-stacked trilayer graphene. 2022 , 105,	
394	Band conductivity oscillations in a gate-tunable graphene superlattice. 2022 , 13,	1

393	Current Injection into Single-Crystalline Carbon-Doped h-BN toward Electronic and Optoelectronic Applications.	О
392	Epitaxial single-crystal hexagonal boron nitride multilayers on Ni (111). 2022 , 606, 88-93	14
391	Boron nitride on SiC(0001). 2022 , 6,	
390	Unbiased Plasmonic-Assisted Integrated Graphene Photodetectors.	1
389	Theoretical prediction of superconductivity in monolayer B3N. 2022, 105,	О
388	Chemically exfoliated inorganic nanosheets for nanoelectronics. 2022 , 9, 021313	O
387	Beyond T-graphene: Two-dimensional tetragonal allotropes and their potential applications. 2022 , 9, 021314	1
386	Towards n-type conductivity in hexagonal boron nitride. 2022 , 13,	4
385	Quantum spin Hall effect in two-dimensional transition-metal chalcogenides MX5 (M = Zr, Hf and X = S, Se, Te). 2022 , 143, 115325	О
384	Lattice relaxation and substrate effects on the electronic properties of graphene superlattice. 2022 ,	
383	Highly Sensitive Pressure Sensor Based on h-BN/Graphene/h-BN Heterojunction and Cu B n Solid L iquid Interdiffusion Bonding. 2022 , 1-6	2
382	Site-selective Growth of Two-Dimensional Materials: Strategies and Applications.	
381	The role of permanent and induced electrostatic dipole moments for Schottky barriers in Janus MXY/graphene heterostructures: a first-principles study.	1
380	Abnormal anti-oxidation behavior of hexagonal boron nitride grown on copper.	
379	Quantum oscillations in a hexagonal boron nitride-supported single crystalline InSb nanosheet.	
378	Engineering van der Waals Materials for Advanced Metaphotonics.	2
377	2D materials: increscent quantum flatland with immense potential for applications. 2022 , 9,	4
376	Influence of Hexagonal Boron Nitride on Electronic Structure of Graphene. 2022, 27, 3740	1

375	Exploring Interface Through Synchrotron Radiation Characterization Techniques: A Graphene Case. 2202469	О
374	Electrical charge control of h-BN single photon sources. 2022 , 9, 035020	1
373	Directional Damping of Plasmons at MetalBemiconductor Interfaces.	1
372	Quantification of Ion-Implanted Single-Atom Dopants in Monolayer MoS2 via HAADF STEM Using the TEMUL Toolkit. 1-10	
371	Advances in Flexible Optoelectronics Based on Chemical Vapor Deposition-Grown Graphene. 2203115	1
370	Superconducting Proximity Effect in d -Wave Cuprate/Graphene Heterostructures. 2100559	O
369	First-Principles Calculations on Janus MoSSe/Graphene van der Waals Heterostructures: Implications for Electronic Devices. 2022 , 5, 8371-8381	3
368	Large-Area Hexagonal Boron Nitride Layers by Chemical Vapor Deposition: Growth and Applications for Substrates, Encapsulation, and Membranes.	2
367	1D van der Waals Nb 2 Pd 3 Se 8 -Based n-Type Field-Effect Transistors Prepared by Liquid Phase Exfoliation. 2200620	
366	Strong Interfacial Charge Trapping in Ultrathin SrRuO3 on SrTiO3 Probed by Noise Spectroscopy. 2022 , 13, 5618-5625	
365	Hexagonal Boron Nitride for Next-Generation Photonics and Electronics. 2204161	2
364	Frequency Memorizing Shape Morphing Microstrip Monopole Antenna using Hybrid Programmable 3-Dimensional Printing. 2022 , 102988	
363	Ferroelectricity in hBN intercalated double-layer graphene. 2022 , 17,	1
362	Recent Development of Morphology-Controlled Hybrid Nanomaterials for Triboelectric Nanogenerator: A Review.	1
361	Hexagonal Boron Nitride on IIII Compounds: A Review of the Synthesis and Applications. 2022, 15, 4396	О
360	Positioning of edge states in a quantum Hall graphene pn junction. 2022 , 105,	O
359	Surface charge-transfer doping a quantum-confined silver monolayer beneath epitaxial graphene. 2022 , 105,	1
358	Observation of photoluminescence from a natural van der Waals heterostructure. 2022 , 120, 253101	

357	Chemical Vapor-Deposited Graphene on Ultraflat Copper Foils for van der Waals Hetero-Assembly.	
356	Ab Initio Study of Graphene/hBN Van der Waals Heterostructures: Effect of Electric Field, Twist Angles and p-n Doping on the Electronic Properties. 2022 , 12, 2118	Ο
355	2D MoS2-hBN hybrid coatings for enhanced corrosion resistance of solid lubricant coatings. 2022 , 443, 128612	1
354	Physical properties of novel Tin-chalcogenides heterostructures: A first-principles study. 2022 , 149, 106820	0
353	Modulation of the MoSH/WSi₂N₄ Schottky-junction Barrier by External Electric Field and Biaxial Strain. 2022 ,	
352	Interlayer spacing control of boron nitride sheets with hydrated cations.	
351	In situ synthesis of boron nitride flanonoodlesfbased epoxy nanocomposites with enhanced thermal and dielectric properties.	Ο
350	Magneto-optical Kerr effect in surface engineered 2D hexagonal boron nitride. 2022 , 12,	
349	Phonon-assisted carrier cooling in h -BN/graphene van der Waals heterostructures. 2022 , 105,	
348	Two-dimensional diamonds from sp2-to-sp3 phase transitions.	7
347	Properties of Composite Powder Based on Boron Nitride Prepared under Concentrated Light. 2022 , 7, 42	
346	Boron nitride materials as emerging catalysts for oxidative dehydrogenation of light alkanes.	Ο
345	Improving carrier mobility in two-dimensional semiconductors with rippled materials.	2
344	Sub-femto-Joule energy consumption memory device based on van der Waals heterostructure for in-memory computing. 2022 , 1, 100014	0
343	Doping of Graphene Films: Open the way to Applications in Electronics and Optoelectronics. 2203179	4
342	Evaluation of polyvinyl chloride adhesion to 2D crystal flakes. 2022 , 6,	
341	Suspended Graphene Membranes to Control Au Nucleation and Growth.	1
340	High-Efficiency Infrared Sensing with Optically Excited Graphene-Transition Metal Dichalcogenide Heterostructures. 2202626	O

339	Spontaneous transport of water nanodroplets on graphene and hexagonal boron nitride in-plane heterostructure.	2
338	Multi-scale electronics transport properties in non-ideal CVD graphene sheet. 2022 , 12,	
337	Charge carrier modulation in graphene on ferroelectric single-crystal substrates. 2022, 14,	
336	Large-Scale Synthesis h-BN Films on Copper-Nickel Alloy by Atmospheric Pressure Chemical Vapor Deposition. 2022 , 12, 985	
335	Power-delay-product optimal repeater design for horizontal and vertical multilayer graphene nanoribbon interconnects.	
334	Density functional theory study of the hydrogen evolution reaction in haeckelite boron nitride quantum dots. 2022 ,	1
333	Memristive, Spintronic, and 2D-Materials-Based Devices to Improve and Complement Computing Hardware. 2200068	1
332	Engineering Grain Boundaries in Two-dimensional Electronic Materials. 2203425	
331	Properties at the interface of the pristine CdSe and core@hell CdSe-ZnS quantum dots with ultrathin monolayers of two-dimensional MX2 (M: Mo, W; X: S, Se, Te) heterostructures from density functional theory. 2022 , 28,	
330	Angstrofluidics: Walking to the Limit. 2022 , 52, 189-218	3
330	Angstrofluidics: Walking to the Limit. 2022, 52, 189-218 Robust superconductivity in magic-angle multilayer graphene family.	4
329	Robust superconductivity in magic-angle multilayer graphene family. Non-volatile flash memory based on Van der Waals gate stack using bandgap tunability of	
329 328	Robust superconductivity in magic-angle multilayer graphene family. Non-volatile flash memory based on Van der Waals gate stack using bandgap tunability of hexagonal boron nitride. 2022, 32, 102179 Surface termination effects on the terahertz-range optical responses of two-dimensional MXenes:	
329 328 327	Robust superconductivity in magic-angle multilayer graphene family. Non-volatile flash memory based on Van der Waals gate stack using bandgap tunability of hexagonal boron nitride. 2022, 32, 102179 Surface termination effects on the terahertz-range optical responses of two-dimensional MXenes: Density functional theory study. 2022, 32, 103917 Carbon-dot confined in graphene-analogous boron nitride for enhanced oxidative desulfurization.	4
329 328 327 326	Robust superconductivity in magic-angle multilayer graphene family. Non-volatile flash memory based on Van der Waals gate stack using bandgap tunability of hexagonal boron nitride. 2022, 32, 102179 Surface termination effects on the terahertz-range optical responses of two-dimensional MXenes: Density functional theory study. 2022, 32, 103917 Carbon-dot confined in graphene-analogous boron nitride for enhanced oxidative desulfurization. 2022, 15, 104084 BN white graphene well-dispersed solar salt nanofluids with significant improved thermal	1
329 328 327 326 325	Robust superconductivity in magic-angle multilayer graphene family. Non-volatile flash memory based on Van der Waals gate stack using bandgap tunability of hexagonal boron nitride. 2022, 32, 102179 Surface termination effects on the terahertz-range optical responses of two-dimensional MXenes: Density functional theory study. 2022, 32, 103917 Carbon-dot confined in graphene-analogous boron nitride for enhanced oxidative desulfurization. 2022, 15, 104084 BN white graphene well-dispersed solar salt nanofluids with significant improved thermal properties for concentrated solar power plants. 2022, 245, 111875	1 2

321	Strain-tunable pure H- conduction in one-atom-thick hexagonal boron nitride for high-energy-density fuel cells. 2022 , 138223	0
320	A minireview on 2D materials-enabled optoelectronic artificial synaptic devices. 2022 , 10, 070702	1
319	Chemically Induced Surface Potential Modulation at Pd Al2O3 Graphene Field Effect Transistors: Implications for Enhanced H2 Sensing.	Ο
318	Open level lines of a superposition of periodic potentials on a plane. 2022 , 169039	
317	Fingerprints of quantum criticality in locally resolved transport. 2022 , 13,	O
316	Transport Spectroscopy of Ultraclean Tunable Band Gaps in Bilayer Graphene. 2200510	1
315	Substrate influence on transition metal dichalcogenide monolayer exciton absorption linewidth broadening. 2022 , 6,	Ο
314	Magnetic two-dimensional chromium trihalides: structure, properties and modulation.	Ο
313	First-principles perspective on full-spectrum infrared photodetectors from doping an excitonic insulator. 2022 , 106,	
312	Highly anisotropic thermal conductivity of few-layer CrOCl for efficient heat dissipation in graphene device.	1
311	On Functional Boron Nitride: Electronic Structures and Thermal Properties. 2022 , 100005	Ο
310	Van der Waals heterostructures. 2022 , 2,	2
309	Linear and nonlinear optical propagation in 2D materials. 2021 , 2021, 19-37	
308	Direct growth of h-BN multilayers with controlled thickness on non-crystalline dielectric substrates without metal catalysts.	1
307	Isolated Ni atoms induced edge stabilities and equilibrium shapes of CVD-prepared hexagonal boron nitride on Ni(111) surface.	5
306	A clean dry transfer of hexagonal boron nitride with improved oxidation resistance.	
305	Anomalous Charge Transport Properties and Band Flattening in Graphene: A Quasi-Relativistic Tight-Binding Study of Pseudo-Majorana States.	
304	Large-area transfer of two-dimensional materials free of cracks, contamination and wrinkles via controllable conformal contact. 2022 , 13,	O

303	Planar Optical Cavities Hybridized with Low-Dimensional Light-Emitting Materials. 2203889	1
302	Enhancement of the contrast for a hexagonal boron nitride monolayer placed on a silicon nitride/silicon substrate. 2022 , 15, 086502	
301	Transmission-Electron-Microscopy-Generated Atomic Defects in Two-Dimensional Nanosheets and Their Integration in Devices for Electronic and Optical Sensing. 2022 , 5, 11429-11436	
300	Zeolite-like molecules: Promising dielectrics for two-dimensional semiconductors.	
299	Lighting Nanoscale Insulators by Steric Restriction-Induced Emissions.	
298	Fabricating Graphene Oxide/h-BN Metal Insulator Semiconductor Diodes by Nanosecond Laser Irradiation. 2022 , 12, 2718	
297	An Inventive Method for Graphene-Based Optofluidic Tweezer to Actively Detection, Sorting, and Manipulation of Nano-bioparticles below 2.5 nm.	
296	Magneto-optical measurements of the negatively charged 2s exciton in WSe2. 2022 , 106,	
295	Giant Carrier Mobility in Graphene with Enhanced Shubnikov de Haas Quantum Oscillations: Implications for Low-Power-Consumption Device Applications. 2022 , 5, 10860-10866	
294	Structure and electronic properties of stable facets in the 2D material hexagonal boron nitride (hBN) on curved platinum. 2022 , 100071	
293	Carbon-related defect control of bulk hBN single crystals growth by atmospheric-pressure metal-flux-based fusion synthesis. 2022 , 57, 14668-14680	
292	Heat transfer in transversely coupled qubits: Optically controlled thermal modulator with common reservoirs.	O
291	Activation of h -BN and SiC monolayer sheets through foreign atom substitution; a comparative study based on ab-initio method.	1
290	Strain-Engineered Wrinkles on Graphene Using Polymeric Actuators. 2022 , 18,	O
289	Effect of boundary scattering on magneto-transport performance in BN-encapsulated graphene.	
288	Tunable Sample-Wide Electronic Kagome Lattice in Low-Angle Twisted Bilayer Graphene. 2022 , 129,	2
287	Superconducting quantum interference effect in NbSe2/NbSe2 van der Waals junctions. 2022 , 34, 405702	
286	Recent Progress in Fabrication and Physical Properties of 2D TMDC-Based Multilayered Vertical Heterostructures. 2022 , 11, 2401	

285	Recent Advances of Preparation and Application of Two-Dimension van der Waals Heterostructure. 2022 , 12, 1152	О
284	Ultrafast photoluminescence at telecom wavelengths from wafer-scale monolayer graphene enabled by Fabry-Perot interferences.	
283	Preparation and Charge Transfer at Sb2Se3/1L-MoS2 Heterojunction. 2022, 11, 2574	
282	Investigation on photocatalytic property of SiH/GaSe and SiH/InSe heterojunctions for photocatalytic water splitting. 2022 ,	O
281	Ultrahigh resistance of hexagonal boron nitride to mineral scale formation. 2022, 13,	О
280	Controlled Growth of Two-Dimensional Heterostructures: In-Plane Epitaxy or Vertical Stack.	
279	Direct growth of hBN/Graphene heterostructure via surface deposition and segregation for independent thickness regulation.	
278	A brief review on the spin valve magnetic tunnel junction composed of 2D materials. 2022 , 55, 423001	2
277	Irreversible Conductive Filament Contacts for Passivated van der Waals Heterostructure Devices. 2207351	
276	Tunable Emission from Localized Excitons Deterministically Positioned in Monolayer pli Junctions.	
275	Strain Quantum Sensing with Spin Defects in Hexagonal Boron Nitride. 2022, 22, 6553-6559	1
274	Electrical and optical properties of InSe with various interfaces. 2022 , 121, 071603	
273	SnS Nanoflakes/Graphene Hybrid: Towards Broadband Spectral Response and Fast Photoresponse. 2022 , 12, 2777	
272	Advances in Two-Dimensional Materials for Optoelectronics Applications. 2022 , 12, 1087	3
271	Effect of buffer layer and substrate growth temperature on the microstructural evolution of hexagonal boron nitride thin films. 2022 , 447, 128805	О
270	Interlayer interactions in transition metal dichalcogenides heterostructures. 2022, 9, 100077	
269	Two novel easily exfoliated quaternary chalcogenides with high performance of photocatalytic hydrogen production. 2022 , 604, 154555	1
268	Recent progress in 2D van der Waals heterostructures: fabrication, properties, and applications. 2022 , 65,	1

267	Programmable Photo-Induced Doping in 2D Materials. 2201219	2
266	Non-thermal and thermal effects on mechanical strain in substrate-transferred wafer-scale hBN films. 2022 , 132, 104303	O
265	Fabricating one-dimensional van der Waals heterostructures on chirality-sorted single-walled carbon nanotubes. 2022 , 199, 407-414	О
264	Tuning electronic and optical properties of graphene/h-BN heterobilayer via surface modification. 2022 , 605, 154591	3
263	Salt-promoted growth of monolayer tungsten disulfide on hexagonal boron nitride using all chemical vapor deposition approach. 2022 , 605, 154812	О
262	Electric field tunability of the electronic properties and contact types in the MoS2/SiH heterostructure. 2022 , 12, 24172-24177	О
261	Ballistic Transport in Square Junctions of Delafossite Metals. 2022 , 87-135	О
260	Chapter 1. Introduction. 2022 , 1-32	O
259	Introduction to 2-Dimensional Materials and Moir Superlattices. 2022, 5-28	О
258	Introduction. 2022 , 1-7	O
257	Surface etching and edge control of hexagonal boron nitride assisted by triangular Sn nanoplates. 2022 , 4, 3786-3792	О
256	Ultrahigh anisotropic carrier mobility in ZnSb monolayers functionalized with halogen atoms. 2022,	
	12, 26994-27001	О
255		0
255 254	12, 26994-27001 A two-dimensional Sb/InS van der Waals heterostructure for electronic and optical related	
	12, 26994-27001 A two-dimensional Sb/InS van der Waals heterostructure for electronic and optical related applications. 2022, 24, 22000-22006	0
254	12, 26994-27001 A two-dimensional Sb/InS van der Waals heterostructure for electronic and optical related applications. 2022, 24, 22000-22006 2D MXene nanocomposites: electrochemical and biomedical applications.	0
²⁵⁴	12, 26994-27001 A two-dimensional Sb/InS van der Waals heterostructure for electronic and optical related applications. 2022, 24, 22000-22006 2D MXene nanocomposites: electrochemical and biomedical applications. Fabrication Techniques. 2022, 29-47	0 2

249	Boron Nitride Fabrication Techniques and Physical Properties.	O
248	Is the Bandgap of Bulk PdSe 2 Located Truly in the Far-Infrared Region? Determination by Fourier-Transform Photocurrent Spectroscopy. 2200231	О
247	Mass transfer techniques for large-scale and high-density microLED arrays.	0
246	Synthesis of two-dimensional materials: How computational studies can help?.	О
245	Interband scattering across the Lifshitz transition in WTe2. 2022 , 106,	0
244	Effects of Mono-Vacancies and Co-Vacancies of Nitrogen and Boron on the Energetics and Electronic Properties of Heterobilayer h-BN/graphene. 2022 , 15, 6369	O
243	Chemical vapor deposition: a potential tool for wafer scale growth of two-dimensional layered materials. 2022 , 55, 473001	1
242	Gate-Tunable Junctions within Monolayer MoS2WS2 Lateral Heterostructures.	О
241	Strong Dzyaloshinskii-Moriya interaction in monolayer CrI3 on metal substrates. 2022 , 106,	1
240	2+ 🛮 Dimensional Materials via Atomistic Z-Welding. 2202695	О
239	In Situ Measurements of Strain Evolution in Graphene/Boron Nitride Heterostructures Using a Non-Destructive Raman Spectroscopy Approach. 2022 , 12, 3060	0
238	Integrated wafer-scale ultra-flat graphene by gradient surface energy modulation. 2022, 13,	1
237	Emerging low-dimensional materials for nanoelectromechanical systems resonators. 2023 , 11, 21-52	0
236	Natural band alignment of BAlN and BGaN alloys. 2022 , 55, 455102	О
235	Combining Freestanding Ferroelectric Perovskite Oxides with Two-Dimensional Semiconductors for High Performance Transistors. 2022 , 22, 7457-7466	0
234	Tuning Schottky Barrier of Single-Layer MoS2 Field-Effect Transistors with Graphene Electrodes. 2022 , 12, 3038	1
233	Observation of well-defined Kohn-anomaly in high-quality graphene devices at room temperature. 2022 , 9, 045028	0
232	Epitaxy of III-nitrides on two-dimensional materials and its applications.	O

231	Low-resistance metal contacts to encapsulated semiconductor monolayers with long transfer length. 2022 , 5, 579-585	О
230	Ferroelectrics-Integrated Two-Dimensional Devices toward Next-Generation Electronics. 2022 , 16, 1359	5-1361 <u>1</u>
229	Lifetime-Limited and Tunable Quantum Light Emission in h-BN via Electric Field Modulation.	2
228	Two-Dimensional Semiconductors for Photodetection. 1-22	O
227	Multivalley Superconductivity in Monolayer Transition Metal Dichalcogenides.	О
226	Molecular Dynamics Simulation on In-Plane Thermal Conductivity of Graphene/Hexagonal Boron Nitride van der Waals Heterostructures.	O
225	Lattice dynamics, elastic, magnetic, thermodynamic and thermoelectric properties of the two-dimensional semiconductors MPSe3 (M=Cd, Fe and NI): a first-principles study.	О
224	Charge carrier dynamics in 2D materials probed by ultrafast THzspectroscopy. 2023 , 8,	O
223	Towards the Growth of Hexagonal Boron Nitride on Ge(001)/Si Substrates by Chemical Vapor Deposition. 2022 , 12, 3260	O
222	Manipulation of antichiral edge state based on modified Haldane model.	O
221	Recent progress on the interfacial regulation and application of 2D antimonene-based van der Waals heterostructures. 2022 , 121, 100501	1
220	Graphene hyperbolic metamaterials: Fundamentals and applications.	O
219	Time-dependent transport in graphene Mach-Zender interferometers. 2022, 106,	O
218	Probing the interaction between 2D materials and oligoglycine tectomers. 2022 , 9, 045033	1
217	Hexagonal-boron nitride/graphene van der Waals heterostructure-based wavelength-selective infrared absorbers using plasmonic metasurfaces for multi-spectral infrared photodetectors.	1
216	Prediction of Room-Temperature Ferromagnetic Semiconductors in $CrMoA2B2$ (A = Se and Te ; B = Br and I) $Monolayers$.	O
215	Band alignment and interlayer hybridisation in transition metal dichalcogenide/hexagonal boron nitride heterostructures.	О
214	Trivalent and pentavalent atoms doped boron nitride nanosheets as Favipiravir drug carriers for the treatment of COVID-19 using computational approaches. 2022 , 1217, 113902	Ο

213	Electrolyte adsorption in graphene and hexagonal boron nitride nanochannels. 2022, 367, 120474	0
212	Substrate effects on the speed limiting factor of WSe2 photodetectors. 2022 , 24, 25383-25390	O
211	Two-dimensional van der Waals heterostructures (vdWHs) with band alignment transformation in multi-functional devices. 2022 , 12, 31456-31465	0
210	Van der Waals Integration of Artificial Heterostructures and High-Order Superlattices. 2022,	O
209	Highly Confined and Tunable Mid-IR Polaritonics in Symmetric Nonlinear-Graphene-hBN Heterostructures.	О
208	Wrinkle-mediated CVD synthesis of wafer scale Graphene/h-BN heterostructures. 2023, 34, 025601	O
207	Emergence of Interlayer Coherence in Twist-Controlled Graphene Double Layers. 2022, 129,	O
206	Gate Dielectrics Integration for Two-Dimensional Electronics: Challenges, Advances and Outlook. 2207901	1
205	Tailorable Electronic and Electric Properties of Graphene with Selective Decoration of Silver Nanoparticles by Laser-Assisted Photoreduction. 2022 , 12, 3549	O
204	Evolution of Reverse-Biased Current of a Barristor Junction by Varying Temperature and Barrier Height of the Junction. 2200761	O
203	Effect of dilute impurities on short graphene Josephson junctions. 2022 , 5,	0
202	The rise of boron nitride nanotubes for applications in energy harvesting, nanoelectronics, quantum materials, and biomedicine.	O
201	hBN-based enhancement and regulation of radiative heat transfer between two monolayer graphene sheets. 2022 , 121, 171104	0
200	A light-controllable topological transistor based on quantum tunneling of anomalous topological edge states. 2022 , 15, 115003	1
199	Multifractal Conductance Fluctuations in High-Mobility Graphene in the Integer Quantum Hall Regime. 2022 , 129,	О
198	Two-dimensional heterostructures formed by graphenelike ZnO and MgO monolayers for optoelectronic applications. 2022 , 6,	O
197	A compact model of the backscattering coefficient and mobility of a graphene FET for \$\$hbox {SiO}_2\$\$ and h-BN substrates.	O
196	2D Van der Waals Heterostructures for Chemical Sensing. 2207065	3

195	Formation of One-Dimensional van der Waals Heterostructures via Self-Assembly of Blue Phosphorene Nanoribbons to Carbon Nanotubes.	О
194	Gate-Tunable Resonance State and Screening Effects for Proton-Like Atomic Charge in Graphene.	O
193	Bias-Modified Schottky Barrier Height-Dependent Graphene/ReSe2 van der Waals Heterostructures for Excellent Photodetector and NO2 Gas Sensing Applications. 2022 , 12, 3713	1
192	Continuous epitaxy of single-crystal graphite films by isothermal carbon diffusion through nickel.	1
191	High-Energy-Density and High Efficiency Polymer Dielectrics for High Temperature Electrostatic Energy Storage: A Review. 2205247	0
190	Mechanical characterization of Nanoporous two-dimensional Ti3C2 MXene membranes. 2022,	O
189	Electron Beam as Straightener to De-Wrinkle Large 2D Black Phosphorus Flake: An In Situ TEM Monitoring. 2201320	O
188	Ballistic graphene arrays for ultra-high pressure sensing. 2022 , 132, 154501	O
187	Strongly enhanced THz generation enabled by a graphene hot-carrier fast lane. 2022, 13,	1
186	High-Temperature Quantum Hall Effect in Graphite-Gated Graphene Heterostructure Devices with High Carrier Mobility. 2022 , 12, 3777	O
185	Graphene and Its Derivatives: Synthesis and Application in the Electrochemical Detection of Analytes in Sweat. 2022 , 12, 910	5
184	Challenges for Nanoscale CMOS Logic Based on Two-Dimensional Materials. 2022 , 12, 3548	1
183	Anti-Stokes excitation of optically active point defects in semiconductor materials. 2022 , 2, 042001	0
182	Fully Encapsulated and Stable Black Phosphorus Field-Effect Transistors. 2200546	1
181	Poly(vinyl alcohol)-Assisted Exfoliation of van der Waals Materials. 2022, 7, 38774-38781	О
180	Exciton optics, dynamics, and transport in atomically thin semiconductors. 2022 , 10, 100701	2
179	Dual-gated hBN/bilayer-graphene superlattices and the transitions between the insulating phases at the charge neutrality point. 2022 , 106,	О
178	Molecular beam epitaxial growth of multilayer 2D-boron nitride on Ni substrates from borazine and plasma-activated nitrogen.	O

177	Roadmap on nanogenerators and piezotronics. 2022 , 10, 109201	O
176	Helicity exchange and symmetry breaking of in-plane phonon scattering of h-BN probed by polarized Raman spectroscopy. 2022 , 121, 182203	O
175	Electronic Structure of Folded Hexagonal Boron Nitride. 2022 , 126, 17746-17752	0
174	Development of Broadband PbS Quantum Dot/Graphene Photodetector Arrays with High-Speed Readout Circuits for Flexible Imagers.	O
173	Sensing Remote Bulk Defects through Resistance Noise in a Large-Area Graphene Field-Effect Transistor.	0
172	Nanoscale infrared imaging and spectroscopy of few-layer hexagonal boron nitride. 2022 , 132, 174301	O
171	A Review of Scalable Hexagonal Boron Nitride (h -BN) Synthesis for Present and Future Applications. 2207374	2
170	The Winner Takes It All: Carbon Supersedes Hexagonal Boron Nitride with Graphene on Transition Metals at High Temperatures. 2205184	O
169	Constructing Fast Transmembrane Pathways in a Layered Double Hydroxide Nanosheets/Nanoparticles Composite Film for an Inorganic Anion-Exchange Membrane.	0
168	Boron nitride based polymer nanocomposites for heat dissipation and thermal management applications. 2022 , 29, 101672	1
167	First-principles investigate on the electronic structure and magnetic properties of 3d transition metal doped honeycomb InS monolayer. 2023 , 608, 155240	O
166	Group IIIIV hexagonal pnictide clusters and their promise for graphene-like materials. 2023, 139-155	O
165	MOCVD of WSe2 crystals on highly crystalline single- and multi-layer CVD graphene. 2023, 202, 150-160	Ο
164	Perspectives on weak interactions in complex materials at different length scales.	O
163	A highly anisotropic polymorph.	Ο
162	Hydrodynamics of charged two-dimensional Dirac systems. I. Thermoelectric transport. 2022 , 106,	O
161	Graphene Incorporated Electrospun Nanofiber for Electrochemical Sensing and Biomedical Applications: A Critical Review. 2022 , 22, 8661	4
160	Absolute N-atom density measurement in an Ar/N2 micro-hollow cathode discharge jet by means of ns-two-photon absorption laser-induced fluorescence. 2022 , 29, 113508	Ο

159	Emerging Two-Dimensional Metal Oxides: From Synthesis to Device Integration. 2207774	О
158	Correlated and topological physics in ABC-trilayer graphene moir uperlattices. 2022, 1,	O
157	Gate-tunable Veselago interference in a bipolar graphene microcavity. 2022, 13,	0
156	Van der Waals Interface-dominated all-2D Electronics. 2207966	O
155	Structural, mechanical, and electro-optical properties of hydrogenated graphene/h-BN heterobilayer. 2022 , 137,	O
154	Multifunctional Graphene-based photodetector/modulator/absorber enhanced by metallic Nano-Antenna by employing an ingenious Fabry-Perot cavity.	O
153	Role of External Electric Field in Carrier Mobility of Graphene/ZnO Heterojunction Adsorbed H 2 O and O 2 Molecules. 2022 , 7,	O
152	Proximity induced longitudinal and transverse thermoelectric response in graphene-ferromagnetic CrBr3 vdW heterostructure.	O
151	Carbon Layer Formation on Hexagonal Boron Nitride by Plasma Processing in Hydroquinone Aqueous Solution.	2
150	Defective graphene/SiGe heterostructures as anodes of Li-ion batteries: a first-principles calculation study. 2022 , 25, 617-624	O
149	Dielectric Material Technologies for 2-D Semiconductor Transistor Scaling. 2022 , 1-20	2
148	Preparation, properties and applications of two-dimensional superlattices.	O
147	Interfacial thermal conductance between atomically thin boron nitride and graphene. 2022, 15, 122-126	O
146	Mixed dimensional Transition Metal Dichalcogenides (TMDs) vdW Heterostructure based Photodetectors: A review. 2023 , 269, 111926	O
145	Thermal stability of thin hexagonal boron nitride grown by MOVPE on epigraphene. 2023, 603, 127030	0
144	Solution-processed 2D materials on paper substrates for photodetection and photomechanical applications. 2022 , 10, 18326-18335	O
143	Superconductivity and bosonic fluid emerging from moir[flat bands. 2022, 106,	O
142	Diamond p-FETs Using Two-Dimensional Hole Gas for High Frequency and High Voltage Complementary Circuits.	O

141	Tunable Sensing and Transport Properties of Doped Hexagonal Boron Nitride Quantum Dots for Efficient Gas Sensors. 2022 , 12, 1684	О
140	Passivating Graphene and Suppressing Interfacial Phonon Scattering with Mechanically Transferred Large-Area Ga2O3.	1
139	Graphene-Based Quantum Hall Interferometer with Self-Aligned Side Gates. 2022 , 22, 9645-9651	0
138	The VdW Heterostructure Interface Physics. 2022, 125-156	O
137	Modulations in Superconductors: Probes of Underlying Physics. 2209457	О
136	The 2D Semiconductor Library. 2022 , 1-31	O
135	Reduction in residual impurities in CVDgrown hexagonal boron nitride thin films.	О
134	Growth Mechanism of High-Quality hBN Monolayers on Cu through Chemical Vapor Deposition with Inductively Coupled Plasma. 2022 , 126, 21287-21296	O
133	Temperature-dependent zero-field splittings in graphene. 2022 , 106,	Ο
132	Fabrication, Optimization, and Mechanism Analysis of Graphene/Hexagonal Boron Nitride Stacked Film. 2022 , 44, 1163-1177	O
131	Two-dimensional optoelectronic devices for silicon photonic integration. 2022,	О
130	Excitonpolaritons of hBN/WS2 heterostructure in cavity observed at room temperature. 2022 , 121, 231106	O
129	Rhombohedral and Turbostratic Boron Nitride Polytypes Investigated by X-ray Absorption Spectroscopy. 2022 , 126, 21101-21108	О
128	Three-dimensional transistors and integration based on low-dimensional materials for the post-Moore law era. 2022 ,	О
127	Graphene and Two-Dimensional Materials-Based Flexible Electronics for Wearable Biomedical Sensors. 2023 , 12, 45	О
126	Advanced 2D Nanomaterials for Additive Manufacturing. 2023 , 335-368	Ο
125	Charge transport in single polymer fiber transistors in the sub-100 nm regime: temperature dependence and Coulomb blockade. 2023 , 6, 015001	Ο
124	Recent progress of two-dimensional heterostructures for thermoelectric applications. 2023, 35, 073001	1

123	Optoelectronic properties and applications of two-dimensional layered semiconductor van der Waals heterostructures: perspective from theory. 2023 , 35, 043001	O
122	The 2D Semiconductor Synthesis and Performances. 2022 , 33-67	O
121	Graphene Microheater Chips for In Situ TEM.	1
120	One-pot liquid-phase synthesis of MoS2-WS2 van der Waals heterostructures for broadband photodetection.	O
119	All-dry flip-over stacking of van der Waals junctions of 2D materials using polyvinyl chloride. 2022 , 12,	O
118	Non-Additive Optical Response in Transition Metal Dichalcogenides Heterostructures. 2022 , 12, 4436	O
117	Exotic states in moir uperlattices of twisted semiconducting transition metal dichalcogenides. 2023 , 72, 027802	O
116	Graphene spin valve for spin logic devices. 2209137	O
115	First-principles study on GeC/FAsP heterostructure with type-II band alignment for photocatalytic water splitting. 2023 , 156298	O
114	Coupled Evolution of Sliding and Rolling of Carbon Nanotubes: Effect of Lattice Mismatch and Size.	O
113	Self-Assembly in Matrix-FreelFunctionalized Boron Nitride Sheets as Free-Standing Thin Film Sieves for Stable Forward Osmosis and Robust Dye Removal Applications. 2200385	O
112	Optical and Electrical Properties of Low-Dimensional Crystalline Materials: A Review. 2023 , 13, 108	O
111	Electrical Contacts With 2D Materials: Current Developments and Future Prospects. 2206550	О
110	Graphene Nano-Electromechanical Mass Sensor with High Resolution at Room Temperature. 2023, 105958	O
109	Defect physics in 2D monolayer I-VII semiconductor AgI. 2023 , 100304	O
108	Bioactive inorganic nanomaterials for cancer theranostics.	O
107	Oxygen Activated CVD Growth of Large-Area Multilayer h-BN on Polycrystalline Copper Foils. 2023 , 127088	O
106	High Temperature Phases of Borophene: Borophene Glass and Liquid.	O

105	Electrochemically Exfoliated Two-Dimensional Nanomaterials for Electronics. 2022, 25, 427-436	0
104	Vapor-phase Precise-synthesis of 2D Inorganic materials for optoelectronics.	O
103	High-Q Nanophotonics Over the Full Visible Spectrum Enabled by Hexagonal Boron Nitride Metasurfaces. 2209688	O
102	Ion-gel-based light-emitting devices using transition metal dichalcogenides and hexagonal boron nitride heterostructures.	Ο
101	Eddy Current Measurement of Chemiresistive Sensing Transients in Graphene-hBN Heterostructures.	0
100	Graphene Bridge Heterostructure Devices for Negative Differential Transconductance Circuit Applications. 2023 , 15,	O
99	Scalable synthesis of 2D materials. 2023 , 1-54	0
98	Exploring the world of functional materials. 2023 , 1-19	O
97	Research Process on Photodetectors based on Group-10 Transition Metal Dichalcogenides. 2207641	1
96	Anisotropy and Hybrid Heterosurface-Modulated Two-Dimensional Hydrogen Bond Network of Water. 2023 , 127, 2544-2557	О
95	Efficient computational design of two-dimensional van der Waals heterostructures: Band alignment, lattice mismatch, and machine learning. 2023 , 7,	0
94	Low-Temperature Direct Growth of Amorphous Boron Nitride Films for High-Performance Nanoelectronic Device Applications. 2023 , 15, 7274-7281	O
93	Design, mechanism, and performance of cement-based materials with 1D nanomaterials. 2023, 93-126	0
92	Anomalous optical response of graphene on hexagonal boron nitride substrates. 2023, 6,	O
91	Nonlinear diffusion of negatively charged excitons in monolayer WSe2. 2023 , 107,	0
90	Low-Temperature Direct Synthesis of Multilayered h-BN without Catalysts by Inductively Coupled Plasma-Enhanced Chemical Vapor Deposition.	Ο
89	Strong gate-tunability of flat bands in bilayer graphene due to moirlencapsulation between hBN monolayers.	Ο
88	Graphene-Based Drug Delivery System. 2023 , 189-210	O

87	Graphene in Field Effect Transistor-Based Biosensors. 2023 , 49-78	О
86	From two-dimensional materials to polymer nanocomposites with emerging multifunctional applications: A critical review.	1
85	Modeling metamaterials: Planar heterostructures based on graphene, silicene, and germanene. 2023 , 27-50	0
84	Coherence protection of spin qubits in hexagonal boron nitride. 2023, 14,	O
83	Graphene-Based Touch Sensors. 2023 , 54-70	O
82	2D nanomaterials as lubricant additives. 2023 , 97-112	Ο
81	Electrostatic restacking of two-dimensional materials to generate novel hetero-superlattices and their energy applications. 2023 , 11, 020901	Ο
80	Two Dimensional Heterostructures for Optoelectronics: Current Status and Future Perspective. 2023 , 28, 2275	O
79	Unfolding the band structure of van der Waals heterostructures. 2023, 7,	О
78	Wafer-Scale Single Crystal Hexagonal Boron Nitride Layers Grown by Submicron-Spacing Vapor Deposition. 2301086	O
77	The Controllable Synthesis of High-Quality Two-Dimensional Iron Sulfide with Specific Phases. 2207325	О
76	Moir[phonons in graphene/hexagonal boron nitride moir[superlattice. 2023, 107,	O
75	Complete Determination of Thermoelectric and Thermal Properties of Supported Few-Layer Two-Dimensional Materials. 2023 , 19,	O
74	Andreev Reflection and Klein Tunneling in High-Temperature Superconductor-Graphene Junctions. 2023 , 130,	O
73	Adhesion of 2D MoS2 to Graphite and Metal Substrates Measured by a Blister Test. 2023 , 23, 2607-2614	Ο
72	Realization of multifunction in perovskite-based van der Waals heterostructure by interface engineering strategy: The case of CsPbBr3/Janus MoSSe. 2023 , 618, 156626	O
71	First-principles study of electronic and optical properties of NH3-adsorbed Sc2CO2 monolayer and its application in gas sensors. 2023 , 24, 173-184	0
70	Chemically modified graphene sheets as potential sensors for organophosphate compounds(pesticide): A DFT study. 2023 , 619, 156745	O

69	Machine learning insight into h-BN growth on Pt(111) from atomic states. 2023, 621, 156893	O
68	hBN-based regulation of near-field radiative heat transfer between planar structures. 2023 , 301, 108540	O
67	First-principles prediction of room-temperature half-metallicity in strain- and carrier-tunable monolayer Mn2Sn2Te6. 2023 , 150, 115704	0
66	Thermal stability of twin graphene: A Reaxff molecular dynamics study. 2023 , 623, 157038	O
65	Increasing coverage of mono-layer graphene grown on hexagonal boron nitride. 2023, 34, 165601	О
64	Unidirectional domain growth of hexagonal boron nitride thin films. 2023 , 30, 101734	O
63	Sensitivity and Stability Analysis of Double-Gate Graphene Nanoribbon Vertical Tunnel FET for Different Gas Sensing. 2023 , 12, 027003	О
62	Boron Nitride-Graphene (BN-G) Bilayer as a Channel of Graphene Based Field Effect Transistor. 2023 , 12, 021001	O
61	Direct observation of cation diffusion driven surface reconstruction at van der Waals gaps. 2023 , 14,	О
60	Graphene-based optofluidic tweezers for refractive-index and size-based nanoparticle sorting, manipulation, and detection. 2023 , 13,	O
59	A primer on twistronics: a massless Dirac fermion journey to moir patterns and flat bands in twisted bilayer graphene. 2023 , 35, 143001	0
58	Terminal Atom-Controlled Etching of 2D-TMDs. 2211252	O
57	Large-area synthesis and transfer of multilayer hexagonal boron nitride for enhanced graphene device arrays. 2023 , 6, 126-136	О
56	Ultra-High Interfacial Thermal Conductance via Double hBN Encapsulation for Efficient Thermal Management of 2D Electronics. 2023 , 19, 2205726	O
55	Fast Fabrication of WS2/Bi2Se3 Heterostructures for High-Performance Photodetection.	О
54	Crosslinked PAES-based sandwich-structured polymer nanocomposites with covalently strengthened interface towards high-temperature capacitive energy storage. 2023 , 9, 10-17	O
53	Molecular Bridges Link Monolayers of Hexagonal Boron Nitride during Dielectric Breakdown. 2023 , 5, 1262-1276	O
52	Efficiency of electron doping to monolayer hexagonal boron nitride by alkali metals. 2023 , 122, 071601	O

51	Engineering Transistorlike Optical Gain in Two-Dimensional Materials with Berry Curvature Dipoles. 2023 , 130,	Ο
50	Imaging the breaking of electrostatic dams in graphene for ballistic and viscous fluids. 2023, 379, 671-676	O
49	Locally-enhanced optical properties in a hybrid organic/inorganic (coronene/MoS2) Van der Waals heterostructure. 2023 , 10, 025015	0
48	Horizontal Arrays of One-Dimensional van der Waals Heterostructures as Transistor Channels. 2023 , 15, 10965-10973	O
47	Unravelling the room temperature growth of two-dimensional h-BN nanosheets for multifunctional applications.	0
46	Electronic and magnetic behaviors of lanthanide atoms intercalated G/MoS2 heterostructures: A first-principles study. 2023 , 363, 115115	Ο
45	Predicting Synthesizability using Machine Learning on Databases of Existing Inorganic Materials. 2023 , 8, 8210-8218	O
44	Lithium adsorption on the interface of graphene/boron nitride nanoribbons. 2023, 58, 4513-4524	O
43	2D Material Infrared Photonics and Plasmonics. 2023 , 17, 4134-4179	1
42	Growth mechanisms of hBN crystalline nanostructures with rf sputtering deposition: challenges, opportunities, and future perspectives. 2023 , 98, 042001	O
41	Pyrolysis process for boron nitride fiber derived from tris(methylamino)borane: Evolution of the molecular structure.	O
40	Manipulating optical micrograph contrast for visualizing monolayer graphene encapsulated by hBN layers. 2023 , 16, 035004	O
39	Thickness-Dependent Cross-Plane Thermal Conductivity Measurements of Exfoliated Hexagonal Boron Nitride. 2023 , 15, 12545-12550	0
38	Hexagonal Boron Nitride for Photonic Device Applications: A Review. 2023 , 16, 2005	O
37	Band structure engineering and transport properties of graphene/BN van der Waals heterostructures. 2023 , 46, 106315	0
36	Direct Imaging of Band Structure for Powdered Rhombohedral Boron Monosulfide by Microfocused ARPES. 2023 , 23, 1673-1679	O
35	Novel electrodes and gate dielectrics for field-effect transistors based on two-dimensional materials.	0
34	Stacking Order, Perfect Spin Polarization, and Giant Magnetoresistance in Zigzag Graphene/ h - BN Heterobilayer Nanoribbons. 2023 , 19,	O

33	Field-controlled quantum anomalous Hall effect in electron-doped CrSiTe3 monolayer. 2023, 7,	1
32	2D material-based sensing devices: an update. 2023 , 11, 6016-6063	O
31	Single-Crystalline BaZr 0.2 Ti 0.8 O 3 Membranes Enabled High Energy Density in PEI-Based Composites for High-Temperature Electrostatic Capacitors.	0
30	Raman spectroscopic characterizations of graphene on oxide substrates for remote epitaxy. 2023 , 133, 105301	O
29	Self-doped graphite nanobelts. 2023, 207, 240-244	0
28	Single-crystalline van der Waals layered dielectric with high dielectric constant.	O
27	Emergent second-harmonic generation in van der Waals heterostructure of bilayer MoS 2 and monolayer graphene. 2023 , 9,	0
26	Temperature dependence of carrier mobility in hydrogenated germanane field-effect transistor with various electrode materials. 2023 , 62, 030905	O
25	Coexistence of reconstructed and unreconstructed structures in the structural transition regime of twisted bilayer graphene. 2023 , 107,	O
24	Ordered Van der Waals Hetero-nanoribbon from Pressure-Induced Topochemical Polymerization of Azobenzene. 2023 , 145, 6845-6852	O
23	Signature of quantum interference effect in inter-layer Coulomb drag in graphene-based electronic double-layer systems. 2023 , 14,	O
22	Doping- and strain-tuned high Curie temperature half-metallicity and quantum anomalous Hall effect in monolayer NiAl2S4 with non-Dirac and Dirac states. 2023 , 107,	O
21	Electronic Properties of Vertically Stacked h-BN/B1\(\textbf{B}\)AlxN Heterojunction on Si(100). 2023 , 15, 16211-16220	0
20	2D SiP2/h-BN for a Gate-Controlled Phototransistor with Ultrahigh Sensitivity. 2023 , 15, 15810-15818	O
19	Signal Integrity Assessment of GNRFET-Based Ternary Logic for Multi Layered GNR Interconnects with Dielectric Insertion. 2023 , 12, 041001	O
18	van der Waals heterostructures. 2022 ,	O
17	Charge Carrier Statistics-Based Analytical Model and Simulation of Optical Mechanisms in White Graphene for High-Quality FETs and Optoelectronic Applications. 2023 , 12, 041002	0
16	Fabrication and applications of van der Waals heterostructures. 2023 , 5, 022007	O

15	Automated One-Drop Assembly for Facile 2D Film Deposition.	0
14	High-Throughput Growth of Hexagonal Boron Nitride Film Using Porous-Structure Isolation Layer. 2023 , 11, 45-51	О
13	Observation of Robust and Long-Ranged Superperiodicity of Electronic Density Induced by Intervalley Scattering in Graphene/Transition Metal Dichalcogenide Heterostructures. 2023 , 23, 2630-2635	О
12	Smith B urcell Radiation from Highly Mobile Carriers in 2D Quantum Materials.	О
11	High-field 1/f noise in hBN-encapsulated graphene transistors. 2023, 107,	О
10	Rational and key strategies toward enhancing the performance of graphene/silicon solar cells.	О
9	Graphene-based Composite Materials as Catalyst for Organic Transformations. 2023, 8,	O
8	Identification of Exciton Complexes in Charge-Tunable Janus WSeS Monolayers.	О
7	Theoretical Study on Origin of CVD Growth Direction Difference in Graphene/hBN Heterostructures. 2023 ,	O
6	Dielectric function of epitaxial quasi-freestanding monolayer graphene on Si-face 6H-SiC in a broad spectral range. 2023 , 7,	O
5	Perspectives and recent advances of two-dimensional III-nitrides: Material synthesis and emerging device applications. 2023 , 122, 160501	О
4	Majorana bound states in encapsulated bilayer graphene. 2023 , 14,	O
3	Highly dispersed and functionalized boron nitride nanosheets contribute to ultra-stable long-life all-solid-state batteries.	0
2	Charge and heat transport of doped 8Pmmn borophene with and without relaxation time approximation. 2023 , 107,	O
1	Fabrication and chemical modification of carbon nanodots/monolayer hexagonal boron nitride/substrate heterostructures and their terahertz optoelectronic properties. 2023 , 629, 157441	0